Leibniz Institute for Age Research
Fritz Lipmann Institute (FLI)

ER retention signals in the γ-secretase and their role in complex assembly

DISSERTATION

zur Erlangung des akademischen Grades doctor rerum naturalium
(Dr. rer. nat.)

vorgelegt dem Rat der Biologisch-Pharmazeutischen Fakultät der
Friedrich-Schiller-Universität Jena

von Diplom-Biochemiker

Matthias Faßler

geboren am 28.10.1980 in Jena

– 2009 –

Gutachter:

1. Dr. habil. Christoph Kaether, FLI Jena
2. Prof. Dr. Frank-Dietmar Böhmer, FSU Jena
3. Prof. Dr. Sascha Weggen, Universität Düsseldorf

Datum der Disputation: 22.04.2010

Diese Arbeit ist meinem Paten Dieter Faßler gewidmet. Er hat meine Arbeit mit Neugier und Begeisterung verfolgt und mich an entscheidender Stelle dazu motiviert, dieses Projekt fortzusetzen. Er hätte diese Arbeit sicher mit Freude gelesen und meine Verteidigung mit Interesse verfolgt.

Contents

List of Figures

List of Tables

Abbreviations

Aβ	amyloid β-protein
ACE1	angiotensin I converting enzyme 1
AChR	nicotinic acetylcholine receptor
AD	Alzheimer's Disease
ADAM	a disintegrin and metalloproteinase
AICD	APP intracellular domain
Aph-1	anterior pharynx-defective-1
APOE	apolipoprotein E
APP	β-amyloid precursor protein
APP_{sw}	β-amyloid precursor protein with the Swedish double mutation
BACE1	β-site APP-cleaving enzyme 1
C25H	cholesterol 25-hydroxylase
CD4	Cluster of differentiation 4
CFTR	cystic brosis transmembrane conductance regulator
CGN	cis-Golgi network
CHRNB2	nicotinic acetylcholine receptor β2 subunit
CHX	cycloheximide
CTF	C-terminal fragment
EDEM	ER degradation-enhancing α-mannosidase-like protein
EndoH	Endoglycosidase H
(E)GFP	(enhanced) green fluorescent protein
ER	endoplasmatic reticulum
ERAD	ER-associated degradation
ERGIC	ER-Golgi intermediate compartment
ERGIC	ER-Golgi intermediate compartment
FAD	familial AD
FcϵRI	high a?nity receptor for immunoglobulin E
GABA	γ-aminobutyric acid
GRP94	glucose-regulated protein 94
GT	glycoprotein glucosyltransferase
Iip33	human-specic p33 isoform of the MCH class II-associated invariant chain Ii of MHC
Iip35	human-specic p35 isoform of the MCH class II-associated invariant chain Ii of MHC
IP	immunoprecipitation
K_{ATP}	ATP-sensitive K^+ channel
KCNK3	K^+ channel, subfamily K, member 3
Nct	nicastrin
NGF	N-glycosidase F
NICD	Notch intracellular domain
NMDA	N-methyl-D-aspartic acid

NTF	N-terminal fragment
PAS	protein A sepharose
PDI	protein disulde isomerase
PE	PS1-EGFP
Pen2	presenilin enhancer-2
PGS	protein G sepharose
PM	plasma membrane
PPI	peptidyl-prolyl isomerase
PS1	presenilin-1
PS2	presenilin-2
PSDKO cells	$PS1^{-/-}/PS2^{-/-}$ MEF cells
RER1	return to the ER OR retention in the ER
TGN	trans-Golgi network
TMD	transmembrane domain

Zusammenfassung

Die Alzheimer Erkrankung ist die häufigste Form von Demenz bei älteren Menschen. Die Hauptkomponente der amyloiden Plaques im Gehirn von Alzheimer Patienten sind die Aβ Peptide, welche durch die Aktivität der γ-Sekretase in den extrazellulären Raum gelangen. Die γ-Sekretase ist ein multimerer Komplex von hohem Molekulargewicht und besteht aus den Untereinheiten Präsenilin (PS), Nicastrin, anterior pharynx-defective phenotype 1 (Aph1) und PS enhancer 2 (Pen2). In einer vorausgehenden Arbeit wurde ein Qualitätskontrollmechanismus für den Zusammenbau der γ-Sekretase vorgeschlagen. Dieser Mechanismus basiert auf Retentionssignalen, welche die isolierten Untereinheiten und Zwischenformen des Zusammenbaus im endoplasmatischen Retikulum (ER) halten. Diese Signale werden im korrekt assemblierten Komplex inaktiviert und die γ-Sekretase wird an die Plasmamembran und in die Endosomen transportiert, wo sie aktiv ist. Das Ziel der vorliegenden Arbeit war es, Belege für die vorgeschlagene Qualitätskontrolle beim Zusammenbau der γ-Sekretase zu finden.

Der erste Schritt dieser Arbeit war die Identifizierung von ER Retentionssignalen in den verschiedenen Untereinheiten der γ-Sekretase. Durch die Anwendung von Reporterproteinen konnten zwei neuartige ER Retentionssignale identifiziert werden, welche in der Transmembrandomäne (TMD) 4 von PS1 und der TMD1 von Pen2 liegen. Beide Signale basieren auf polaren Aminosäuren im hydrophoben Umfeld einer TMD. Das Signal in der Pen2-TMD1 trägt außerdem zur Stabilität von Pen2 bei. Die Mutagenese der zwei bekannten Retentionssignale in PS1 (TMD4 und TMD9) führte nicht zum Export von PS1 aus dem ER. Daher ist zu vermuten, dass es weitere Signale in PS1 gibt, entweder in den verbleibenden 7 TMD oder in den zytoplasmatischen Bereichen von PS1.

Der zweite Teil der vorliegenden Arbeit zielte auf die Identifizierung von Komponenten, welche die TMD-basierte ER Retention vermitteln. Retention in the ER 1 (Rer1) wurde als ein Protein identifiziert, das zur ER Retention von Pen2, jedoch nicht von PS1, beiträgt. Pen2 ist das erste bekannte Substrat von Rer1 in Säugetierzellen wobei Rer1 mit Pen2 durch die Bindung an die Pen2-TMD1 interagiert. Die Unabhängigkeit des Signals in der PS1-TMD4 von Rer1 impliziert, dass es weitere bisher unbekannte Mechanismen gibt, welche zur TMD-basierten ER Retention beitragen.

Als Drittes wurde ein Mechanismus aufgeklärt, durch welchen ER Retentionssignale in der assemblierten γ-Sekretase inaktiviert werden. Ergebnisse von uns und anderen zeigten bereits, dass die Pen2-TMD1 und die PS1-TMD4 notwendig für die Interaktion von PS1 und Pen2 sind. Dementsprechend sind beide TMD bifunktional, da sie sowohl zu einer Protein-Protein Interaktion als auch zur ER Retention beitragen. In der vorliegenden Arbeit konnte gezeigt werden, dass diese Protein-Protein Interaktion zu einer Maskierung und somit zur Inaktivierung der Retentionssignale in beiden TMD führt. Auf diese Art und Weise sind beide Funktionen der TMD aneinander gekoppelt. Diese Kopplung kann von der ER Qualitätskontrolle genutzt werden, um den Prozess des Zusammenbaus der γ-Sekretase zu überwachen. Höchstwahrscheinlich kann dieser Mechanismus für andere multimere Proteine wie Ionenkanäle und Rezeptoren an der Plasmamembran verallgemeinert werden.

Darüber hinaus wurde hier gezeigt, dass die stabile Überexpression der PS1-TMD4 den beschriebenen Qualitätskontrollmechanismus stört und somit den Zusammenbau der γ-Sekretase verhindert. Diese Beobachtung hebt die Rolle der TMD der γ-Sekretase nochmals hervor. Zudem eröffnet sie eine Möglichkeit zur pharmakologischen Beeinflussung der γ-Sekretase über ihre TMD, welche genutzt werden könnte, um dieses wichtige Enzym bei pathologischen Zuständen zu inhibieren.

Abstract

Alzheimer's Disease (AD) is the most frequent form of dementia found in the elderly. The Aβ peptides that are the principal component of the amyloid plaques in the brains of AD patients are released to the extracellular space by the activity of γ-secretase. The γ-secretase is a multimeric, high-molecular-weight complex composed of presenilin (PS), nicastrin, anterior pharynx-defective phenotype 1 (Aph1) and PS enhancer 2 (Pen2). In previous work a quality control mechanism for γ-secretase assembly was suggested that is based on retention signals, which keep unassembled subunits and assembly intermediates in the endoplasmic reticulum (ER). These signals become inactivated in the properly assembled complex and the γ-secretase is transported to the plasma membrane and the endosomes where it is active. It was the aim of the present study to provide evidence for the proposed quality control hypothesis for γ-secretase assembly.

The first step in this work was the identification of ER retention signals in the different subunits of γ-secretase. By applying a reporter protein approach, two novel ER retention signals were identified in the transmembrane domain (TMD) 4 of PS1 and the TMD1 of Pen2. Both signals are based on polar residues in the hydrophobic context of a TMD. The signal in the Pen2-TMD1 also contributes to the stability of Pen2. Mutagenesis of the two known signals in PS1 (TMD4 and TMD9) did not result in the ER export of full-length PS1. Thus, it is suggested here that further signals exist in PS1, either in the remaining 7 TMDs or in the cytoplasmic domains.

The second part of the present study aimed on the identification of the machinery accomplishing TMD-based ER retention. Retention in the ER 1 (Rer1) was identified as a protein involved in the ER retention of Pen2 but not PS1. Pen2 was the first identified mammalian substrate of Rer1 and Rer1 interacts with Pen2 via the binding to the Pen2-TMD1. The signal in the PS1-TMD4 is independent of Rer1, suggesting that other, so far unknown mechanisms exist which contribute to TMD-based ER retention.

Third, the mechanisms by which ER retention signals become inactivated in the assembled γ-secretase was elucidated. Data from our lab and by others already demonstrated that the Pen2-TMD1 and the PS1-TMD4 are necessary for the interaction of PS1 and Pen2. Thus, both TMDs are bifunctional, since they contribute to protein-protein interaction and to ER retention. It was shown here, that the protein-protein interaction between the TMDs results in the masking and inactivation of the retention signals in both TMDs. In this way both functions of the TMDs are connected and this mechanism can be used by the ER quality control to probe the assembly status of γ-secretase. Most likely, this mechanism can be generalised for other multimeric proteins like ion channels and cell surface receptors.

Furthermore, it was shown that the stable overexpression of the PS1-TMD4 interferes with the described quality control mechanism and thus with the assembly of the γ-secretase. This finding highlights the relevance of TMDs for γ-secretase function and it discloses the possibility that pharmacological targeting of γ-secretase TMDs could be used to inhibit this important enzyme under pathological conditions.

1 Introduction

1.1 Alzheimer's Disease

1.1.1 Relevance of Alzheimer's Disease to modern societies

Alzheimer's Disease (AD) has been described for the first time in 1906 by Alois Alzheimer and has been thought to be a special form of presenile dementia. Nowadays, it is commonly accepted that dementias of the Alzheimer type are the most frequent form also of senile dementias (Selkoe, 2001). Early symptoms of AD are problems in concentration or forgetfulness, which are often considered as ″normal″ signs of ageing. The progression of the disease is accompanied for instance by language deterioration, depression, impaired ability to process visual information and confusion. In the end stage the entire loss of the personality may occur. Due to the advancing loss of independence in day-to-day situations intensive care for the patients is necessary.

The risk to develop AD exponentially grows with age, especially after the age of 65, leading to a prevalence of almost 25 % for people older than 85 years in Germany (Ott *et al.*, 1995; Bickel, 2000). The second most important risk factor after age is genetic predisposition. Yet, the inherited, familial AD (FAD) accounts only for less than 5 % of all AD cases (Bertram and Tanzi, 2005). FAD cases are very often characterised by an early onset before the age of 65 and a fast progression of the disease. Considering the demographical development the number AD patients in Germany will increase from 935,000 in the year 2000 to an estimated number of 2,620,000 by 2050 (Deutsche Alzheimer Gesellschaft).

The increasing case numbers in combination with the extensive care needed by the patients, highlight the necessity to develop a cure or at least a prophylaxis for AD. Otherwise AD will become a socioeconomic challenge within the next decades.

1.1.2 Neuropathological hallmarks of Alzheimer's Disease

AD results from a loss of neurons in regions important for memory and learning, like the neocortex, limbic structures (e.g. hippocampus and amygdala) and some brainstem nuclei. Ultimately, this neuronal loss results in the severe brain atrophy observed in the brains of AD patients (figure 1.1A). On a microscopic level three more hallmarks were identified. The two most prominent ones were already described by Alois Alzheimer: Neurofibrillary tangles and senile or neuritic plaques.

Neurofibrillary tangles are large, intraneuronal bundles of abnormal fibres, which consist of so-called paired helical filaments. These paired helical filaments are highly insoluble aggregates of a hyperphosphorylated form of the microtubule-associated protein tau (figure 1.1B). Neurofibrillar tangles have been also described in other neurodegenerative diseases (Selkoe, 2001). The second microscopic hallmark of AD, neuritic plaques, are extracellular deposits of the amyloid β-protein (Aβ). Plaques have a compact, fibrillary structure and can vary in size between 10 to more than 120 μm (figure 1.1C). The majority of the amyloid β-protein found in the plaques is the more aggregation prone Aβ_{42} form. Dystrophic neurites are found within and immediately surrounding the plaques (Selkoe, 2001). Third, additionally to protein aggregates visible in AD brains, cellular changes have been detected using immunohistochemistry. The formation of neuritic plaques is intimately coupled to the activation of an inflammatory response resulting in microgliosis and astrocytosis(figure 1.1D)(Weiner and Frenkel, 2006).

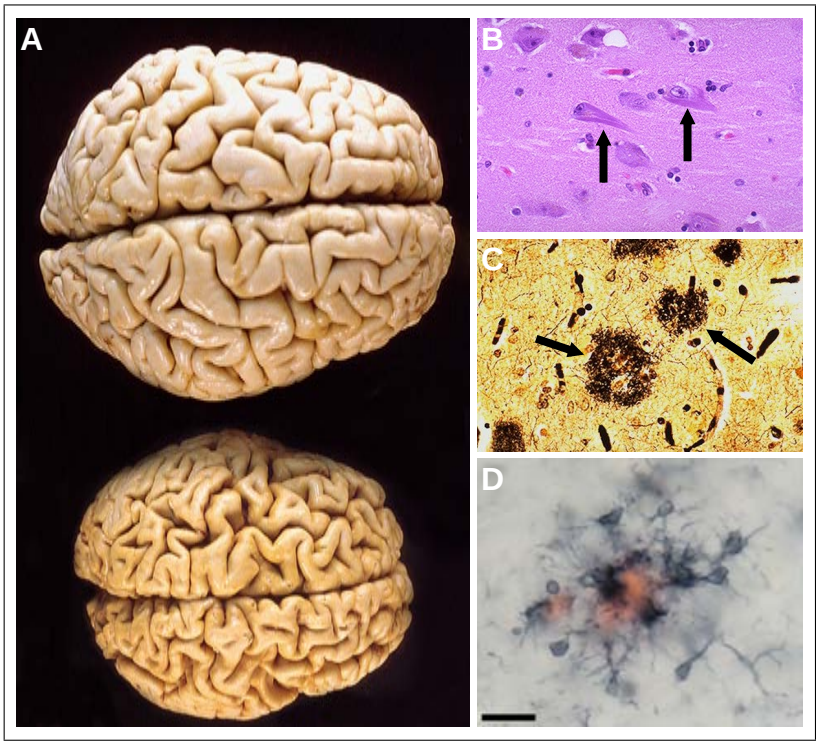

Figure 1.1: *Pathological hallmarks of Alzheimer's Disease. A) Brain atrophy. Normal brain (top) and AD patient brain (bottom). Picture from PEIR digital library. B) Neurofibrillary tangles. HE staining. C) Neuritic plaques. Bielschowsky silver stain. Pictures B) and C) from WebPath: The Internet Pathology Laboratory, 2009. D) Microgliosis in APPPS1-21 transgenic mouse model. Iba-1 immunostaining and Congo red staining in the neocortex of an 8 month old APPPS-21 mouse. Iba-1 positive microglia clustered around a plaque. Scale bar 20 μm. Picture from Radde* et al.*, 2006.*

1.2 Molecular basis of Alzheimer's Disease

Although hereditary forms of AD comprise only a small fraction of all AD cases, they have provided great insight into the molecular processes underlying Alzheimer's Disease. So far 200 mutations were identified that lead to FAD (Alzheimer Disease & Frontotemporal Dementia Mutation Database). All mutations were identified within only 3 genes: APP, PSEN1 and PSEN2 (Bertram and Tanzi, 2005). APP encodes the β-amyloid precursor protein and PSEN1 and PSEN2 encode presenilin-1 (PS1) and presenilin-2 (PS2), respectively.

In addition to mutations that ultimately cause FAD several susceptibility genes were identified that lead to a late onset AD. The best studied is the apolipoprotein E (APOE) genotype, with the $\epsilon 4$ allele being an AD risk factor and the $\epsilon 2$ allele being protective (Corder *et al.*, 1993; Strittmatter *et al.*, 1993). More recently, genome wide association studies revealed further genetic risk factors for AD which were integrated into the AlzGene database (Bertram *et al.*, 2007). Among these susceptibility genes are for instance angiotensin I converting enzyme 1 (ACE1), cholesterol 25-hydroxylase (C25H) and the nicotinic acetylcholine receptor $\beta 2$ subunit (CHRNB2) (Bertram *et al.*, 2007; Bertram and Tanzi, 2008).

1.2.1 The β-amyloid precursor protein (APP)

Biochemical analysis of the neuritic plaques in AD patients postmortem brains led to the isolation and partial sequencing of Aβ in the 80s of the last century (Glenner and Wong, 1984; Masters *et al.*, 1985). Using this information the APP gene cloned shortly thereafter in several laboratories (Kang *et al.*, 1987; Goldgaber *et al.*, 1987; Tanzi *et al.*, 1987). The localisation of the APP gene on chromosome 21 was consistent with the finding of an AD pathology in middle-aged patients with Down syndrome (Robakis *et al.*, 1987). APP is a member of a small and highly conserved gene family comprised of APLP1 and APLP2 (*H. sapiens*), Appl (*D. melanogaster*) and apl-1 (*C. elegans*). All encode for large type I membrane proteins with a large extracellular domain and a short cytoplasmic tail, yet only APP contains the domain giving rise to the Aβ peptide. Alternative splicing leads to mainly three different APP isoforms of different length (APP_{695}, APP_{751} and APP_{770}). Neuronal APP is almost exclusively expressed as the APP_{695} isoform (Kang and Müller-Hill, 1990). As of today, the most consistently established function for APP is an autocrine and paracrine role in growth regulation (Thinakaran and Koo, 2008; Nikolaev *et al.*, 2009).

The APP ectodomain is shedded by α- or β-secretase generating small membrane bound C-terminal fragments (CTF). αAPP-CTF and βAPP-CTF are an immediate substrate to several cleavages by γ-secretase which lead to the release of p3 and Aβ, respectively, into the extracellular space and of the APP intracellular domain (AICD) into the cytosol (Thinakaran and Koo, 2008)(figure 1.2). α-secretase activity was found for several different proteases with zinc metalloproteases of the ADAM family (A disintegrin and metalloproteinase; ADAM-9, ADAM-10, ADAM-17/TACE) as the most prominent enzymes (Allinson *et al.*, 2003). α-secretases cleave APP within the Aβ domain at position K612 and the p3 protein released by

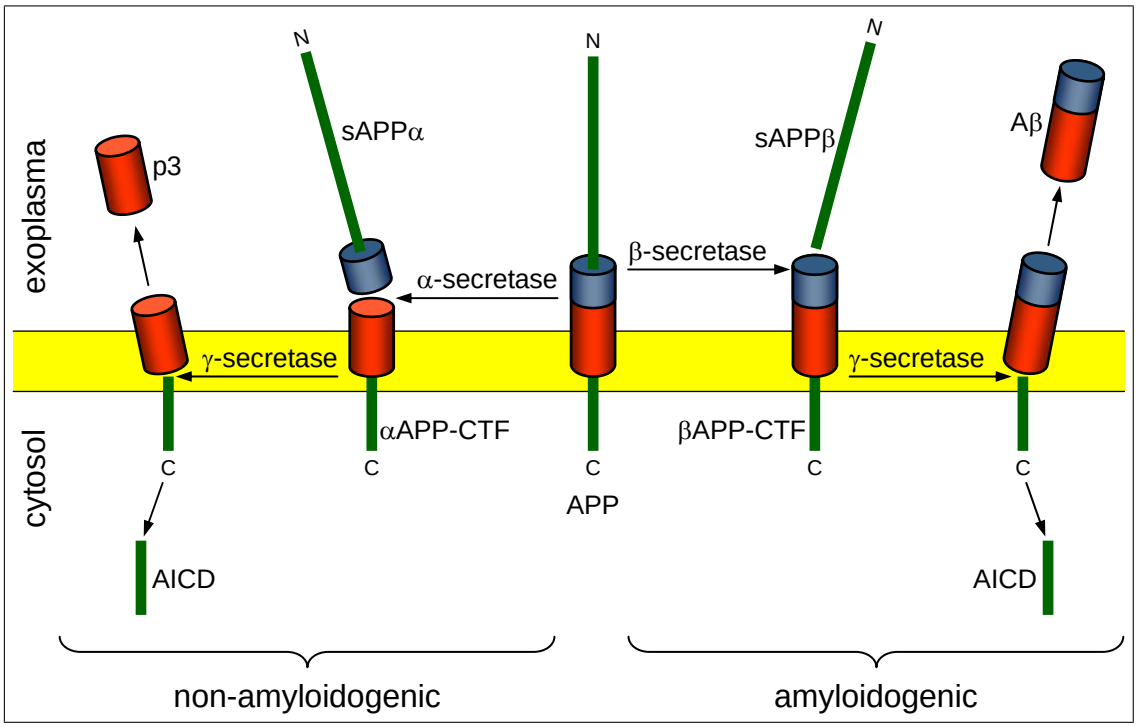

Figure 1.2: *APP is cleaved by α-, β- and γ-secretase. Cleavage by α-secretase initiates the non-amyloidogenic pathway resulting in the release of p3. In contrast, β-secretase cleavage initiates the amyloidogenic pathway that ultimately leads to the release of the Aβ peptides of different length. Both pathways result in the release of AICD into the cytosol and of the respective sAPP fragments into the extracellular space (Thinakaran and Koo, 2008).*

subsequent γ-secretase cleavage is not aggregation prone. Thus, α-secretase triggers a non-amyloidogenic series of cleavage events. Neuronal β-secretase activity was demonstrated for BACE1 (β-site APP-cleaving enzyme 1). BACE1 is an aspartyl protease and a type I membrane protein that cleaves APP at position M596, thus generating the Aβ N-terminus with D597 as the first residue (Cole and Vassar, 2008). More recently, another cleavage site was postulated in the N-terminal domain of APP. However, neither the protease nor the functional relevance of this cleavage was shown (Nikolaev *et al.*, 2009).

FAD-linked mutations in the APP gene were named after the geographical origin of the affected families (e.g. Swedish, Arctic, London, ...). The found mutations either increase the propensity of the released Aβ peptide to aggregate or they affect the proteolytic processing of APP (figure 1.3). For instance, the Swedish double mutation (K595M, M596L) increases the frequency of a β-secretase cleavage, hence the overall production of Aβ species is increased (Citron *et al.*, 1992). Other mutations affect the generation of the Aβ C-terminus by γ-secretase, thus the ratio between the longer $A\beta_{42}$ and the shorter $A\beta_{40}$ is increased. Since $A\beta_{42}$ is more aggregation-prone whereas $A\beta_{40}$ was supposed to be an anti-aggregation factor (McGowan *et al.*, 2005) this causes an increase in the formation of neurotoxic Aβ oligomers (see section 1.2.3). Additionally, duplications of the entire APP gene lead to genetically

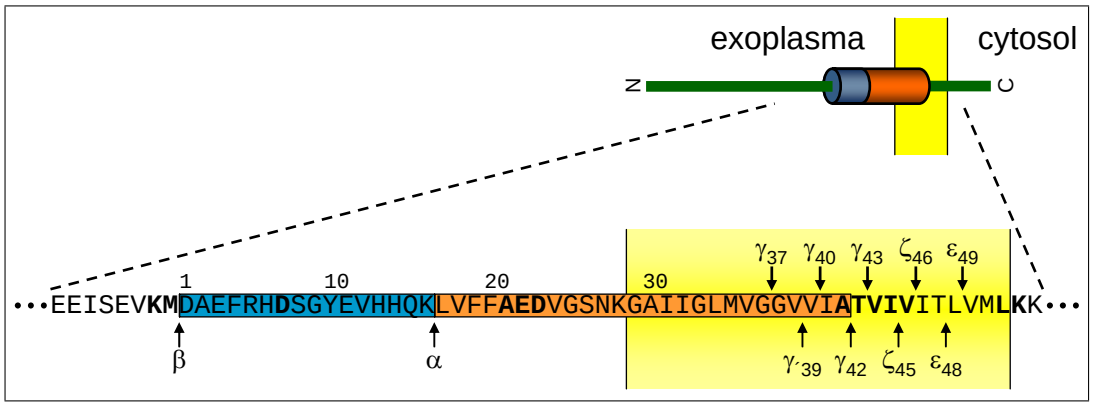

Figure 1.3: *APP is cleaved at multiple sites and a variety of FAD-linked mutations have been identified in APP. FAD-linked mutations in APP are depicted in bold and the TMD region in APP was marked with yellow. βAPP-CTF processing by γ-secretase leads to two product lines generated by stepwise cleavages at every third amino acid. The different cleavage sites were denominated with greek letters. The first cleavage at the ϵ-site determines which line is chosen, either from ϵ_{49} to γ_{37} or from ϵ_{48} to γ_{39}. Both product lines do not necessarily proceed until the last cleavage. Modified after Steiner* et al.*, 2008a.*

determined AD for instance in patients with Down syndrome.

1.2.2 The γ-secretase

γ-secretase is an aspartyl protease that cleaves a variety of substrates within their transmembrane domains (TMD). As of today, there are more than 60 substrates known with APP and Notch as the most prominent ones (McCarthy *et al.*, 2009). γ-secretase is composed of the four subunits Aph-1 (anterior pharynx-defective-1), Pen2 (presenilin enhancer-2), Nct (nicastrin) and PS1 or PS2. All four subunits were necessary and sufficient to yield proteolytic activity (Kimberly *et al.*, 2003; Edbauer *et al.*, 2003) and were found in a 1:1:1:1 stoichiometry within the complex (Sato *et al.*, 2007)(figure 1.4). Estimation of the size of γ-secretase by native gel electrophoresis revealed a molecular mass of ∼500 kDa, although the mass of the individual subunits sums up to approximately 200 kDa (Pen2 ∼12 kDa, Aph-1 ∼20 kDa, PS1/2 ∼50 kDa, mature Nct ∼120 kDa). Schroeter *et al.*, 2003 suggested a dimerisation of the tetrameric complex to explain the observed differences in the complex size though these findings are still controversial. Besides the four core subunits several other proteins were found to interact with γ-secretase and/or to modulate its activity such as CD147 (Zhou *et al.*, 2005), TMP21 (Chen *et al.*, 2006) and GPR3 (Thathiah *et al.*, 2009). The detailed assembly of γ-secretase is described in section 1.5.

Presenilins were the first identified γ-secretase subunits because FAD-linked mutations were discovered in the PS genes (Sherrington *et al.*, 1995; Rogaev *et al.*, 1995). Presenilins contain 9 TMDs and the N-terminus faces the cytosol, whereas the C-terminus folds back into the membrane from the lumenal side (Spasic *et al.*,

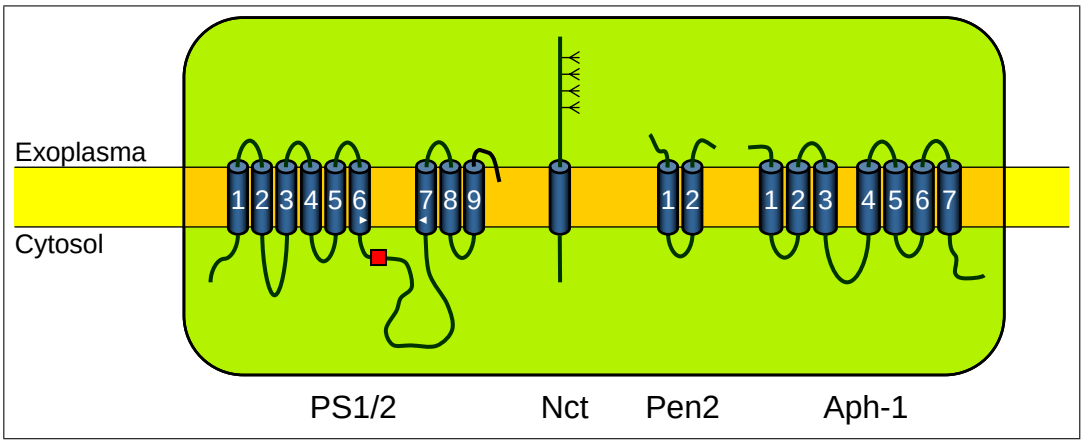

Figure 1.4: *γ-secretase is composed of Presenilin, Nicastrin, Aph-1 and Pen2. The topology of all four essential subunits is shown. The arrowheads indicate the positions of the catalytic aspartates and the red rectangle the endoproteolytic cleavage site in PS1/2. The Nct ectodomain contains several glycosylation sites.*

2006). The two aspartate residues forming the active site of γ-secretase are located within the TMD6 and TMD7 of PS1/2 and mutation of either of these residues abolished γ-secretase activity (Wolfe *et al.*, 1999). The D385 residue within TMD7 is part of a highly conserved GXGD motif, thus giving rise to the name GXGD-type aspartyl proteases for the family of such proteases. After the assembly of all subunits the PS1/2 holoprotein is cleaved into an N-terminal (PS-NTF, ∼30 kDa) and C-terminal (PS-CTF, ∼20 kDa) fragment most likely in an autoproteolytic way (Thinakaran *et al.*, 1996; Edbauer *et al.*, 2003). The cleavage site is located in an intracellular loop between the TMD6 and TMD7 that possibly folds back into the membrane to be cleaved by the holoprotein. As of today, there are 177 and 14 FAD-linked mutations described for PS1 and PS2, respectively (Alzheimer Disease & Frontotemporal Dementia Mutation Database, 2009). The FAD-linked mutations in PS1/2 lead to an altered specificity of the γ-secretase cleavage within βAPP-CTF. Thus, the ratio of generated Aβ_{42} versus Aβ_{40} is increased as it was described for FAD-linked mutations in APP before (see 1.2.1).

The presence of PS in a high-molecular-weight complex already suggested that other subunits are involved in the γ-secretase activity (Li *et al.*, 2000). Accordingly, Nct was identified as a second subunit (Yu *et al.*, 2000; Edbauer *et al.*, 2002). In its mature form it is a highly glycosylated type I transmembrane protein of ∼120 kDa. Nct binds to the new N-terminus of shedded substrates via its ectodomain, thereby acting as a substrate receptor for γ-secretase (Shah *et al.*, 2005). Aph-1 and Pen2 were identified in a genetic screen in *C. elegans* (Francis *et al.*, 2002). Both proteins are highly hydrophobic with 7 and 2 TMDs, respectively (figure 1.4). Aph-1 has 2 human homologs (Aph-1a and Aph-1b) of which Aph-1a has a short and long splice form (Aph-1aS and Aph-1aL). The three Aph-1 isoforms and the two presenilins permit up to 6 different γ-secretase complexes (Shirotani *et al.*, 2004b) that differ in specificity (Serneels *et al.*, 2005; Lai *et al.*, 2003; Mastrangelo *et al.*,

2005). Pen2 has a pivotal role in the stabilisation of the PS fragments (Prokop *et al.*, 2004; Hasegawa *et al.*, 2004) and there is first evidence that FAD-linked mutations exist therein (Frigerio *et al.*, 2005). In contrast, no function was assigned to Aph-1 so far.

The cleavage of APP by γ-secretase is a stepwise process (figure 1.3) and the different cleavage sites were denominated with greek letters. The first cleavage at the ϵ-site releases AICD to the cytosol. Subsequently, the remaining stub is cleaved at ζ-site and several γ-sites until the respective Aβ or p3 peptide is short enough to be released from the membrane into the extracellular space. It was demonstrated that already the ϵ-cleavage determines the subsequent cleavages since γ-secretase cleaves the remaining stub at every third amino acid. Thus, two sequences of Aβ cleavages can occur depending on the position of the first ϵ-cleavage: Aβ49(ϵ) - Aβ46(ζ) - Aβ43(γ) - Aβ40(γ) - Aβ37(γ) or Aβ48(ϵ) - Aβ45(ζ) - Aβ42(γ) - Aβ39(γ) (Qi-Takahara *et al.*, 2005, reviewed in Steiner *et al.*, 2008a)(figure 1.3). However, the situation observed *in vivo* is much more complicated since N- and C-terminal truncations lead to a broad range of detectable Aβ peptides (Haass *et al.*, 1992; Wang *et al.*, 1996). The variability of detectable Aβ peptides ranges from the prominent $A\beta_{1-40}$ and $A\beta_{1-42}$ over $A\beta_{3-40}$ and $A\beta_{1-38}$ to rare species like $A\beta_{11-34}$.

1.2.3 The amyloid cascade hypothesis

All FAD-linked mutations lead to an increased ratio of generated $A\beta_{42}$ versus $A\beta_{40}$ or to an overall increase in Aβ production. Additionally, reduced clearance of Aβ peptides could contribute to elevated Aβ levels in the brain. These changes in Aβ metabolism are supposed to be the first step in the cascade of pathogenic events leading to AD (Selkoe, 2001, revised in Haass and Selkoe, 2007)(figure 1.5).

1.3 The secretory pathway

1.3.1 Overview

By revealing the importance of organelles like the endoplasmic reticulum (ER) and the Golgi apparatus for protein secretion in the 1960s, Pallade and others laid the ground for our current understanding of intracellular transport. Using ultrastructural analysis and pulse chase experiments they disclosed the role of different organelles in exocrine cells of the pancreas and they separated protein secretion from other processes like translation (Jamieson and Palade, 1967a,b, 1968a,b). The secretory pathway consists of the following organelles: ER, ER-Golgi intermediate compartment (ERGIC), cis-Golgi network (CGN), Golgi apparatus and the trans-Golgi network (TGN). These organelles differ in structure, function, lipid composition and enzymatic instrumentation, but they are interconnected by dynamic membrane traffic (Harter and Wieland, 1996; Dalbey and Heijne, 2002). The tasks of the secretory pathway include membrane insertion, folding and complex assembly, modification, transport and (regulated) secretion of proteins. All in all, the secretory pathway is the cellular factory for the majority of membrane bound and secreted proteins

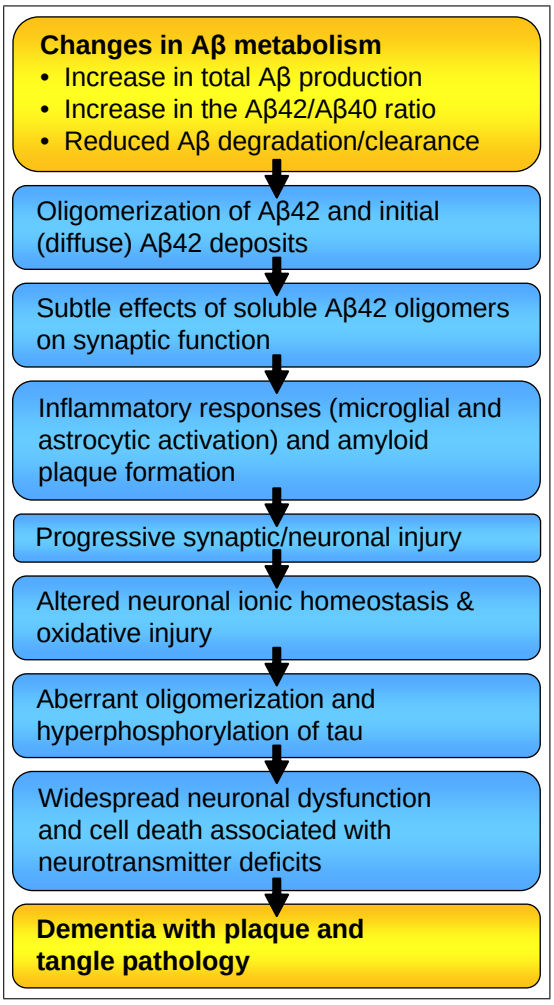

Figure 1.5: *The amyloid cascade hypothesis (Selkoe, 2001; Haass and Selkoe, 2007).*

(summarised in figure 1.6).

Proteins enter the secretory pathway by co-translational translocation into the ER, where they are properly folded and glycoproteins obtain initial glycosylations. In parallel, the TMDs of membrane proteins are inserted into the ER membrane (Dalbey and Heijne, 2002). Once proteins are in a proper conformation, they are sorted into budding vesicles that are coated with COPII coatomer proteins. COPII vesicles then move anterogradely to the ERGIC which comprises an additional sorting station between the ER and the cis-Golgi. Larger ERGIC compartments that are generated by the fusion of COPII vesicles (Klumperman, 2000) most likely develope into early Golgi cisternae. Movement through the Golgi apparatus results from cisternal maturation and does according to current models not involve budding of anterograde vesicles (Pelham, 2001). An entire Golgi cisternae physically moves from the CGN to the TGN while its enzymatic instrumentation is modified by retrogradely moving vesicles from later Golgi stages. In the course of Golgi transit glycoproteins are heavily modified by the stepwise exposure to different glycosyl transferases (Helenius and Aebi, 2001). The TGN is the major branch point of the

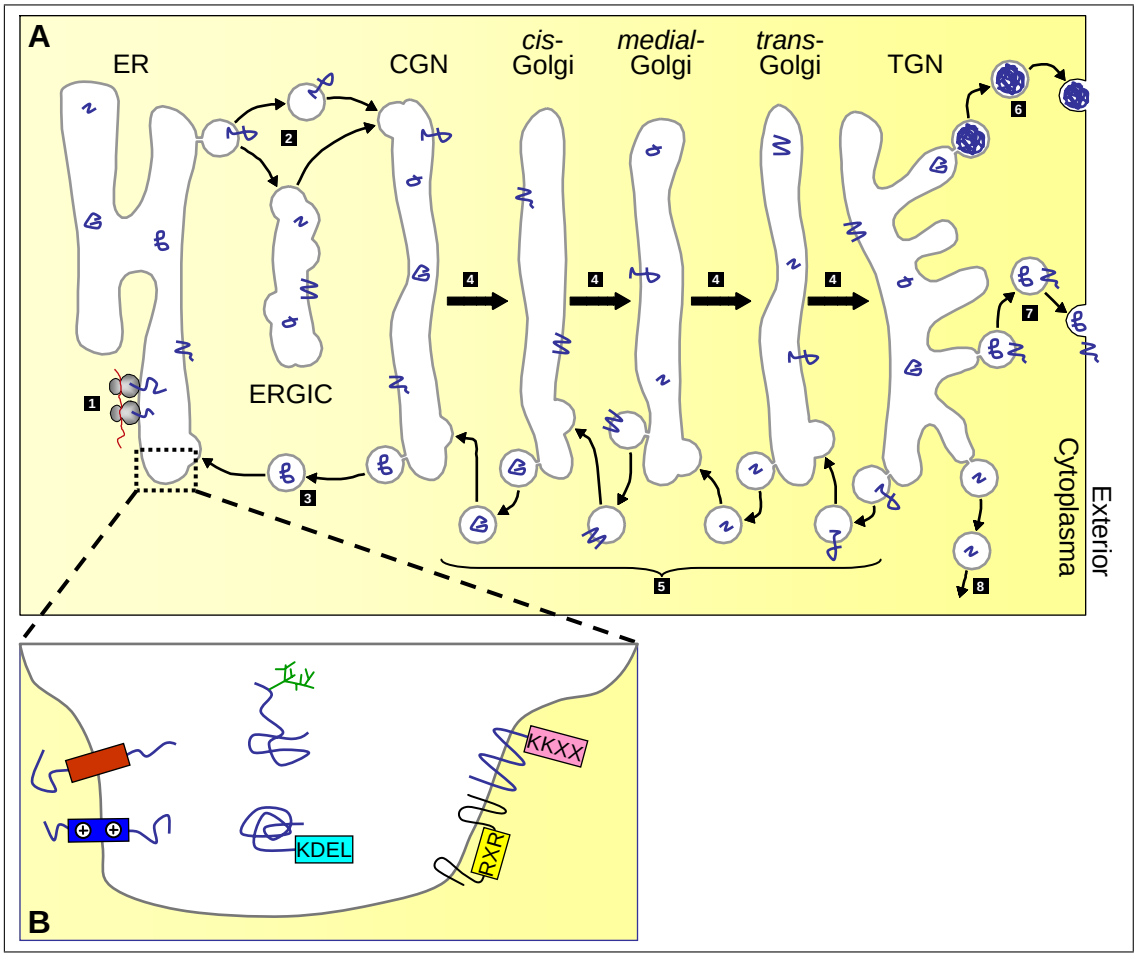

Figure 1.6: *Overview over the secretory pathway and ER retention signals. A) Protein secretion through the secretory pathway requires a complex machinery.* 1 *Proteins that are determined for the secretory pathway are co-translationally transported into the ER.* 2 *Anterograde transport via COPII vesicles from the ER to the ERGIC or CGN.* 3 *and* 5 *Retrograde transport via COPI vesicles to the ER and between different compartments of the Golgi apparatus, respectively.* 4 *Anterograde transport within the Golgi apparatus via cisternal maturation.* 6 *Regulated protein secretion via densely packed secretory granules.* 7 *Continuous secretion via exocytosis.* 8 *Transport to the lysosomal/endosomal compartment. Figure modified after Lodish, 2007. B) Different ER retention signals were identified. TMD-based signals might be divided into two groups since signals with charged residues (dark blue) seem to work differently than non-charged signals (red). In membrane proteins KKXX (pink) and RXR (yellow) signals have been described. For lumenal proteins the KDEL signal (light blue) is known. Additionally, for all glycoproteins (membrane bound or soluble) the glycans (green) may facilitate ER retention.*

secretory pathway, where proteins are sorted to at least three different vesicle types. Type one is dedicated to exocytosis, releasing proteins to the plasma membrane or the cell exterior in a continuous process. The second type is also targeted to the plasma membrane, although these vesicles undergo exocytosis only after a distinct stimulus. These vesicles are called secretory granules or secretory vesicles and are mainly found in highly specialised secretory active cells. The last type transports proteins to the lysosomes. The entire process is guided by signal sequences that cause either retention in or exit from a distinct compartment (Ikonen and Simons, 1998).

1.3.2 ER retention signals

Different reasons necessitate that proteins stay in the ER. On the one hand, misfolding and improper assembly of secreted proteins have to be recognised by the ER quality control and the affected proteins have to be retained in the ER (see section 1.3.3). On the other hand, resident ER proteins (e.g. chaperones) exert their function in the ER and therefore they have to be kept in place. ER localisation of proteins is achieved in different ways. Exclusion from anterogradely moving COPII vesicles is supposed to be the primary mechanism localising proteins to the ER (Barlowe, 2000; Dalbey and Heijne, 2002). Moreover, specific signal sequences were identified that mediate ER retention or promote retrograde transport via COPI vesicles once a protein is mislocalised to the ERGIC or cis-Golgi. These signals can be cytoplasmic, lumenal or within TMDs (figure 1.6B).

The best characterised signal is the KDEL sequence (HDEL in yeast) found at the very C-terminus of ER resident chaperones like BiP and it is bound by the KDEL receptor (Erd2p in yeast) in the cis-Golgi. The complex of the KDEL receptor and the substrate protein is subsequently packaged into COPI vesicles and transported to the ER (Aoe *et al.*, 1998). The KDEL receptor itself has a dilysine motif (KKXX, with X = any amino acid) at the end of the cytoplasmic C-terminus, which is found in several ER localised transmembrane proteins (Pelham, 1995). The KKXX motive directly interacts with COPI coatomers, thus promoting the sorting into COPI vesicles and the retrograde transport to the ER (Cosson and Letourneur, 1997).

Zerangue *et al.*, 1999 identified a novel type of ER retention signals in the cytoplasmic domains of Kir6.2 and SUR1, both subunits of ATP-sensitive K^+ channels (K_{ATP}). These signals are based on two arginines (RXR). Meanwhile, signals of the RXR type were identified for example in the γ-aminobutyric acid (GABA) receptor subunit $GABA_B$-R1 (Margeta-Mitrovic *et al.*, 2000), the human-specific p33 isoform of the MHC class II-associated invariant chain Ii (Iip33)(Schutze *et al.*, 1994) and the N-methyl-D-aspartic acid (NMDA) receptor splice variants NR1-1 and NR1-3 (Standley *et al.*, 2000). Similarly to KKXX signals, ER retention triggered by RXR type signals is mediated by the binding of COPI coatomers to the arginines (O'Kelly *et al.*, 2002; Yuan *et al.*, 2003; Michelsen *et al.*, 2007).

The knowledge about TMD-based ER retention signals is less clear. In their ground breaking work in the early 1990s the Klausner group characterised a degradation and ER retention signal in the TMD of TCRα. This signal depends on

two positively charged residues within the TMD, that most likely destabilise the entire TMD (Bonifacino *et al.*, 1990a,b). Hence, it appears that the identified signal primarily targets the carrying protein to ER-associated degradation (ERAD) and in this way causes ER localisation. This view is supported by the findings of Letourneur *et al.*, 1995 for the TMD of human high affinity receptor for immunoglobulin E (FcϵRI) that contains a negatively charged amino acid.

On the other hand, TMD-based ER retention signals were described that depend on polar amino acids. Such signals were identified for example in the nicotinic acetylcholine receptor (AChR)(Wang *et al.*, 2002), Nct (Spasic *et al.*, 2007) and Pen2 (this study). In yeast Rer1p was implicated in the retention of TMD-based retention signals that are based on polar residues (Sato *et al.*, 1995, 1996, 1997, 2003, 2004)(see section 1.4). This finding was confirmed in mammals for Pen2 (this study) and Nct (Spasic *et al.*, 2007). All in all, no agreement exists which determinants lead to TMD-based ER retention and how this retention is accomplished.

Interestingly, there exist also ER export signals like the diacidic DXD motif in CFTR (cystic fibrosis transmembrane conductance regulator). In contrast to ER retention signals, these signals mediate the binding to COPII coatomers and thus promote anterograde transport via COPII vesicles (Wang *et al.*, 2004).

1.3.3 Quality control in the ER

All proteins that traffic through the secretory pathway are subjected to a quality control in the ER. Since later Golgi compartments do not generally support protein folding or exert quality control, it is of highest importance to keep misfolded or unassembled proteins in the ER (Mezzacasa and Helenius, 2002). Folding and quality control in the ER include formation of disulfide bonds, addition and modification of glycans, proteolytic cleavages, minimisation of free energy and assembly of multimeric complexes. An entire set of ER-resident chaperones and folding sensors is facilitating and controlling these processes. Among these proteins are BiP, calnexin, calreticulin, glucose-regulated protein 94 (GRP94) and members of the families of peptidyl-prolyl isomerases (PPI) and protein disulfide isomerases (PDI)(Ellgaard and Helenius, 2003).

The best understood mechanism of quality control in the ER is the calnexin/calreticulin cycle. This cycle applies for glycoproteins that have their folding status marked by specific modifications of their glycan trees. To this end, the preformed glycan trees that were added to asparagines by oligosaccharyltransferase are trimmed by two glucose units by glucosidases I and II. The monoglucosylated glycoprotein is then bound by calreticulin (ER lumen) or calnexin (ER membrane) which are themselves associated with further chaperones. Cleavage of the last glucose releases the glycoprotein from calnexin/calreticulin and the folding status is probed by UDP-glucose:glycoprotein glucosyltransferase (GT). If misfolding is detected, GT adds a terminal glucose to the glycoprotein and thereby promotes reassociation with calnexin/calreticulin. If this cycle of association to and dissociation from calnexin/calreticulin exceeds a distinct time span, the glycoprotein is targeted for ERAD by the removal of a mannose in another branch of the glycan tree. Glycoproteins marked in this way are bound by the lectin EDEM (ER degradation-

enhancing α-mannosidase-like protein) that most likely promotes retrotranslocation to the cytoplasm. There the misfolded protein is ubiquitinylated and degraded via the proteasome (Yoshida *et al.*, 2002; Ellgaard and Helenius, 2003; Helenius and Aebi, 2004).

Different mechanisms are involved in probing the assembly status of multimeric complexes like ion channels or cell surface receptors. These mechanisms are based on ER retention signals (see section 1.3.2) that are masked after correct assembly of the multimeric complex (for reviews see Nufer and Hauri, 2003; Michelsen *et al.*, 2005). In case of the $GABA_B$ receptor the masking of an ER retention signal was characterised down to the structural level. The $GABA_B$-R1 subunit carries a RSRR (RXR type) ER retention motif in the cytoplasmic C-terminus. This motif immediately follows a region that mediates the binding to the $GABA_B$-R2 subunit by forming a coiled-coil between the C-termini of the two subunits. The structural rearrangement in this area causes the masking of the ER retention signal after the coiled-coil has formed (Margeta-Mitrovic *et al.*, 2000)(figure 1.7A).

Other examples describe the involvement of 14-3-3 proteins. K_{ATP} channels contain RXR type retention signals in their α (Kir6.1/2) and β (SUR1) subunits. At least for the ER retention signal in Kir6.2 it was demonstrated that oligomerization of this signal sequence recruits 14-3-3 proteins *in vitro* and *in vivo*. The recruited

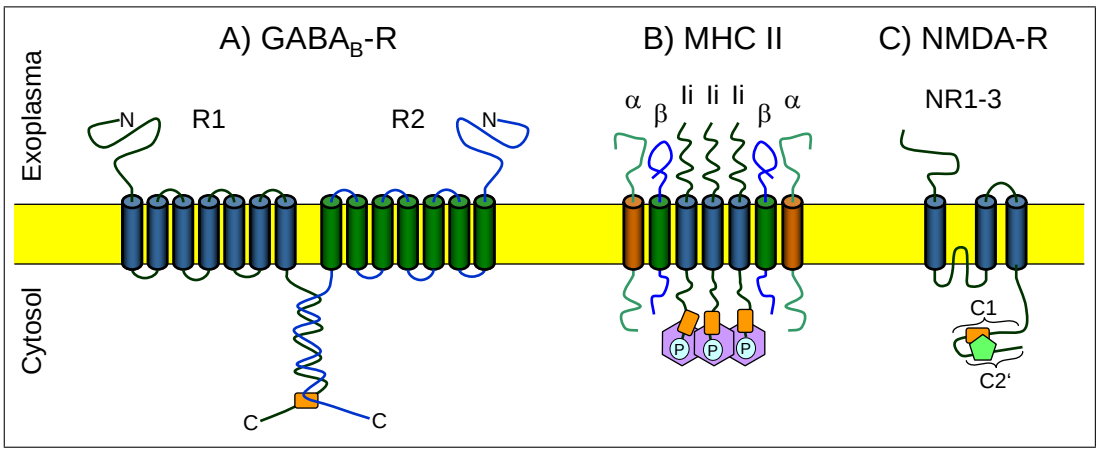

Figure 1.7: *Masking of cytoplasmic ER retention signals is achieved in different ways. Orange rectangles indicate cytoplasmic ER retention signals. A) Steric masking: coiled-coil formation between the C-termini of the two $GABA_B$ receptor subunits R1 and R2 cause the masking of an adjacent ER retention signal in the R1 subunit (Margeta-Mitrovic* et al.*, 2000). B) Masking by 14-3-3 proteins: Iip35 (Ii) is phosphorylated at a residue in the vicinity of the Arg-based signal. Subsequent recruitment of 14-3-3 protein (purple hexagons) causes masking of the signal (Kuwana* et al.*, 1998). Additionally, steric masking has also been implicated for the MHC class II complex (Khalil* et al.*, 2003). C) Masking by PDZ-domain protein: NMDA receptor splice form NR1-3 has the C1 and C2' cassette present in its C-terminus. The C1 contains a cytosolic ER retention signal that is masked by binding of a PDZ-domain protein (green pentagon) to the adjacent C2' cassette (Standley* et al.*, 2000). Modified after Michelsen* et al.*, 2005.*

14-3-3 proteins compete with the COPI vesicle coat and thus with ER retention (Zerangue *et al.*, 1999; Yuan *et al.*, 2003). 14-3-3 protein have also been implicated in the ER exit of Iip35 that also contains a RXR type signal. In this case the phosphorylation of the serine residue next to the retention signal results in the binding of 14-3-3 proteins and the masking of the ER retention motif. However, the impact of this masking on the assembly of the entire Ii-MHC-complex is not completely clarified (Kuwana *et al.*, 1998; Khalil *et al.*, 2003, 2005)(figure 1.7B). A very similar mechanism was described for KCNK3 (K^+ channel, subfamily K, member 3)(O'Kelly *et al.*, 2002).

Furthermore, Standley *et al.*, 2000 described a RXR type ER retention motif in the C1 cassette of the NMDA receptor splice variants NR1-1 and NR1-3. The NR1-3 splice variant contains a PDZ binding site within the C2' cassette and binding of PSD-95 family members causes masking of the retention signal in the C1 cassette (figure 1.7C). Moreover, Scott *et al.*, 2001 described that the very same signal can be inactivated by PKC-mediated phosphorylation in the NMDA receptor splice form NR1-1 that also contains the C1 but lacks the C2' cassette. The masking of dilysine ER retention signals by nonspecific sterical hindrance was shown for the cytoplasmic C-terminus of FcϵRI(Letourneur *et al.*, 1995).

Less knowledge exists on the masking of TMD-based ER retention signals. Bonifacino *et al.*, 1990a demonstrated that the positively charged residues of the ER retention signal in the TMD of TCRα interacts with the negatively charged residues in the TMD of another subunit of the TCR complex, namely CD3-δ. Most notably, this interaction causes stabilisation of a Tac reporter protein carrying the TCRα-TMD, since the processes of TMD-mediated ER retention and protein degradation are intimately coupled in their study (Bonifacino *et al.*, 1990a,b). More recently, a study by Horak *et al.*, 2008 revealed an ER retention signal in TMD3 of NMDA receptor subunits NR1 and NR2B. In the functional, tetrameric receptor (NR1-NR1-NR2B-NR2B stoichiometry) these signals are masked by an interaction of $NR1_{TMD3}$ and $NR2B_{TMD3}$ with the TMD4 of NR1.

Taken together, the literature shows a diversity of mechanisms causing masking of cytoplasmic ER retention signals. In contrast, the picture of TMD-based retention signals seems to be split. On the one hand, detailed knowledge exists on signals that are based on charged residues (like TCRα). Masking of these ER retention signals is accompanied by stabilisation of the harbouring protein, which makes both processes hard to dissect. On the other hand, only little knowledge exists on the masking of other TMD-based retention signals.

1.4 The sorting receptor Rer1

The *RER1* gene (Return to the ER OR Retention in the ER) was found mutated in a yeast strain that failed to localise Sec12p to the early compartments of the secretory pathway (cis-Golgi and ER)(Nishikawa and Nakano, 1993; Boehm *et al.*, 1994). *RER1* encodes a hydrophobic protein of 188 amino acids with a molecular mass of 22 kDa and four TMDs (Boehm *et al.*, 1994; Sato *et al.*, 1995)(figure 1.8). Rer1p cycles between the ER and the Golgi apparatus via COPI and COPII vesicles,

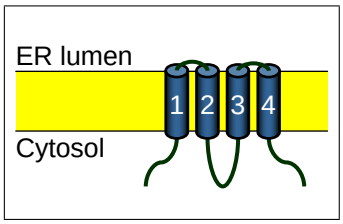

Figure 1.8: *Rer1 has a W-topology. N- and C-terminus face the cytosol and only 6 residues are exposed to the ER lumen (Boehm* et al.*, 1994; Sato* et al.*, 1995).*

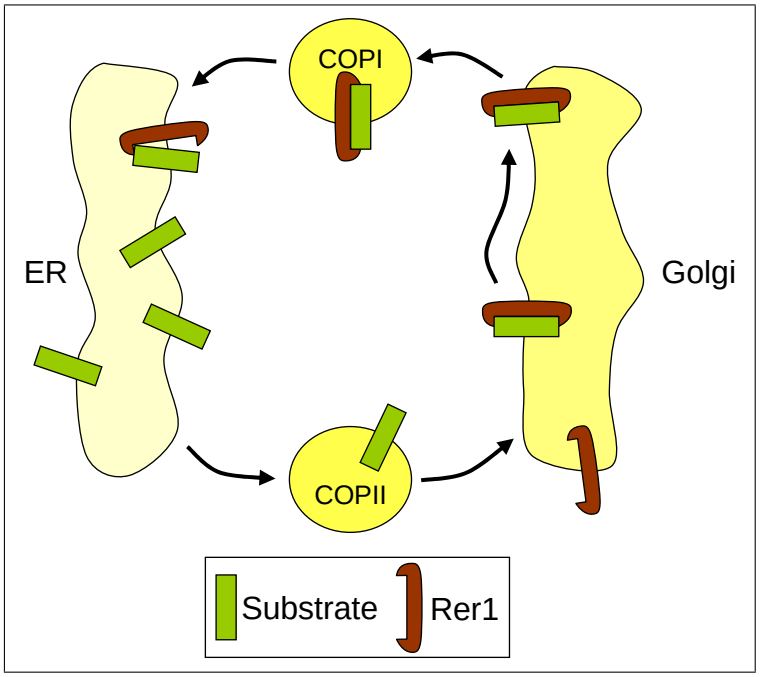

Figure 1.9: *Rer1 is a retrieval receptor for mislocalised ER proteins. Rer1 recognises a signal in a TMD of an escaped (mislocalised) ER protein (substrate of Rer1). After binding to its substrate the Rer1-substrate complex is sorted into COPI vesicles and transported to the ER where the substrate is released. Subsequently, Rer1 cycles back to the cis-Golgi via COPII vesicles (not shown here). Alternatively, Rer1 could act as a sorting factor leading its substrate to COPI vesicles without entering the vesicles itself.*

although the steady state shows localisation to the cis-Golgi (Boehm *et al.*, 1997; Sato *et al.*, 1995, 2001). Rer1p binds to COPI subunits via a dilysine-like motif in its C-terminus perfectly matching to its dynamical localisation (Sato *et al.*, 2001).

Robust evidence exists that Rer1p mediates the localisation of target proteins to the ER via an interaction with the TMDs of target proteins. Although no clear consensus sequence for Rer1p binding was identified, the presence of polar residues in the hydrophobic context of a TMD is a common feature of all Rer1p substrates. The identified substrates of Rer1p exhibit different types of membrane topology and can also be subunits of multimeric complexes (Sato *et al.*, 1996, 1997, 2001, 2003, 2004). The steady-state localisation and the cycling between the ER and

the Golgi suggests that it functions very similar to the well studied KDEL receptor (HDEL in yeast)(Pelham, 1996)(figure 1.9). Thus, the localisation of proteins to the ER by Rer1p is more by retrieval than by retention, although both terms are used synonymously in this study. On the other hand, it is also possible that Rer1p acts as a sorting factor in the Golgi. In this case Rer1p would not enter COPI vesicles in a complex with its substrate. However, both proposed models are hard to distinguish (Boehm *et al.*, 1997).

Rer1p is highly conserved from yeast to human and the human homolog Rer1 complements Rer1p deficient yeast strains (Fullekrug *et al.*, 1997). Human Rer1 has 196 amino acids and shares 64 % similarity (44 % identity) with Rer1p. Unlike yeast Rer1p, the mammalian homolog Rer1 shows co-localisation with ERGIC-53, indicating its presence in the ERGIC besides its localisation in the Golgi. In mammalians only the γ-secretase subunits Nct (Spasic *et al.*, 2007) and Pen2 (this study) were described to be Rer1 substrates. Nevertheless, a search for proteins carrying polar residues in their TMDs in the TMbase database (`ftp://ftp.ncbi.nih.gov/repository/TMbase/`) revealed a bulk of potential Rer1 substrates in mammals (Christoph Kaether, unpublished data).

1.5 Assembly of the γ-secretase

The spatial and temporal aspects of γ-secretase assembly were intensively studied in the recent years. The major findings are: (1) Stable knock down of Nct causes reduced levels of PS (Edbauer *et al.*, 2002), Aph-1 (Capell *et al.*, 2003) and Pen2 (Steiner *et al.*, 2002). Furthermore, Nct forms a stable interaction with Aph-1 also in the absence of PS and Pen2 (Shirotani *et al.*, 2004a). (2) Aph-1 overexpression stabilises the PS holoprotein (Takasugi *et al.*, 2003) and Aph-1 directly interacts with PS and Nct (Lee *et al.*, 2002; Gu *et al.*, 2003). (3) $PS1^{-/-}/PS2^{-/-}$ double knock out MEFs (PSDKO cells) show dramatically reduced levels of Pen2 while the levels of Nct and Aph-1 are only slightly reduced (Steiner *et al.*, 2002; Gu *et al.*, 2003). In PSDKO cells Nct is only present in its immature form due to retention in the ER (Edbauer *et al.*, 2002). (4) Stable knock down of Pen2 results in attenuation of PS endoproteolysis and Nct maturation (Prokop *et al.*, 2004) and Pen2 directly binds to PS (Watanabe *et al.*, 2005; Kim and Sisodia, 2005a). Additionally, triple knock down of Nct, Aph-1 and Pen2 decreases the levels of PS holoprotein to a similar extent as knock down of Nct and Aph-1 alone. This places the function of Pen2 downstream of those of Nct and Aph-1 (Takasugi *et al.*, 2003). (5) Immediately after complex assembly the Nct ectodomain undergoes a conformational change and PS is endoproteolysed (Shirotani *et al.*, 2003; Capell *et al.*, 2005). (6) Chemical crosslinking of γ-secretase subunits reveals close neighbourhood between Pen2 and PS1-NTF, Aph-1 and PS1-CTF, Aph-1 and Nct and of course PS1-NTF and PS1-CTF (Steiner *et al.*, 2008b). (7) γ-secretase is assembled in the ER (Kim *et al.*, 2004; Capell *et al.*, 2005) and the assembled complex exerts its function at the plasma membrane or in the endosomal/lysosomal system (Kaether *et al.*, 2006).

These findings led to a model suggesting a stepwise assembly of γ-secretase. First, Aph-1 and Nct form an initial scaffold in the ER membrane. Subsequently,

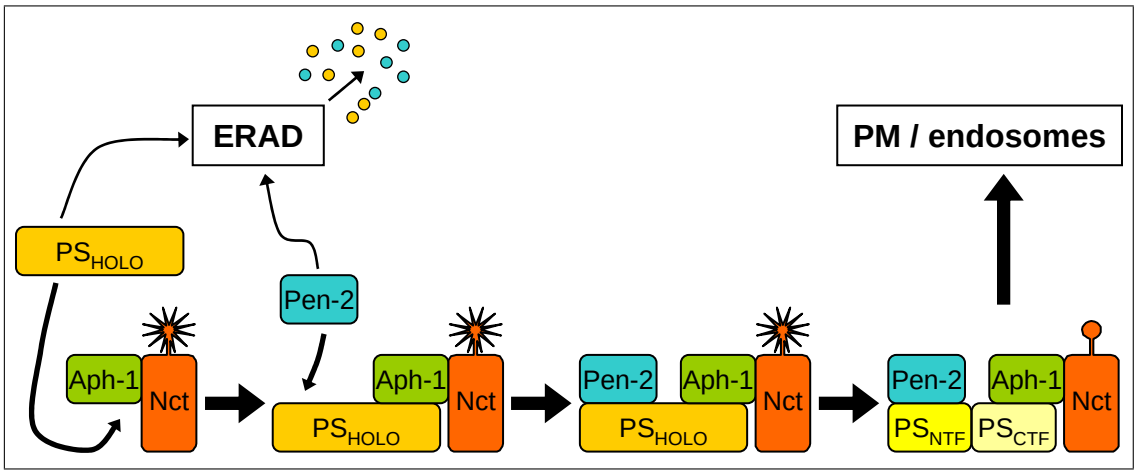

Figure 1.10: *γ-secretase assembles in a stepwise manner. Nct and Aph-1 form an ER-localised scaffold that recruits PS. Pen2 binds to the trimeric complex via an interaction with the PS-TMD4. Unassembled complex subunits can be degraded via ERAD. Once the quaternary complex has formed, PS undergoes endoproteolytic cleavage, the Nct ectodomain folds into a compact trypsin-resistent conformation and the complex is transported to the plasma membrane.*

PS binds to this scaffold and is thereby stabilised. Last, Pen2 is incorporated into the complex resulting in endoproteolytic cleavage of PS and structural changes in the Nct ectodomain (reviewed in Dries and Yu, 2008)(see figure 1.10).

Kaether *et al.*, 2004 proposed a hypothetical model for the quality control of γ-secretase assembly that adopts ER quality control mechanisms known from ion channels and cell surface receptors. In this model ER retention signals on each γ-secretase subunit assure ER localisation of the isolated subunits and assembly intermediates. The non-assembled subunits might be degraded by ERAD as it was shown for Pen2 (Bergman *et al.*, 2004a). Supporting this model, ER retention signals were identified in the PS1 C-terminus (PS1-TMD9)(Kaether *et al.*, 2004), Nct-TMD (Spasic *et al.*, 2007) and Pen2-TMD1 and PS1-TMD4 (this study). The proposed model implies that upon complex assembly all ER retention signals are inactivated and the ER export is permitted.

1.6 Aims of this work

This work focused on quality control mechanisms acting in the course of the assembly of the γ-secretase complex. In particular, additional evidence should be provided supporting the hypothesis suggested by Kaether *et al.*, 2004, who proposed ER retention signals as a checkpoint in the ER quality control of γ-secretase. Specifically, the following aims were addressed:

(a) Identification of novel ER retention signals
In a first step novel ER retention signals should be identified on different γ-secretase subunits. The identified signals should be intensively characterised and their relevance for the full-length protein had to be tested. This work concentrated on signals within the TMDs of γ-secretase.

(b) Identification of the machinery involved in TMD-based retention
Since only little knowledge existed on the mechanisms contributing to TMD-based ER retention, these mechanisms should be intensively studied. A potential candidate protein involved in ER retention in yeast was Rer1.

(c) Analysis of processes leading to the masking of ER retention signals
ER retention signals that are involved in the ER quality control of complex assembly need to be inactivated after correct assembly to allow ER export of the complex. Thus, mechanisms resulting in the masking of ER retention signals in γ-secretase should be identified.

2 Material and methods

2.1 Cell culture

2.1.1 Cell lines

The eucaryotic cell lines used to express proteins are listed in table 2.1.

Table 2.1: *Cell lines used*

cell line	specifications	reference/source
HEK-293	Ad5 transformed human embryonic kidney cells	ATCC-number CRL-1573
HeLa Kyoto	strongly adherent HeLa isolate	gift by R. Pepperkok (EMBL, Heidelberg)
Swe	HEK-293 cells, stably expressing APP with the Swedish double mutation	Citron *et al.*, 1992
CHO	Chinese hamster ovary cell line	gift by B. Schwappach (Manchester, UK)

2.1.2 Culture conditions

All cells were cultured under standard conditions (37 ℃, 5 % CO2, 90 % humidity). Cell culture work was performed under sterile conditions using a sterile laminar flow box. Cell lines were cultured in DMEM medium (Gibco, #61965) supplemented with 1 % Penicillin/Streptomycin (PAA, #P11-010) and 10 % FCS (Invitrogen, #10270). Every 3-4 days cells were detached from cell culture dish (BD Falcon) with 0.05 % Trypsin/EDTA-solution (Invitrogen, #25300) and split in appropriate ratios.

2.1.3 Transfection

To transfect cells with Plasmid-DNA Lipofectamine 2000 (Invitrogen, #11668) and Turbofect (Fermentas, #R0531) were used. Transfections were carried out strictly according to the manufacturers protocol, yet the amount of used DNA was varied within the range supposed by the manufacturer. Lipofectamine 2000 was used according to the manufacturers protocol for transfecting cells with siRNA, but the amount of used siRNA was increased to 250 pmol per well on a 6-well plate. For bigger or smaller culture vessels, transfections were scaled up or down appropriately. To generate stable cell lines cells were split to 1:20, 1:50, 1:100 and 1:250 the day after the transfection. 12 hours later the respective antibiotic (see table 2.2) was added and selection was performed over approximately 3 weeks. Subsequently, either clones were picked and expanded or a cell pool was generated.

Table 2.2: *Antibiotics used for selection of stable cell lines*

antibiotic	final concentration	supplier
Zeocin™	200 μg/ml	Invitrogen, #R250
Geneticin®	250 μg/ml	PAA, #P27-011
Hygromycin B	100 μg/ml	PAA, #P02-011

2.2 Plasmids

To express proteins in eucaryotic cells several DNA plasmid vectors were constructed. The used constructs are listed in table 2.4. Detailed maps and construction descriptions can be found in the appendix (A.1) for the constructs that were described here for the first time. Details for the used vectors are listed in table 2.3.

Table 2.3: *Vectors used for eucaryotic protein expression*

name	resistances	supplier
pcDNA™3.1/Hygro(+)	Hygromycin B, Ampicillin	Invitrogen, #V87020
pcDNA™3.1/Zeo(+)	Zeocin, Ampicillin	Invitrogen, #V86020
pcDNA™4/myc-His	Zeocin, Ampicillin	Invitrogen, #V86320
pcDNA™6/V5-His	Blasticidin, Ampicillin	Invitrogen #V22020
pCMV-myc	Ampicillin	Clontech #631604
pmaxGFP	Kanamycin	AMAXA
pSuper	Ampicillin	Oligoengine #VEC-PBS-0001

Table 2.4: *List of DNA constructs used for eukaryotic protein expression.*

expressed construct	vector	reference/source
CD4	pcDNA™3.1/Hygro(+)	Christoph Kaether
CD4-Pen2$_{TMD1}$	pcDNA™3.1/Hygro(+)	Christoph Kaether (Kaether *et al.*, 2007)
CD4-RXR	pcDNA™3.1/Hygro(+)	Lily E. Jan (Zerangue *et al.*, 1999)
CD4-PS1$_{TMD4}$	pcDNA™3.1/Zeo(+)	Appendix A.1
CD4-PS1$_{TMD4mut}$	pcDNA™3.1/Zeo(+)	Appendix A.1
CD4-Pen2$_{TMD1}$-EGFP	pcDNA™3.1/Hygro(+)	Appendix A.1
CD4-PS1$_{TMD4}$-myc	pcDNA™4/myc-His	Michael Zocher (Fassler *et al.*, 2009)
CD4-RXR-myc	pcDNA™4/myc-His	Michael Zocher (Fassler *et al.*, 2009)
Tac	pcDNA™3.1/Zeo(+)	Christina Valkova (Fassler *et al.*, 2009)
Tac-PS1$_{TMD4}$	pcDNA™3.1/Zeo(+)	Appendix A.1
Tac-RXR	pcDNA™3.1/Zeo(+)	Appendix A.1
PE	pcDNA™3.1/Zeo(+)	Christoph Kaether (Kaether *et al.*, 2002)
PE$_{-PALP}$	pcDNA™3.1/Zeo(+)	Christoph Kaether (Kaether *et al.*, 2004)
PE$_{-WNF}$	pcDNA™3.1/Zeo(+)	Appendix A.1
PE$_{-PALP-WNF}$	pcDNA™3.1/Zeo(+)	Appendix A.1
PE Δ7	pcDNA™3.1/Zeo(+)	Christoph Kaether (Kaether *et al.*, 2004)
PE Δ7$_{-PALP}$	pcDNA™3.1/Zeo(+)	Christoph Kaether (Kaether *et al.*, 2004)
PE Δ7$_{-WNF}$	pcDNA™3.1/Zeo(+)	Appendix A.1
PE Δ7$_{-PALP-WNF}$	pcDNA™3.1/Zeo(+)	Appendix A.1
Rer1-V5	pcDNA™6/V5-His	Christoph Kaether (Kaether *et al.*, 2007)
mycPen2	pCMV-myc	Christoph Kaether (Kaether *et al.*, 2007)
Pen2-shRNA	pSuper	(Prokop *et al.*, 2004)
NotchΔE-EGFP	pcDNA™3.1/Hygro(+)	Kerstin Hünniger, Raphael Kopan (Schroeter *et al.*, 1998)

Briefly, the needed DNA fragments were amplified by PCR with appropriate primers using standard protocols. PCR fragments were purified from agarose gel using the NucleoSpin®Extract II kit (Macherey-Nagel, #740609) and were cloned into pCR®2.1-TOPO®using TOPO-TA cloning®kit (Invitrogen, #K4500). Clones with inserted PCR fragment were identified by the absence of β-Galactosidase activity and plasmids were isolated using the NucleoSpin®Plasmid kit (Macherey-Nagel, #740588). DNA fragments were excised from pCR®2.1-TOPO®using respective enzymes, purified by agarose gel electrophoresis and ligated into the required destination vector.

2.3 Protein biochemical methods

2.3.1 Preparation of cell pellets

The desired cells were placed on ice and the culture medium was aspirated. Afterwards, cells were washed once with ice cold PBS, 1 ml cold PBS was added and cells were scraped off. The cell suspension was transferred to a microcentrifuge tube and centrifuged for 10 minutes at 2,000 g at 4 ℃. The supernatant was discarded and the cell pellet was frozen at -80 ℃.

2.3.2 Cell lysis

Cell pellets were dissolved in an appropriate volume of STEN lysis buffer (50 mM Tris-HCl pH 7.6, 150 mM NaCl, 2 mM EDTA, 1 % NP-40) or CHAPSO lysis buffer (150 mM Citrate buffer pH 6.4, 2 % CHAPSO), supplemented with 1:500 protease inhibitor cocktail (SIGMA, #P8340). Samples were incubated for 30 min on ice and during that time vortexed regularly. Subsequently, samples were centrifuged 15 minutes at 16,000 g and 4 ℃ and the supernatant (lysate) was transferred to a fresh tube.

2.3.3 Immunoprecipitation

Protein concentration of STEN lysates was measured using the BCA assay kit (Pierce, # 23225) and an equal protein mass was used in every IP sample. Samples were titrated to equal volumes and preincubated with 30 μl slurry of Protein A Sepharose (PAS) (Sigma, #P3391) or Protein G Sepharose (PGS) (GE Healthcare, #17-0618-01) for 1 hour at 4 ℃ on a rotor rod. For rabbit and mouse IgG, PAS and PGS was used, respectively. Preincubated lysates were recovered by centrifugation for 3 minutes at 10,000 g and 0.5 μg of the IP antibody (see 2.5 for used antibodies) was added to each sample. Lysates were incubated for 1 hour at 4 ℃ and afterwards another 30 μl of PAS or PGS were added and the IP was incubated over night. The next day, samples were washed once with 500 μl of STEN-NaCl (STEN + 175 mM NaCl), STEN-SDS (STEN + 0.1 % SDS) and STEN (50 mM Tris-HCl pH 7.6, 150 mM NaCl, 2 mM EDTA, 0.2 % NP-40), respectively. To elute the

immunoprecipitated protein, beads were heated to 65 ℃ for 10 min with 20 μl 2×Laemmli sample buffer.

Table 2.5: *Antibodies used in (co-)immunoprecipitations.*

antibody	origin
mouse monoclonal anti-hCD4	DIATEC (EDU-2)
rabbit polyclonal anti-GFP	Invitrogen (A11122)
mouse monoclonal anti-myc	Santa Cruz (9E10)
mouse monoclonal anti-V5	Invitrogen (R960-25)

2.3.4 Co-immunoprecipitation

The protocol is identical to normal immunoprecipitations, but CHAPSO lysates were used and different wash steps were applied. Beads were washed twice with 0.5 % CHAPSO in 150 mM Citrate buffer pH 6.4 and once with 150 mM Citrate buffer pH 6.4. The used antibodies are listed in table 2.5

2.3.5 Deglycosylation assay

To assess the subcellular localisation of different CD4 reporter species, the resistance to Endoglycosidase H (EndoH) was utilised. Immunoprecipitated CD4 protein was eluted from PGS with 35 μl of deglycosylation elution buffer (100 mM Tris-HCl pH 7.6, 10 mM DTT, 1 % SDS) by boiling 5 minutes at 95 ℃. Of each IP sample 3×10 μl were recovered from the beads and divided into 3 tubes. These 3 samples were subject to 3 different treatments (nt, H, N). The nt (non-treated) sample was directly boiled with 2.5 μl of 5×Laemmli sample buffer and stored at 4 ℃ over night. The samples H and F were subjected to deglycosylation with EndoH or N-glycosidase F, respectively, as it is described in table 2.6. Treatment with N-glycosidase F leads to a complete removal of N-glycosylations, whereas treatment with EndoH removes only glycosylations that have not been processed in later Golgi compartments. Deglycosylation was performed over night at 37 ℃ and the samples were TCA-precipitated the next day. The protein pellets were dissolved in 12.5 μl 1×Laemmli sample buffer (50 mM Tris-HCl pH 6.8, 2 % SDS, 6 % glycerol, 2.5 % β-mercaptoethanol) and boiled 5 minutes at 95 ℃. Connected PAGE samples were loaded in the order nt→H→F onto a 10 % SDS-PAGE gel and a Western blot against CD4 was performed as described in 2.3.6.

2.3.6 Western blot

After cell lysis (see 2.3.2) and measurement of protein concentration (see 2.3.3) equal amounts of protein were boiled with 5× Laemmli sample buffer. For blots against γ-secretase subunits and Rer1, samples were heated to 65 ℃ for 10 minutes

Table 2.6: *Reaction mix for EndoH and NGF treatments. EndoH and G5 reaction buffer were from NEB (#P0702L). NGF buffer is 100 mM phosphate buffer pH 8.0, 25 mM EDTA, 0.1 % Triton-X-100, 0.2 % SDS, 0.1 % β-Mercaptoethanol and NGF was obtained from Roche (#11365185001).*

H		F	
10 μl	IP eluate	10 μl	IP eluate
10 μl	G5 reaction buffer	88 μl	NGF buffer
79 μl	ddH_2O	2 μl	NGF
1 μl	EndoH		

to avoid protein aggregation. For all other blots samples were heated to 95 ℃ for 5 minutes. SDS-PAGE was performed using standard protocols (Sambrook and Russell, 2001) and acrylamide concentrations between 6 % and 14 %. In some cases pre-cast NovexR 10-20 % Tricine gels (Invitrogen, #EC66252 Box) were used. By tank blotting proteins were transferred onto a PVDF membrane (Immobilon-P, Millipore). Subsequently, the membrane was blocked for 1 hour with I-Block (Applied Biosystems, #T2015), cut at appropriate positions if needed and incubated with primary antibody over night at 4 ℃. Wash steps were performed according to standard protocols (Sambrook and Russell, 2001) and the membrane was incubated with secondary antibody for 1 hour at room temperature. The blot was developed using freshly mixed ECL solution (4 ml solution A (100 mM Tris-HCl pH 8.6, 0.025 % (w/v) Luminol), 400 μl solution B (0.11 % (w/v) para-Coumaric acid in DMSO), 1.2 μl 35 % H_2O_2) and a FUJI Super RX X-ray film. To detect another protein on the same membrane, the membrane was stripped for 30 minutes at 50 ℃ with Strip buffer (62.5 mM Tris-HCl pH 6.8, 2 % (w/v) SDS, 100 mM β-Mercaptoethanol). All used antibodies are listed in table 2.7.

2.4 Immunocytochemistry

Cells were seeded onto cover slips, which were coated with 0.05 mg/ml poly-L-lysine in case HEK-293 cells were used for immunocytochemistry. Cells were fixed with 4 % Paraformaldehyde for 20 minutes and quenched with 50 mM NH_4Cl for 10 minutes. To permeabilise the cells, cover slips were incubated in 0.2 % Triton-X-100 for 2 minutes. Unspecific signals were blocked with blockmedium (2 % FCS, 2 % BSA, 0.2 % fish gelatine in PBS pH 7.4) for 10 minutes. Primary and secondary antibodies were diluted in blockmedium as described in table 2.8. and the cells were incubated with the respective antibody solution for 20 minutes each. Nuclei were stained with 1 μg/ml DAPI for 5 minutes. In the end, cover slips were mounted onto a microscope slide with MOWIOL mounting medium and dried at room temperature over night. All solutions were prepared in PBS pH 7.4 and all steps were performed at room temperature. Incubations were performed in a humified, dark chamber.
Optionally, a surface antigen stain was performed prior to fixation. To this end,

Table 2.7: *Primary and secondary (HRP-coupled) antibodies used for Western blot.*

antibody	origin	dilution
mouse monoclonal anti-myc	Santa Cruz (9E10)	1:1,000
mouse monoclonal anti-GFP	Clontech (JL-8)	1:1,000
rabbit polyclonal anti-βActin	Abcam (ab8227)	1:10,000
rabbit polyclonal anti-hRer1	Kaether *et al.*, 2007 (1120)	1:750
rabbit polyclonal anti-hCD4	Santa Cruz (H-370)	1:1,000
rabbit polyclonal anti-Nct	SIGMA (N1660)	1:2,000
rabbit polyclonal anti-GFP	Invitrogen (A11122)	1:1,000
rabbit polyclonal anti-cleaved Notch1	Cell Signaling (Val1744)	1:1,000
rabbit polyclonal anti-βAPP-CT	Steiner *et al.*, 2000 (6687)	1:300
rabbit polyclonal anti-Pen2	Steiner *et al.*, 2002 (1638)	1:200
rabbit polyclonal anti-PS-NTF	Walter *et al.*, 1997 (2953)	1:500
goat polyclonal anti-rabbit IgG (H+L), HRP conjugate	Promega (W4011)	1:5,000
goat polyclonal anti-mouse IgG (H+L), HRP conjugate	Promega (W4021)	1:5,000

cover slips were initially incubated with the primary antibody diluted in cold PBS + 1 mM $CaCl_2$ + 0.5 mM $MgCl_2$ for 20 minutes on ice. Subsequently, cells were fixed with 4 % Paraformaldehyde and processed further as described before.

2.4.1 Quantification of immunocytochemistry

To obtain quantitative results for the localisation of CD4-Pen2$_{TMD1}$-EGFP the CELLOMICS ArrayScan HCS Reader was used, providing a combination of automated microscopy and image analysis software. To this end, HeLa Kyoto CD4-Pen2$_{TMD1}$-EGFP cells were seeded into 96-well plates and transfected with siRNA as described before. After 72 hours 96-well plates were placed on ice, and stained for surface CD4 antigen with anti-mouse IgG Alexa Fluor®555 as secondary antibody. Additionally, cell nuclei were stained with DAPI. Images were acquired with a 10×objective and analysed online by the software. Image acquisition was stopped after the identification of 100 valid objects, which were characterised by a normal nuclear shape (e.g. exclusion of mitotic cells) and a moderate expression of the reporter protein. To obtain quantitative data a region of interest was generated by expanding the nucleus by 7 pixels in all directions. Within the resulting ellipse the average intensities of EGFP signal (representing total reporter protein) and Alexa Fluor®555 signal (representing surface reporter protein) were measured and the ratio was calculated as the ultimate score of the assay.

Table 2.8: *Primary and secondary (fluorophore-coupled) antibodies used for Immunocytochemistry.*

antibody	origin	dilution
mouse monoclonal anti-myc	Santa Cruz (9E10)	1:500
mouse monoclonal anti-CD4	DIATEC (EDU-2)	1:500
mouse monoclonal anti-Calnexin	Chemicon (MAB3126)	1:500
rabbit polyclonal anti-GFP	Invitrogen (A11122)	1:500
rabbit polyclonal anti-Calnexin	Abcam (ab13504)	1:200
rat monoclonal anti-mTac	Jörg Stirnweiss (FSU Jena) (PC61.73)	1:500
goat polyclonal anti-BiP	Santa Cruz (aC-19)	1:80
Alexa Fluor®488 goat polyclonal, highly cross-adsorbed, anti-rabbit IgG (H+L)	Invitrogen (A-11034)	1:500
Alexa Fluor®488 goat polyclonal, highly cross-adsorbed, anti-mouse IgG (H+L)	Invitrogen (A-11029)	1:500
Alexa Fluor®555 goat polyclonal, highly cross-adsorbed, anti-rabbit IgG (H+L)	Invitrogen (A-21429)	1:500
Alexa Fluor®555 goat polyclonal, highly cross-adsorbed, anti-mouse IgG (H+L)	Invitrogen (A-21424)	1:500
Alexa Fluor®555 goat polyclonal anti-rat IgG (H+L)	Invitrogen (A-21434)	1:500
Alexa Fluor®660 goat polyclonal anti-mouse IgG (H+L)	Invitrogen (A-21054)	1:500
Alexa Fluor®488 donkey polyclonal anti-goat IgG (H+L)	Invitrogen (A-21054)	1:500

2.5 FACS analysis

To quantify the surface localisation of CD4 reporter proteins FACS analysis was utilised. To this end, cells were harvested using a sterile EDTA solution (2 mM EDTA, 1 % BSA in PBS) and 2 ×200,000 cells were used per sample. Per sample one set of cells was stained for surface antigens only, while the other set was stained for surface and intracellular CD4 antigens. Cells were washed with FACS buffer (2 % FBS in PBS) prior to the first staining step. Anti-hCD4-APC (Allophycocyanin)(Miltenyi, #130-091-232) was diluted 1:10 in FACS buffer and cells were stained with 25 μl antibody solution for 20 minutes on ice in the dark. After washing twice with FACS buffer, cells were fixed and permeabilised using the BD Cytofix/Cytoperm™Fixation/Permeabilization Solution Kit (BD Biosciences Pharmingen, #554714). Thereafter, internal CD4 antigens were stained in the totally stained sample set with 25 μl of 1:10 diluted anti-hCD4-APC for 20 minutes. Finally, specimens were washed twice with FACS buffer. Additionally, intracellular

myc antigens were stained for the FACS-based masking assay to allow gating on double transfected cells. To this end, cells were stained with 25 μl 1:250 rabbit polyclonal anti-myc (Santa Cruz, A-14) and 1:250 R-PE (R-Phycoerythrin) goat polyclonal anti-rabbit IgG (H+L) (Invitrogen, P-2771MP) for 20 minutes each. Specimen were measured on a BD FACSCalibur™or BD FACSCanto™II Flow Cytometer and the obtained data were evaluated with the FlowJo software (version 5.4.3). The geometric mean of the APC fluorescence intensity of approximately 10,000 cells was used to calculate the percentage of surface CD4 antigen.

2.6 Statistical analysis

Statistical analysis was done using the R software package (R Development Core Team, 2009). To test for a true difference of means, Welch Two Sample t-test was applied via the function t.test() of R. A p-value < 0.05 was considered significant and indicated with $*$ and a p-value < 0.01 was considered highly significant and indicated with $**$.

3 Results

3.1 Pen2-TMD1 contains an ER retention signal

It has been described by Bergman *et al.*, 2004a that γ-secretase subunit Pen2 is localised to the ER in PS1$^{-/-}$/PS2$^{-/-}$-MEF cells (PSDKO cells), which lack a γ-secretase complex. Additionally, this finding was confirmed by our lab using N-terminally EGFP-tagged Pen2 (Kaether *et al.*, 2007). Thus, the unassembled Pen2 must be retained in the ER via intrinsic retention signals. Such signals could be localised either in its cytoplasmic loop (Zerangue *et al.*, 1999) or its TMDs, as it was shown for a other proteins (Zerangue *et al.*, 1999; Bonifacino *et al.*, 1991).

To narrow down ER retention signals in Pen2, a series of CD4 reporter proteins were constructed. Cluster of differentiation 4 (CD4) is a type I transmembrane glycoprotein, with its N-terminus in the ER lumen and the C-terminus in the cytosol. It is rapidly transported to the plasma membrane after synthesis and becomes N-glycosylated at two positions of the lumenal part (Asn296, Asn325; figure 3.1A) during the transport through the secretory pathway. It has been used previously as a reporter protein to identify ER retention signals (Nilsson *et al.*, 1989; Zerangue *et al.*, 2001; Kaether *et al.*, 2004). Previous work in our lab by Johanna Scheuermann suggested that Pen2-TMD1 conferred ER localisation to CD4 when being swapped with the CD4-TMD. The first goal of the thesis presented was to verify and extend these findings.

3.1.1 Pen2-TMD1 confers ER retention to a CD4 reporter protein

The used CD4 reporter proteins CD4, CD4-Pen2$_{TMD1}$ and CD4-RXR are depicted in figure 3.1A,B. In CD4-Pen2$_{TMD1}$ the CD4-TMD was swapped with the TMD1 of Pen2 plus three lumenal residues (REA), whereas CD4-RXR had the last 36 amino acids of Kir6.2 fused to the cytoplasmic CD4 C-terminus. Thus, the RXR ER retention signal within this 36 amino acids conferred ER retention to the otherwise PM localised CD4 protein (Zerangue *et al.*, 1999). CD4-Pen2$_{TMD1}$ was constructed by Johanna Scheuermann, whereas CD4 and CD4-RXR were a kind gift by Lilly E. Jan (Howard Hughes Medical Institute, San Francisco, USA). The CD4 reporter constructs were transiently transfected into Cos-7 cells and immunocytochemistry with antibodies against CD4 and BiP revealed plasma membrane and

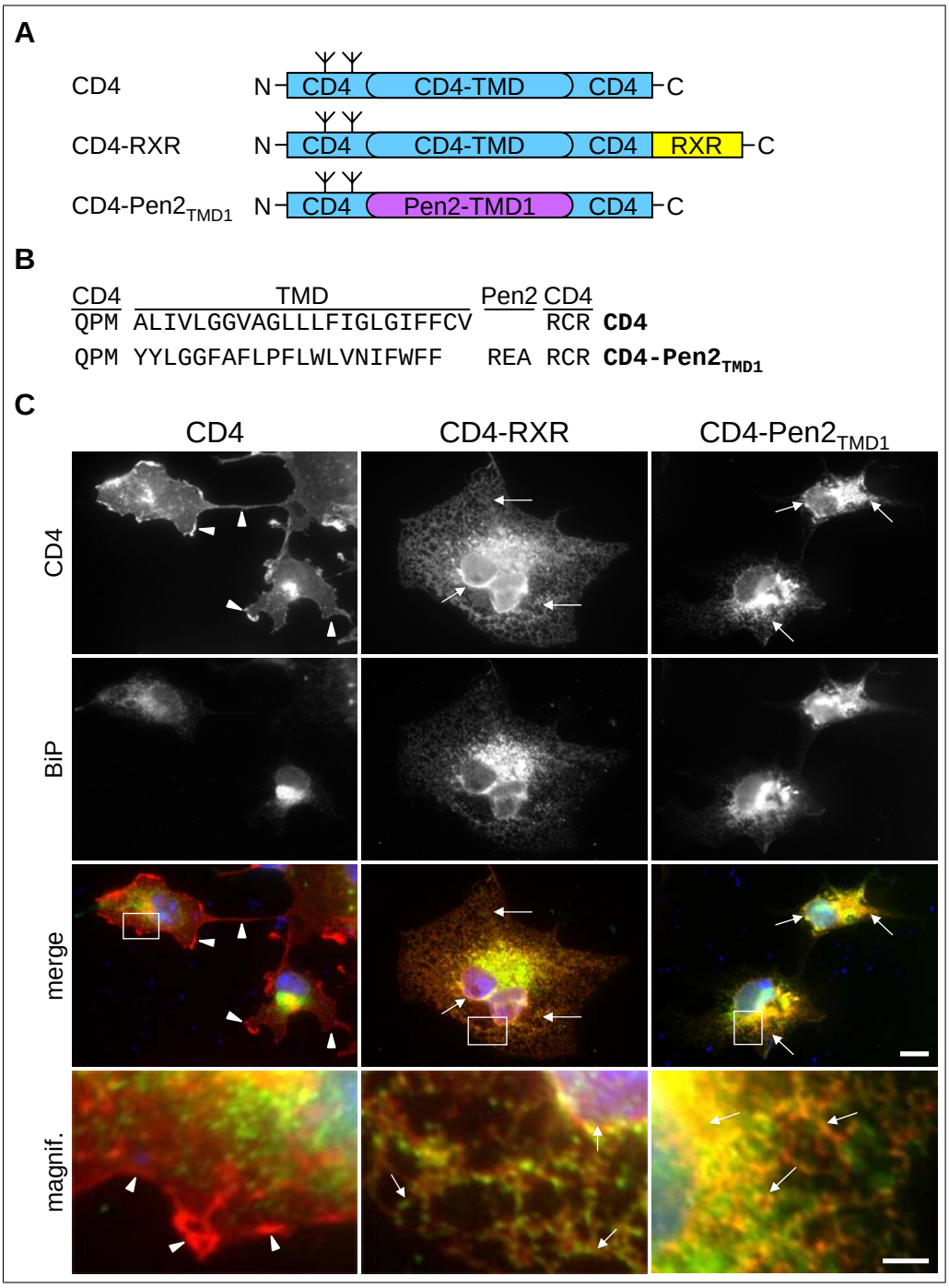

Figure 3.1: *$CD4\text{-}Pen2_{TMD1}$ was retained in the ER in Cos-7 cells. A) Constructed CD4 variants. B) Comparison of the TMD regions of the CD4 constructs. In $CD4\text{-}Pen2_{TMD1}$ the addition of the three following cytoplasmic amino acids REA was necessary to achieve ER retention. C) Cos-7 cells were transiently transfected with different CD4 variants. Cells were subjected to immunofluorescence staining with antibodies against CD4 and the ER marker BiP. Nuclei were stained with DAPI and cells were analysed by fluorescence microscopy. In the merge pictures CD4 was coloured red, BiP green and DAPI blue. Scalebar 10 µm. The lower panel shows magnifications (magnif.) of the boxed areas above. Scalebar 2 µm. Arrowheads, PM localisation; Arrows, ER localisation (nuclear envelope and reticular ER).*

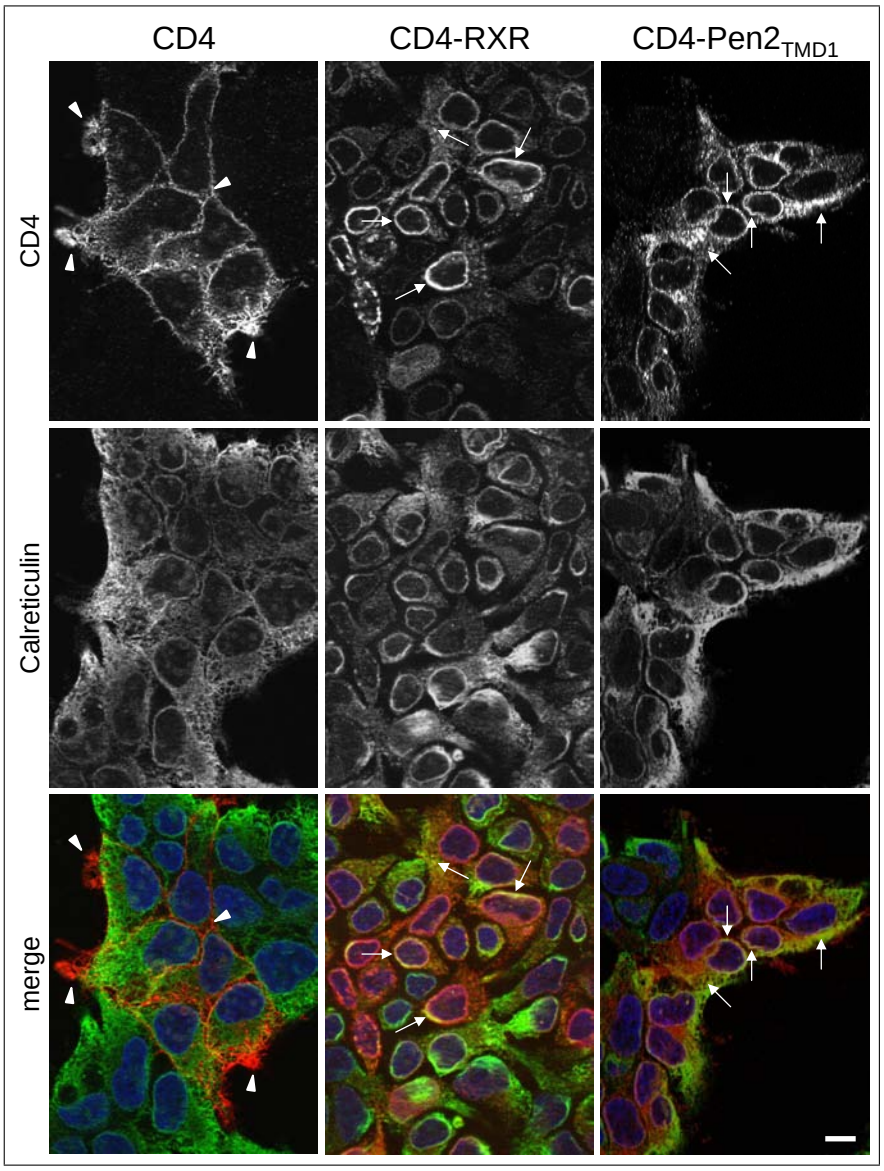

Figure 3.2: *CD4-Pen2$_{TMD1}$ was retained in the ER in Swe cells. Swe cells stably expressing CD4 variants as indicated were subjected to immunofluorescence staining with antibodies against CD4 and the ER marker Calreticulin. Nuclei were stained with DAPI. Pictures show optical sections obtained by fluorescence microscopy with an apotome slider module. In the merge picture CD4 was coloured red, Calreticulin green and DAPI blue. Arrowheads, PM localisation; Arrows, ER localisation (nuclear envelope and reticular ER); Scalebar 10 µm.*

ER localisation for the control constructs CD4 and CD4-RXR, respectively (figure 3.1C, first and second column). CD4-Pen2$_{TMD1}$ was localised to the ER (figure 3.1C, third column), though a few cells showed additional weak plasma membrane staining (data not shown). This indicated the presence of an ER retention signal within the TMD1 of Pen2. Yet, the signal seemed to be weaker than the cytoplasmic RXR signal, where all cells showed exclusively ER staining.

To validate the results obtained in Cos-7 cells, Swe cell lines were generated that stably expressed CD4, CD4-RXR and CD4-Pen2$_{TMD1}$. The Swe cell line was generated from a HEK-293 cells by stably overexpressing the amyloid precursor protein with the Swedish double mutation (APP$_{sw}$). The Swedish double mutation (K595N, M596L) resulted in 6-8-fold increase of Aβ production compared to wild-type APP and it was identified in a hereditary form of AD (Citron *et al.*, 1992). Thus, Swe cells provided the best prerequisites to measure γ-secretase activity in cell-based assays. Since it was initially speculated that overexpression of the Pen2-TMD1 might interfere with the γ-secretase assembly or activity, Swe cells were used here to stably express CD4-Pen2$_{TMD1}$.

The stable cell lines were prepared for immunofluorescence using anti-CD4 and anti-Calreticulin antibodies. Microscopy was carried out on a Zeiss Axio Imager with an ApoTome slider module, allowing confocal-like optical sections through the Swe cells. The control constructs were localised as expected and CD4-Pen2$_{TMD1}$ showed ER localisation (figure 3.2, column 3), confirming the results in the Cos-7 cells (figure 3.1). No additional plasma membrane staining was observed for CD4-Pen2$_{TMD1}$. This could be due to more modest expression in the stably transfected Swe cells.

Next, deglycosylation assay was performed to asses the localisation of the CD4 reporter proteins in the secretory pathway. The oligosaccharides of N-glycosylated proteins are sensitive to cleavage by Endoglycosidase H (EndoH) before they reach medial Golgi cisternae. There, they can be modified by N-acetylglucosamine-transferases and Mannosidases I and II resulting in a resistance against cleavage by EndoH (Dalbey and Heijne, 2002). Hence, ER retention causes EndoH-sensitivity whereas transport to the plasma membrane can result in EndoH-resistance of the oligosaccharides of the CD4 reporter protein. In case of CD4 only one of the two glycosylation sites becomes EndoH-resistant during the maturation of the protein (Nilsson *et al.*, 1989). To perform the assay, CD4 protein was immunoprecipitated from STEN lysates of Swe cells stably expressing the respective CD4 reporter protein. The eluted protein was split into three parts and either left untreated, treated with EndoH or N-glycosidase F (NGF). After the treatment the CD4 protein was precipitated and separated by SDS-PAGE. A Western blot of a deglycosylation assay is shown in Fig-

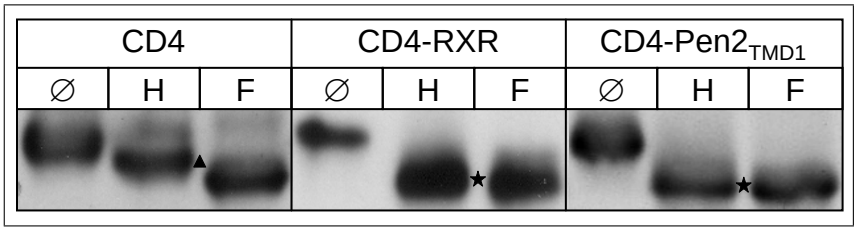

Figure 3.3: *Deglycosylation assay substantiated ER retention of CD4-Pen2$_{TMD1}$. CD4 protein was immunoprecipitated from lysates of Swe cells stably expressing the respective CD4 species. The IP eluates were split into 3 parts and were either left untreated (Ø), treated with Endoglycosidase H (H) or treated with N-glycosidase F (F). The triangle indicates EndoH-resistant species and the star EndoH-sensitive species.*

ure 3.3. A slightly faster mobility was observed even for the PM-localised CD4 after EndoH-treatment, because one glycosylation site stays permanently EndoH sensitive. In contrast, NGF cleaved off all N-glycosylations, yielding the naked protein. Thus, NGF-treated CD4 migrated even faster than EndoH-treated CD4, resulting in the typical stair-like pattern, characteristic for CD4 species that reached later Golgi cisternae (figure 3.3, left lanes). CD4-RXR was EndoH-sensitive. Treatment of CD4-RXR with EndoH or NGF led to equally fast mobilities, showing that CD4-RXR stayed in early compartments of the secretory pathway. The band pattern for CD4-Pen2$_{TMD1}$ was indistinguishable from CD4-RXR clearly demonstrating that CD4-Pen2$_{TMD1}$ was retained in the ER.

3.1.2 FACS-based quantification of ER retention

To asses ER retention in a quantitative manner a FACS-based localisation assay was developed. Briefly, Swe cells stably expressing the respective CD4 reporter protein were stained with an anti-CD4-APC antibody. After the staining of the surface antigens, cells were fixed, permeabilised and each sample was split into two parts. To obtain a sample which has the total CD4 antigens stained, one part was stained a second time with the same anti-CD4-APC antibody to label intracellular CD4 antigens. Subsequently, cells were measured by FACS and single intact cells were gated by size (FSC) and granularity (SSC) in several steps as indicated in figure 3.4. The obtained histogram plots for APC intensities of a representative experiment are shown in the right part of figure 3.4. Although the peaks for totally stained Swe cells stably expressing CD4 and CD4-Pen2$_{TMD1}$ were approximately equal, Swe CD4-Pen2$_{TMD1}$ cells showed much less surface fluorescence than Swe CD4 cells.

The geometric mean of the fluorescence intensities was used to quantify the amount of plasma membrane or total CD4 antigen. As depicted in figure 3.5, in Swe cells 53.8 % of the stably expressed CD4 was at the plasma membrane. In contrast, after the fusion of the cytoplasmic RXR retention signal to CD4 only 4.9 % of this CD4 construct was at the plasma membrane. Swe cells stably expressing CD4-Pen2$_{TMD1}$ have 4.0 % of surface CD4, again confirming a strong intracellular retention of CD4-Pen2$_{TMD1}$.

Taken together, the results confirmed the initial findings of an ER retention signal in the TMD1 of Pen2. The signal could be transferred to a reporter protein and the conferred ER retention was independent of the cell line used. The combination of FACS analysis with a protocol for the staining of intracellular antigens resulted in an assay which allowed quantification of ER retention.

3.1.3 The ER retention signal in Pen2-TMD1 contributes to the stability of Pen2

The first described ER retention signals in TMDs were based on charged residues within the hydrophobic environment of a TMD. These signals intimately coupled the processes of degradation and ER retention (Bonifacino *et al.*, 1990a,b; Letourneur

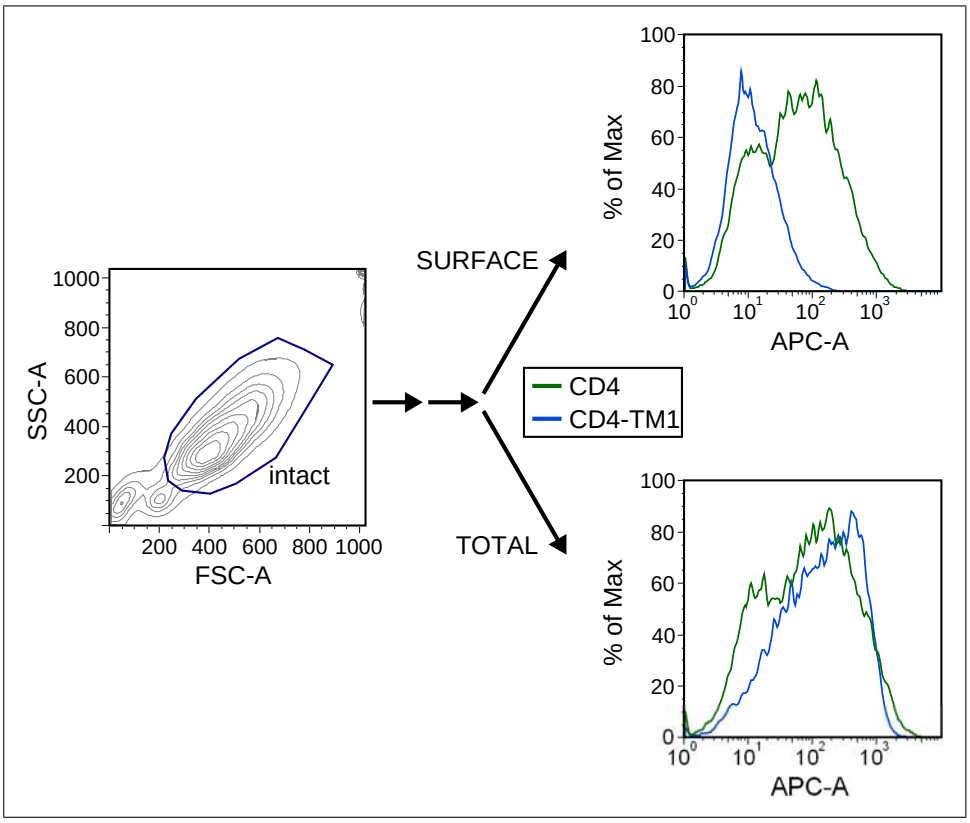

Figure 3.4: *Gating scheme for the FACS analysis of stable Swe cell lines. Swe cell lines stably expressing the respective CD4 species were fixed and stained for either surface or total CD4 antigen. Intact cells were gated via several steps of FSC and SSC gating. The populations used for the measurement of the APC signal are shown in the histogram plots to the right. The percentage of all measured cells that display a distinct fluorescence intensity (% of Max) is plotted against the fluorescence intensity. The APC-A signal reflects the amount of CD4 antigen.*

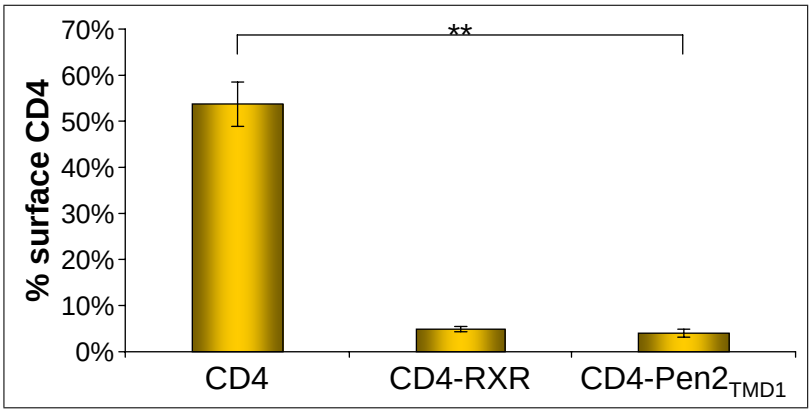

Figure 3.5: *Quantification of surface CD4 antigen confirmed ER retention of CD4-Pen2$_{TMD1}$. Swe cell lines stably expressing the respective CD4 species were either stained for surface CD4 or for total CD4 after permeabilisation. Cells were measured by FACS and the geometric mean of the fluorescence intensities was determined. The ratios of surface CD4 to total CD4 were calculated for the respective CD4 variants. The error bars depict the standard error of n=4-5 experiments.*

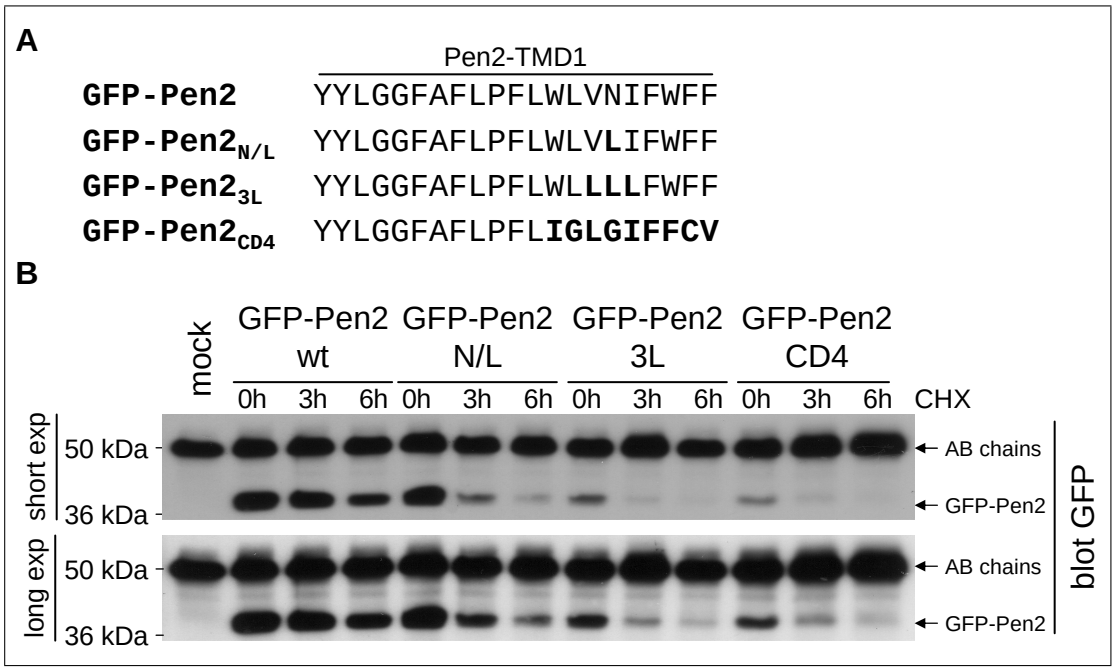

Figure 3.6: *The ER retention signal in Pen2-TMD1 contributed to the stability of Pen2. A) Scheme of the Pen2-TMD1 and the generated mutants in GFP-Pen2 B) PSDKO cells were transiently transfected with GFP-Pen2 variants as indicated or were left untreated (mock). 12 hours later cells were treated with 100 µg/ml cycloheximide (CHX) for the indicated time span. Subsequently, cells were lysed, subjected to immunoprecipitation with a rabbit anti-GFP antibody and the eluates were analysed by Western blot. The figure shows a shorter and a longer exposure of the same blot.*

et al., 1995). Data from our lab revealed that the identified ER retention signal in the Pen2-TMD1 depended on a critical asparagine (Kaether *et al.*, 2007). For this reason, it was tested if a similar mechanism caused the rapid degradation of Pen2 with its polar asparagine in the TMD1.

To this end, N-terminally EGFP-tagged Pen2 was constructed (GFP-Pen2). Data from our lab demonstrated that GFP-Pen2 was fully functional and completely rescued stable Pen2 knock down by shRNA (Johanna Scheuermann, published in Fassler *et al.*, 2009). Subsequently, three different mutations were introduced. The asparagine important for ER retention (GFP-Pen2$_{N/L}$) as well as the asparagine and the two adjacent residues (GFP-Pen2$_{3L}$) were mutated to leucine. Additionally, the 9 most C-terminal amino acids of the Pen2-TMD1 were exchanged with the corresponding sequence from the CD4-TMD (GFP-Pen2$_{CD4}$)(Johanna Scheuermann). The TMDs of all constructs are summarised in figure 3.6A. All constructs were transiently transfected into PSDKO cells. Thus, no interaction with PS could cause a stabilisation or destabilisation of the GFP-Pen2 variants. After 12 hours cells were treated with cycloheximide for different time spans. Subsequently, the stability of the different GFP-Pen2 was analysed by Western blot.

Consistent with earlier findings, GFP-Pen2 was instable and strongly reduced after 6 hours (Bergman *et al.*, 2004a)(figure 3.6B). Nevertheless, wildtype GFP-

Pen2 was more stable than the GFP-Pen2 variants that were lacking the polar asparagine. Thus, the asparagine confers relative stability to wildtype Pen2 when compared with the other GFP-Pen2 mutants. The observed difference in stability was not due to overall misfolding of the protein, since at least GFP-Pen2$_{N/L}$ and GFP-Pen2$_{3L}$ assembled into an active γ-secretase complex in other experiments (Johanna Scheuermann, published in Fassler *et al.*, 2009).

3.2 PS1-TMD4 contains an ER retention signal

In the previous chapter it was shown that the TMD1 of Pen2 harbours an ER retention signal, which depended on a critical asparagine residue (see also Kaether *et al.*, 2007). In a next step, other potential ER retention signals within the γ-secretase complex should be investigated. Two publications by Kim and Sisodia, 2005a and Watanabe *et al.*, 2005 drew the attention to the PS1-TMD4 that was described to contain a binding site for Pen2. This binding site was composed of a ″WNF″ motif. The presence of an asparagine within the PS1-TMD4 raised the question, if this asparagine might also constitute an ER retention signal.

3.2.1 PS1-TMD4 confers ER retention to reporter proteins

Similar to the analysis of the Pen2-TMD1, a CD4 reporter protein was constructed which had its TMD exchanged against the TMD4 of human PS1 (CD4-PS1$_{TMD4}$). Moreover, the WNF motif described in Watanabe *et al.* (2005) was mutated to AAA to assess its contribution to a potential retention signal (CD4-PS1$_{TMD4mut}$). As controls the described CD4 and CD4-RXR constructs were used. All constructs were schematised in figure 3.7A,B.

CD4, CD4-RXR, CD4-PS1$_{TMD4}$ and CD4-PS1$_{TMD4mut}$ were transiently transfected into Cos-7 cells grown on cover slips. Immunocytochemistry with anti-CD4 and anti-BiP antibodies revealed ER localisation for CD4-PS1$_{TMD4}$, as was demonstrated by the colocalisation of CD4 staining with the ER marker BiP (figure 3.7C, third column). The introduction of the WNF→AAA mutation caused partial abrogation of ER retention and a mixed pattern of plasma membrane and ER staining was visible (figure 3.7C, fourth column).

To confirm this results, Swe cell lines stably expressing CD4-PS1$_{TMD4}$ and CD4-PS1$_{TMD4mut}$ were generated. As a control, the described Swe CD4 and Swe CD4-RXR cell lines were used. Cells were grown on cover slips and prepared for immunofluorescence using anti-CD4 and anti-Calreticulin antibodies. Microscopy was carried out on a Zeiss Axio Imager with the ApoTome slider module, allowing confocal-like optical sections through the Swe cells. The ER localisation of CD4-PS1$_{TMD4}$ could be confirmed (figure 3.8, third column) and CD4-PS1$_{TMD4mut}$ showed a mixed distribution between plasma membrane and ER (nuclear envelop) similar to the observations in Cos-7 cells.

Next, deglycosylation assay was performed to obtain further evidence for the ER localisation of CD4-PS1$_{TMD4}$. To this end, lysates of the stable Swe CD4, Swe CD4-RXR, Swe CD4-PS1$_{TMD4}$ and Swe CD4-PS1$_{TMD4mut}$ cell lines were used in the

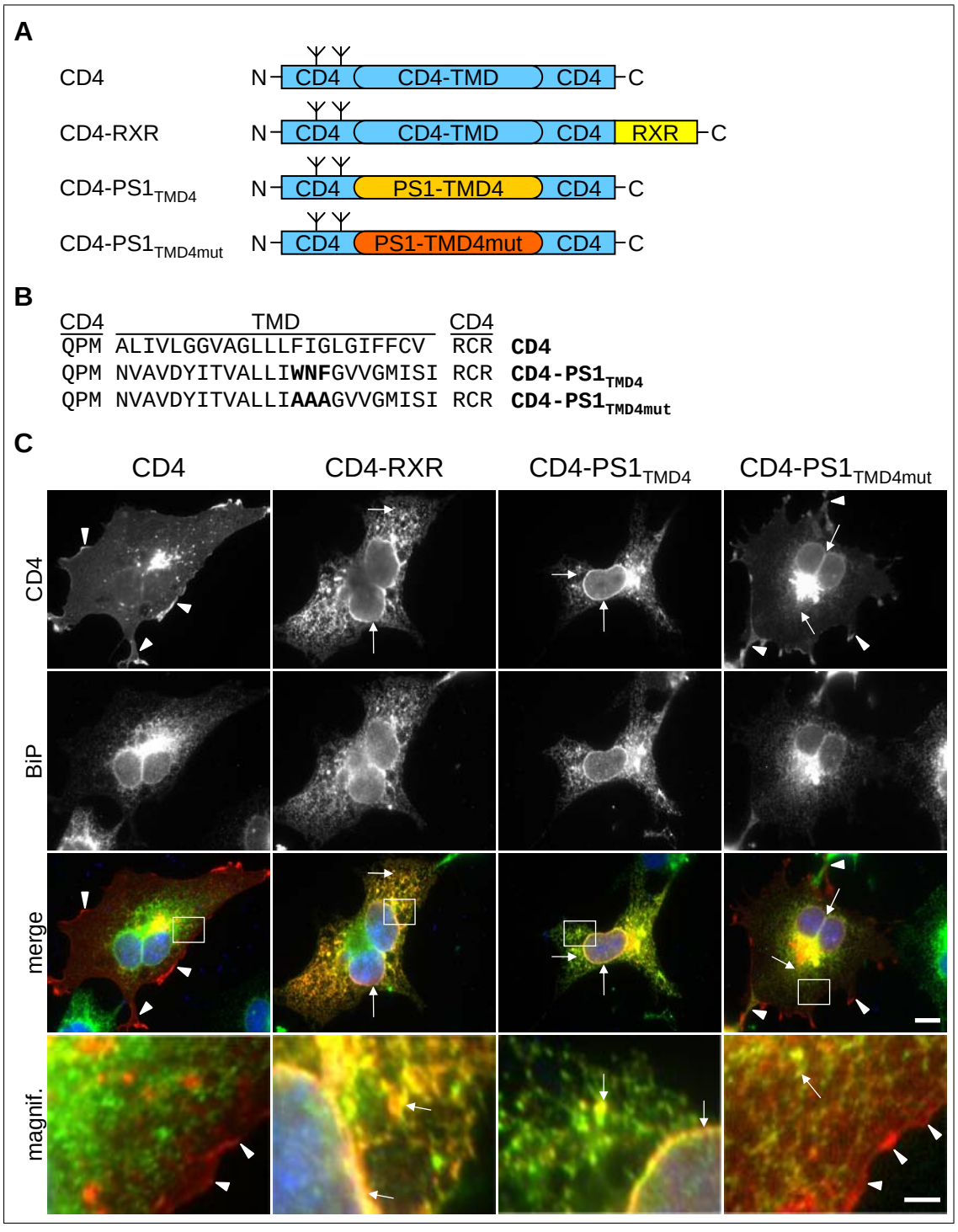

Figure 3.7: *CD4-PS1$_{TMD4}$ was retained in the ER in Cos-7 cells. A) Constructed CD4 variants. B) Comparison of the TMD regions of the CD4 constructs. C) Cos-7 cells were transiently transfected with different CD4 variants. Cells were subjected to immunofluorescence staining with antibodies against CD4 and the ER marker BiP. Nuclei were stained with DAPI and cells were analysed by fluorescence microscopy. In the merge pictures CD4 was coloured red, BiP green and DAPI blue. Scalebar 10 µm. The lower panel shows magnifications (magnif.) of the boxed areas above. Scalebar 2 µm. Arrowheads, PM localisation; Arrows, ER localisation (nuclear envelope and reticular ER).*

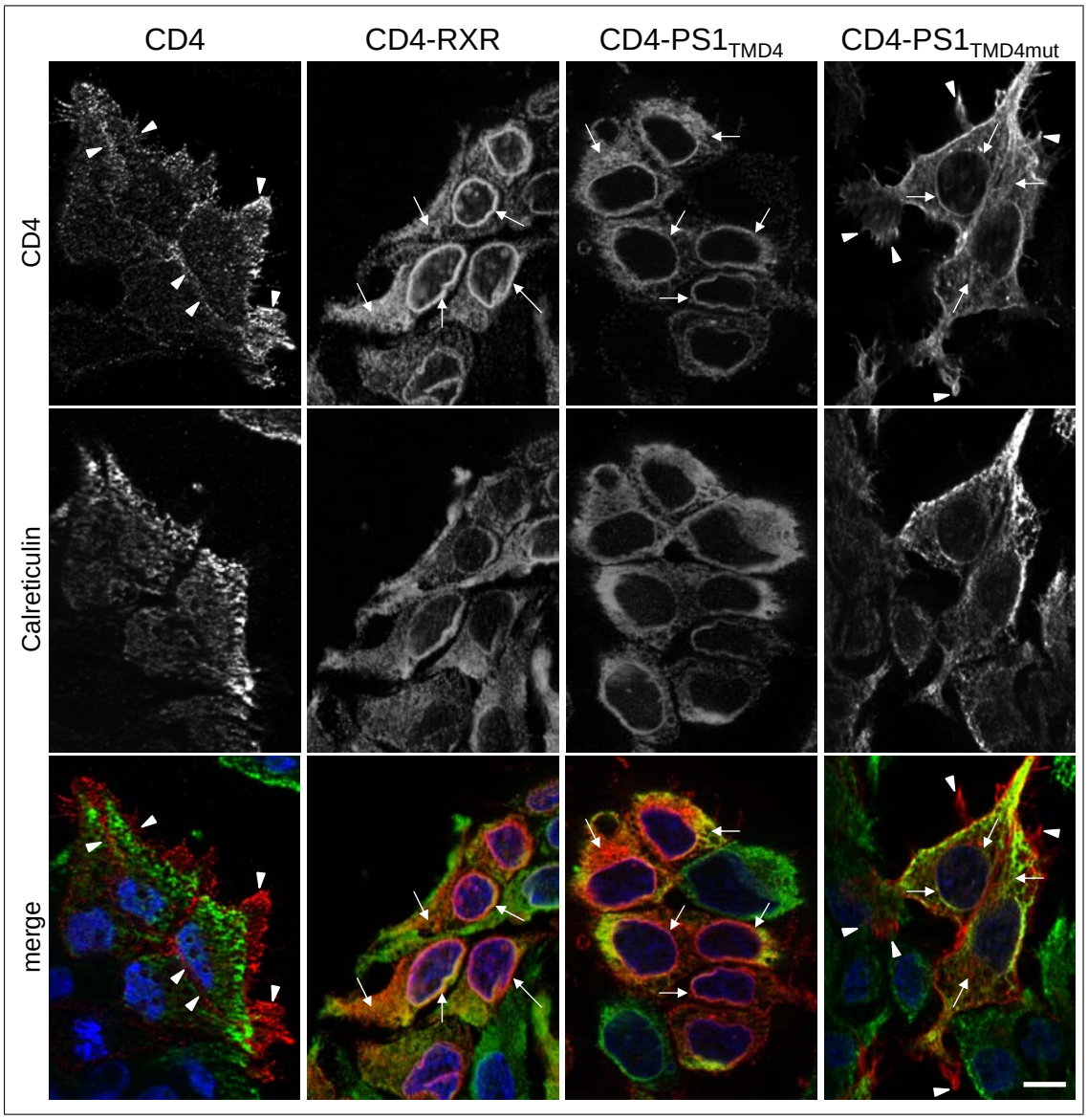

Figure 3.8: *CD4-PS1$_{TMD4}$ was retained in the ER in Swe cells. Swe cells stably expressing CD4 variants as indicated were subjected to immunofluorescence staining with antibodies against CD4 and the ER marker Calreticulin. Nuclei were stained with DAPI. Pictures show optical sections obtained by fluorescence microscopy with an apotome slider module. In the merge picture CD4 was coloured red, Calreticulin green and DAPI blue. Arrowheads, PM localisation; Arrows, ER localisation (nuclear envelope and reticular ER); Scalebar 10 µm.*

assay. As expected, CD4 was EndoH-resistant and CD4-RXR was EndoH-sensitive (figure 3.9, first and second column). CD4-PS1$_{TMD4}$ displayed EndoH-sensitivity indicating a localisation in the early secretory pathway (ER or cis-Golgi)(figure 3.9, third column). In contrast, CD4-PS1$_{TMD4mut}$ showed a mix of EndoH-sensitive and EndoH-resistant CD4 molecules, which resulted in a double band in the EndoH-treated sample (figure 3.9, fourth column, lane H). This result suggested a partial

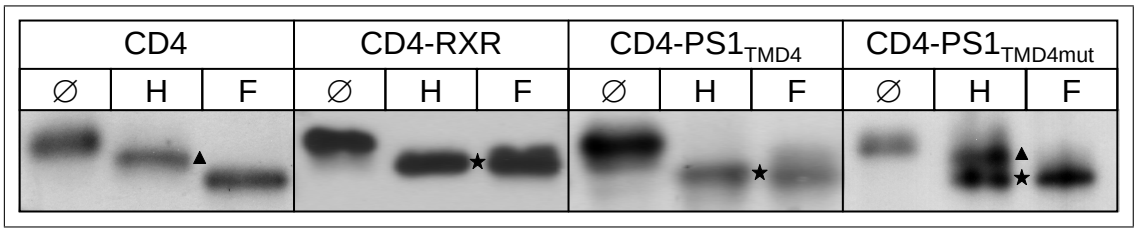

Figure 3.9: *Deglycosylation assay substantiated ER retention of CD4-PS1$_{TMD4}$. CD4 protein was immunoprecipitated from lysates of Swe cells stably expressing the respective CD4 species. The IP eluates were split into 3 parts and were either left untreated (Ø), treated with Endoglycosidase H (H) or treated with N-glycosidase F (F). The triangle indicates endoH resistant species and the star endoH sensitive species.*

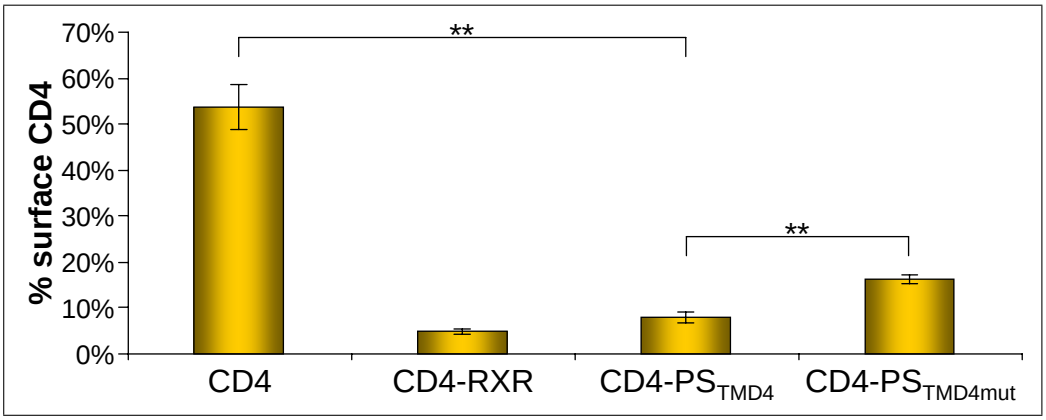

Figure 3.10: *Quantification of surface CD4 antigen confirmed ER retention of CD4-PS1$_{TMD4}$ and showed a partial release of CD4-PS1$_{TMD4mut}$. Swe cell lines stably expressing the respective CD4 species were either stained for surface CD4 or for total CD4 after permeabilisation. Cells were measured by FACS and the geometric mean of the fluorescence intensities was determined. The ratios of surface CD4 to total CD4 were calculated for the respective CD4 variants. The two controls CD4 and CD4-RXR are identical to the data shown in 3.5. The error bars depict the standard error of n=4-6 experiments.*

release of CD4-PS1$_{TMD4mut}$ from the ER to later compartments of the secretory pathway, which perfectly matched the observations by immunofluorescence.

To quantify the ER retention of the different CD4 species the described FACS-based localisation assay was performed (chapters 3.1.2 and 2.5). In Swe cells stably expressing CD4 and CD4-RXR 53.8 % and 4.9 % of the CD4 antigen was at the cell surface, respectively. In Swe CD4-PS1$_{TMD4}$ cells 8.1 % of the CD4 antigen was located at the plasma membrane, demonstrating intracellular retention in the range of CD4-RXR. In contrast, in Swe cells stably expressing CD4-PS1$_{TMD4mut}$ a highly significant increase to 16.3 % of surface CD4 was observed (figure 3.10). This again mirrored the results obtained by immunocytochemistry and the deglycosylation assay, since the introduced mutation did not lead to a complete release of the CD4 antigen to the cell surface.

In addition to the CD4 constructs, mouse Tac reporter proteins were constructed. Mature mouse Tac, also known as mouse interleukin-2 receptor, is a 55 kDa transmembrane glycoprotein with a type I topology. Tac is by default rapidly transported to the plasma membrane (Bonifacino *et al.*, 1990b) and it was used before to analyse TMD-based ER retention signals in TCRα and the nicotinic acetylcholine receptor (Bonifacino *et al.*, 1990a; Wang *et al.*, 2002). To analyse an ER retention signal in the PS1-TMD4, the TMD of Tac was replaced with the TMD4 of human PS1 (Tac-PS1$_{TMD4}$) and a Tac-RXR was constructed for control. Tac-RXR was constructed similarly to CD4-RXR, by fusing the last 36 amino acids of Kir6.2 to the Tac C-terminus, thus introducing a cytoplasmic RXR retention motif (Zerangue *et al.*, 1999). The Tac constructs and a comparison of the respective TMD regions

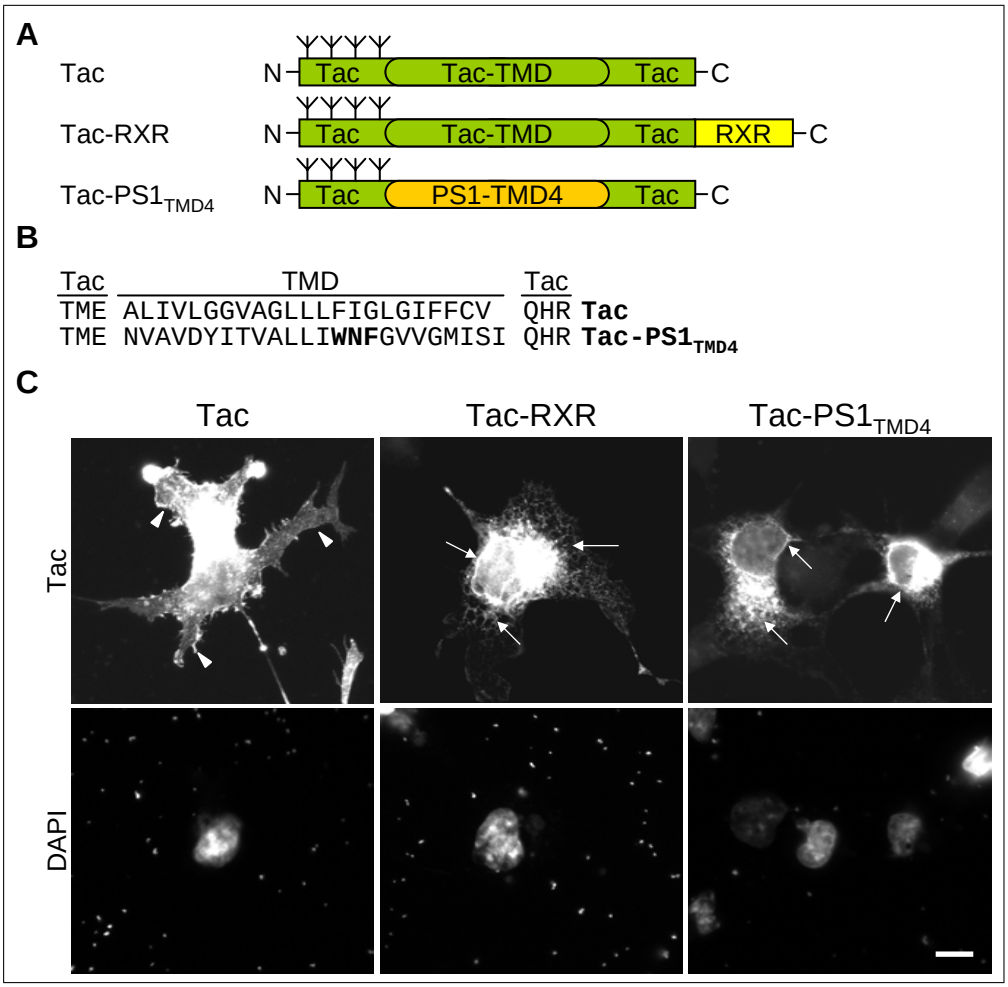

Figure 3.11: *Tac-PS1$_{TMD4}$ was retained in the ER in Cos-7 cells. A) Constructed Tac variants. B) Comparison of the TMD regions of the Tac constructs. C) Cos-7 cells were transiently transfected with different Tac variants. Cells were subjected to immunofluorescence staining with antibodies against Tac and nuclei were stained with DAPI. Cells were analysed by fluorescence microscopy. Arrowheads, PM localisation; Arrows, ER localisation (nuclear envelope and reticular ER); Scalebar 10 µm.*

are shown in figure 3.11A,B.

Tac, Tac-RXR and Tac-PS1$_{TMD4}$ were transiently transfected into Cos-7 cells grown on cover slips. Subsequently, cells were processed for immunocytochemistry with anti-Tac antibodies. As expected, Tac was localised to the plasma membrane, whereas Tac-RXR was retained in the ER (figure 3.11C, first and second column). Tac-PS1$_{TMD4}$ was also localised to ER, supporting the preceding findings of an ER retention signal within the PS1-TMD4.

In conclusion, it was clearly demonstrated that the TMD4 of PS1 contained an ER retention signal, which could confer ER retention to different reporter proteins. Since reporter proteins were retained in the ER in Swe, Cos-7, HeLa Kyoto and NIH3T3 cells (data not shown for the latter two), the retention signal was cell line independent. The WNF sequence in the PS1-TMD4 which was implicated in the binding of Pen2 to PS1 (Watanabe *et al.*, 2005; Kim and Sisodia, 2005a) strongly contributed to the retention signal. Nevertheless, other amino acids of the PS1-TMD4 likely contribute to the ER retention signal, because the WNF→AAA mutation did not lead to a complete ER release of the CD4-PS1$_{TMD4mut}$ reporter protein.

3.2.2 Relevance of PS1-TMD4 for the ER retention of full-length PS1

In the previous section evidence was given on the presence of an ER retention signal in the PS-TMD4. The relevance of the identified signal for the full-length presenilins remained unclear. Furthermore, Kaether *et al.*, 2004 published another ER retention signal within the PS1-TMD9, that depended on a PALP motif. The presence of two retention signals on one protein raised the question, if both were necessary to obtain ER retention of PS1.

To address this concern, a series of mutants of PS1-EGFP (PE) were constructed, which had either a WNF→AAA mutation (PE$_{-WNF}$) or a PALP→AAAA (PE$_{-PALP}$) mutation or both retention signals mutated (PE$_{-PALP-WNF}$). HeLa Kyoto cell lines were generated that stably expressed the four PE variants. The stably expressing cells were seeded onto cover slips and subsequently subjected to immunocytochemistry with anti-GFP and anti-Calnexin antibodies.

PE was located at the plasma membrane (figure 3.12, column 1), although two ER retention signals were present (WNF and PALP). The reason for this observation was the incorporation of PE into fully functional γ-secretase complexes, which were transported to the plasma membrane (Kaether *et al.*, 2004). The absence of ER-located PE molecules indicated that the expression levels were modest, because no unassembled, excessive PE accumulated in the ER. The localisation of PE$_{-PALP}$ was indistinguishable from PE (figure 3.12, column 2). PE$_{-PALP}$ also assembled into complete γ-secretase complexes, although these complexes stayed catalytically inactive. However, the observed lack of activity did not interfere with the trafficking of the assembled γ-secretase (Kaether *et al.*, 2004).

PE$_{-WNF}$ displayed a clear ER staining, nicely overlapping with the ER marker Calnexin (figure 3.12, column 3). In contrast to the PE$_{-PALP}$ mutant, Pen2 could

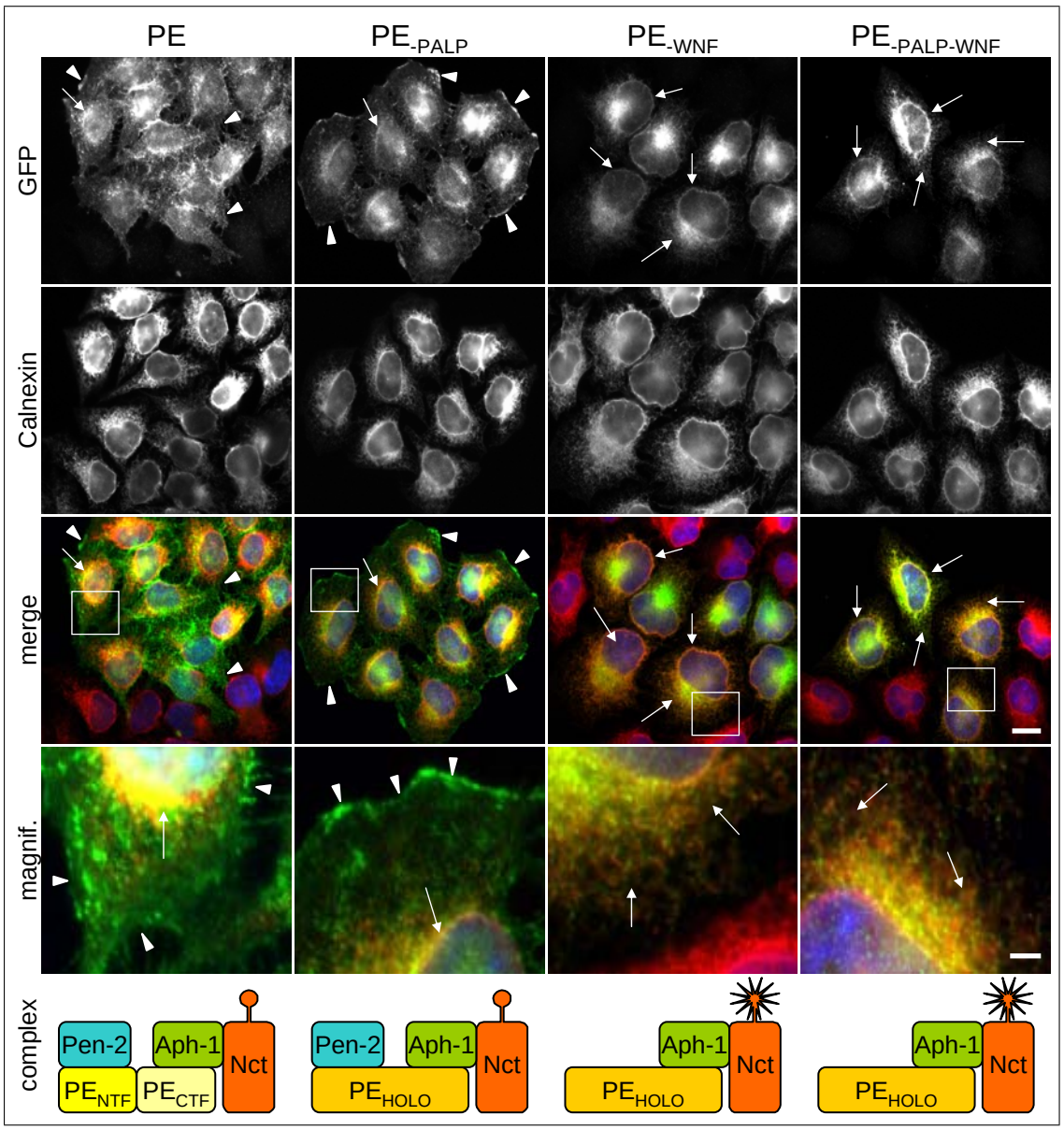

Figure 3.12: *Mutagenesis of two ER retention signals did not cause ER export of PS1-EGFP (PE). HeLa Kyoto cells stably expressing PE and different mutants were subjected to immunofluorescence staining with antibodies against GFP and the ER marker Calnexin. Nuclei were stained with DAPI and cells were analysed by fluorescence microscopy. In the merge pictures GFP was coloured green, Calnexin red and DAPI blue. Scalebar 10 µm. The lower panel shows magnifications (magnif.) of the boxed areas above. Scalebar 2 µm. Arrowheads, PM localisation; Arrows, ER localisation (nuclear envelope and reticular ER). The models at the bottom indicate the assembly state of the γ-secretase complex in the respective cell line (modified after Steiner* et al., *2008b). Most of the observed GFP-derived fluorescence originated from PE molecules that were assembled into the depicted complexes.*

no longer bind to the trimeric assembly intermediate composed of Aph-1, Nct and PE_{-WNF} (see figure 3.12, bottom)(Watanabe *et al.*, 2005; Kim and Sisodia, 2005a). Since the incorporation of Pen2 was the last and rate limiting step during γ-secretase assembly (Takasugi *et al.*, 2003; Prokop *et al.*, 2004), the expressed PE_{-WNF} accumulated in this immature, trimeric complex intermediate. The double mutant $PE_{-PALP-WNF}$ demonstrated the same ER staining like PE_{-WNF} (figure 3.12, column 4). Due to the WNF→AAA mutation, $PE_{-PALP-WNF}$ was trapped in the same assembly state like PE_{-WNF}. The observation of ER retention for $PE_{-PALP-WNF}$ disclosed the presence of further open ER retention signals besides PALP and WNF in the trimer.

In the experimental approach used here, the stable, low level expression of PE and its mutants probably led to a steady state with almost no free PE. This was suggested by the lack of an ER staining in the HeLa Kyoto cells stably expressing PE. Newly synthesised PE was immediately bound by Nct/Aph-1 heterodimers and a complete γ-secretase complex was formed and transported to the plasma membrane. The expression levels in the other HeLa Kyoto cell lines stably expressing the different PE mutants were similar, suggesting that PE molecules are also bound by Nct/Aph-1 heterodimers in these cells. This situation complicated the analysis of the potency of different ER retention signals in PS1, since retention signals on other γ-secretase subunits might have interfered with the signals known in PS1. For example, Spasic *et al.*, 2007 described an ER retention signal in the TMD of Nct, although this signal could not be confirmed in experiments in our lab (Christina Valkova, unpublished data). In summary, it turned out to be of great importance to consider the assembly state of γ-secretase during the analysis of the strength of ER retention signals on one complex subunit.

To exclude the potential influence of ER retention signals on other γ-secretase subunits an assembly mutant of PE was constructed. To this end, the 7 most C-terminal amino acids of all four described PE variants were deleted, giving rise to $PE_{\Delta 7}$ and the respective mutants. $PE_{\Delta 7}$ lacked the binding site for Nct (Kaether *et al.*, 2004; Bergman *et al.*, 2004b) and is not incorporated in any assembly intermediates. Thus, it was possible to analyse the ER retention of PE and its mutants in an isolated manner.

The four $PE_{\Delta 7}$ species were stably expressed in HeLa Kyoto cells. The stable cells were seeded onto cover slips, stained with an anti-GFP antibody and analysed by fluorescence microscopy. All four species clearly localised to the ER. Even in $PE_{\Delta 7-PALP-WNF}$ that lacked both known retention signals and had no contact to other subunits, exclusively ER staining was visible (figure 3.13). This observation provided direct evidence on the presence of a third or even fourth ER retention signal within PS1. Hence, an ultimate answer on the relevance of the novel ER retention signal in the PS1-TMD4 for full-length PS1 could not be given.

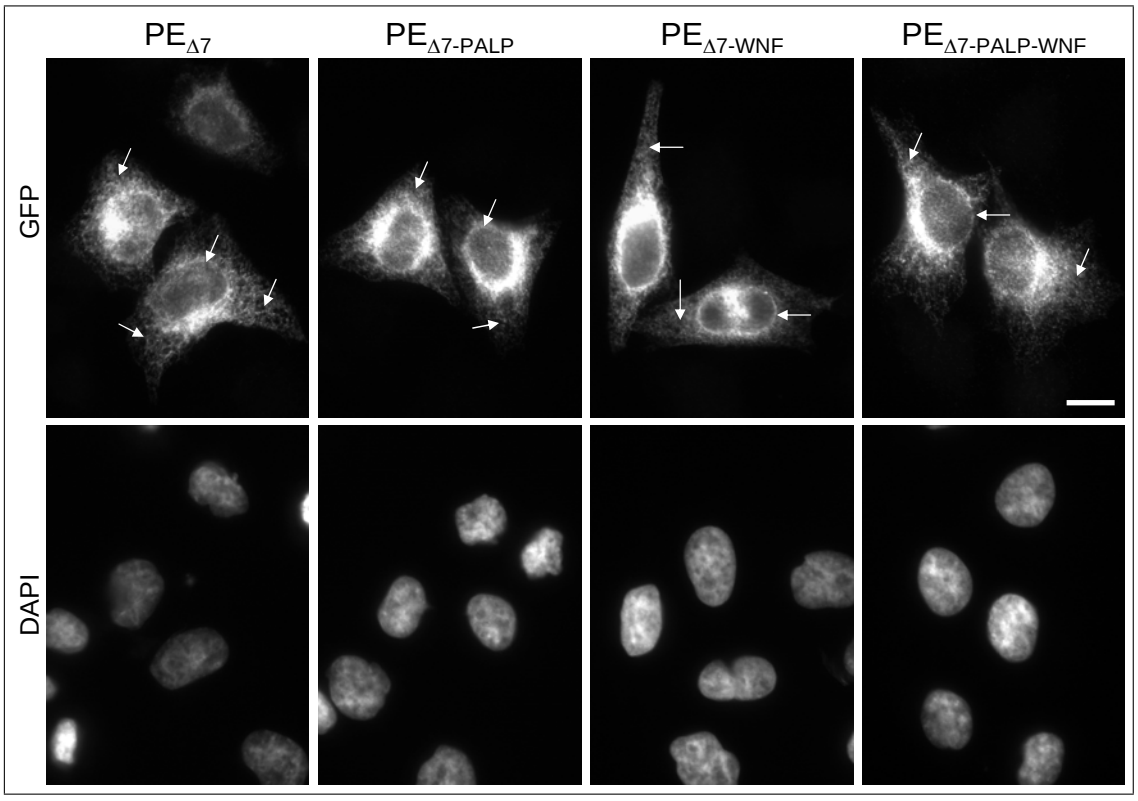

Figure 3.13: *PS1-EGFP Δ7 (PE Δ7) and its mutants were retained in the ER. HeLa Kyoto cells stably expressing PE Δ7 and the indicated mutants were subjected to immunofluorescence staining with antibodies against GFP and nuclei were stained with DAPI. Subsequently cells were analysed by fluorescence microscopy. Arrows, ER localisation (nuclear envelope and reticular ER); Scalebar 10 μm.*

3.3 Rer1-dependency of TMD-based retention signals

Though it has been clear since many years that TMD-based ER retention signals do exist (Bonifacino *et al.*, 1991) only little was known how these signals function in detail and which other proteins were involved in this process. In yeast, Rer1p was described as a retrieval receptor for ER localised proteins and it recognised its target proteins via polar residues in their TMDs (Sato *et al.*, 1995, 1996). In table 3.1 a selection of Rer1p target proteins together with the respective signal-containing TMD is shown. These TMDs were compared to the TMDs of γ-secretase subunits Pen2, Nct and PS1, in which ER retention signals were identified (this work and Spasic *et al.*, 2007). The only common feature of all Rer1p substrates in yeast were one or more polar residues in the hydrophobic context of a TMD. This criteria was met by the ER retention signals in the PS1-TMD4 and the Pen2-TMD1 for which reason it was tested if mammalian Rer1 was involved in the retention of PS1 and/or Pen2.

Table 3.1: *By analogy Pen2 and PS1 could be substrates of Rer1. Comparison of the TMDs of confirmed substrates of Rer1p from yeast with the potential mammalian substrates Nct, Pen2 and PS1. Residues which are important for the (Rer1-mediated) ER retention are underlined.*

protein	TMD sequence	topology type	reference
Sec12p	LSFQLIYSLLVILIFNTFF	II	Sato *et al.*, 1995 Sato *et al.*, 1996
Sec71p	ISVYTPLIYVFILVVSLVMFASSY	III	Sato *et al.*, 1997 Sato *et al.*, 2003
Fet3p	IIAMTFSCFAGILGIITIAIYGMM	I	Sato *et al.*, 2004
Nct	LITLTVGFGILIFSLIVTYCI	I	Spasic *et al.*, 2007
Pen2-TMD1	YYLGGFAFLPFLWLVNIFWFF	IV-B	this study
PS1-TMD4	NVAVDYITVALLIWNFGVVGMISI	IV-A	this study

3.3.1 Rer1 binds to unassembled Pen2 via the Pen2-TMD1

To test if Rer1 can directly bind to the TMD1 of Pen2 a set of double stable Swe cell lines were generated that all expressed C-terminally V5-tagged Rer1 plus either CD4, CD4-Pen2$_{TMD1}$ or CD4-Pen2$_{TMD1mut}$. CD4-Pen2$_{TMD1mut}$ contained a N→L mutation in the Pen2-TMD1, which was shown to partially abrogate ER retention of the CD4 reporter (Kaether *et al.*, 2007). After IP with an anti-V5 antibody only CD4-Pen2$_{TMD1}$ co-immunoprecipitated with Rer1-V5 from CHAPSO lysates. In contrast, CD4-Pen2$_{TMD1mut}$ did not co-immunoprecipitate with Rer1-V5, suggesting that the mutated asparagine was important for the binding to Rer1 (figure 3.14).

In the next step it was tested if Rer1 also binds to the full-length protein and if it binds to free or complex-associated Pen2. To this end, two stable Swe cell lines were created, one expressing N-terminally myc-tagged Pen2 (mycPen2) alone, while the second expressed mycPen2 together with Rer1-V5. CHAPSO lysates of these cells were subjected to two subsequent immunoprecipitations with anti-V5 and anti-myc antibodies, respectively. The first IP of Rer1-V5 showed specific co-immunoprecipitation of mycPen2, but of no other γ-secretase component (figure 3.15, left lanes). From the supernatant of the first immunoprecipitation mycPen2 was immunoprecipitated together with robust amounts of the other components of mature γ-secretase (Aph-1, mature Nct, PS1-NTF), confirming that the majority of Pen2 in the cells was incorporated into the mature complex (figure 3.15, right lanes). In the second immunoprecipitation with anti-myc antibodies also Rer1-V5 co-immunoprecipitated. However, it was shown in other experiments that this was due to unspecific binding of Rer1-V5 to the sepharose beads (data not shown).

The co-immunoprecipitation of mycPen2 with the other γ-secretase components demonstrated that the complex stayed intact under the conditions during immunoprecipitation. Together with the absence of Nct, Aph-1 and PS1 in the Rer1-V5 immunoprecipitation this suggested that Rer1-V5 selectively bound to unassembled mycPen2. This binding depended on a binding site in the Pen2-TMD1, which was

most probably inaccessible for Rer1-V5 in the assembled γ-secretase complex.

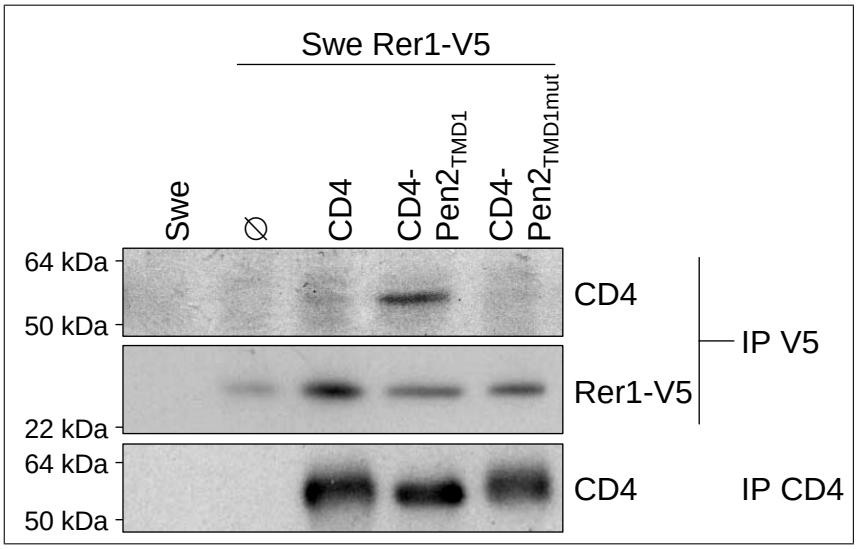

Figure 3.14: *CD4-Pen2$_{TMD1}$ co-immunoprecipitated with Rer1-V5. Rer1-V5 was immunoprecipitated from CHAPSO lysates of Swe cells expressing either Rer1-V5 alone or together with the indicated CD4 variant. After Western blot the proteins were detected with anti-V5 antibody or anti-CD4 antibody. Expression of CD4 species was analysed by IP and Western blot using anti-CD4 antibodies. Data kindly provided by Christoph Kaether.*

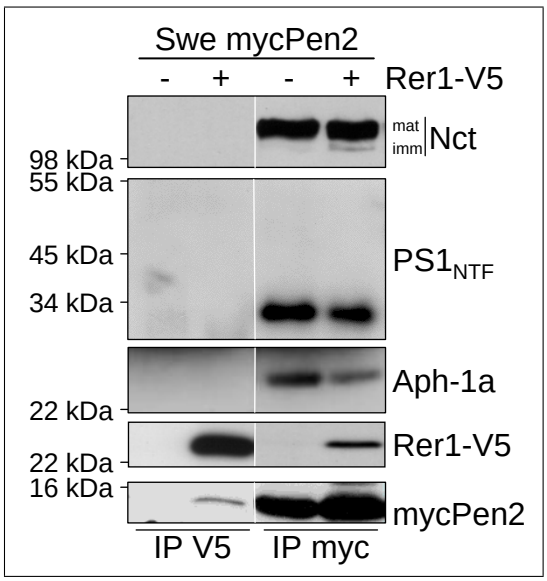

Figure 3.15: *Rer1 selectively bound to unassembled Pen2. CHAPSO lysates of Swe cells stably expressing mycPen2 either alone or together with Rer1-V5 were subjected to two subsequent immunoprecipitations with anti-V5 and anti-myc antibodies, respectively. Immunoprecipitation eluates were analysed by Western blot with antibodies against V5, myc, Nct, Aph-1 and PS1-NTF. The white lines indicate the assembly from different areas of the same blot.*

3.3.2 ER retention of CD4-Pen2$_{TMD1}$ but not CD4-PS1$_{TMD4}$ depends on Rer1

After the demonstration of a direct interaction of the overexpressed proteins it was next tested if that interaction is of functional relevance. To this end, the FACS-based quantification of ER retention described in chapter 3.1.2 was combined with a siRNA approach.

In a first step the delivery of and the knock down by siRNA in Swe cells was validated. The transfection efficiency of siRNA was analysed using an Alexa Fluor®488-conjugated, non-targeting siRNA. 6 hours post-transfection control- or siRNA-transfected cells were analysed by FACS, revealing a transfection of virtually all cells (figure 3.16A). In the next step, the same transfection conditions were used to knock down Rer1 in Swe cells. In figure 3.16B Swe CD4 cells were transfected with control- or Rer1-siRNA. After 24, 48 and 72 hours the Rer1 and CD4 protein levels were analysed by Western blot. A robust knock-down could be observed after 48 and 72 hours with no change in the levels of CD4 protein. These results were reproduced for all stable Swe cell lines, independent of the expressed CD4 variant (data not shown).

As a result from the knock down optimisation the 72 hour time point was chosen for the analysis of Rer1-dependency of the TMD-based retention signals. Stable Swe cells that express CD4, CD4-RXR, CD4-Pen2$_{TMD1}$ or CD4-PS1$_{TMD4}$ were used in the assay. Swe CD4 cells were not transfected with any siRNA, serving as a (theoretical) endpoint in the assay by depicting the maximum of surface CD4. Swe CD4-RXR cells served as a negative control, since the RXR retention signal de-

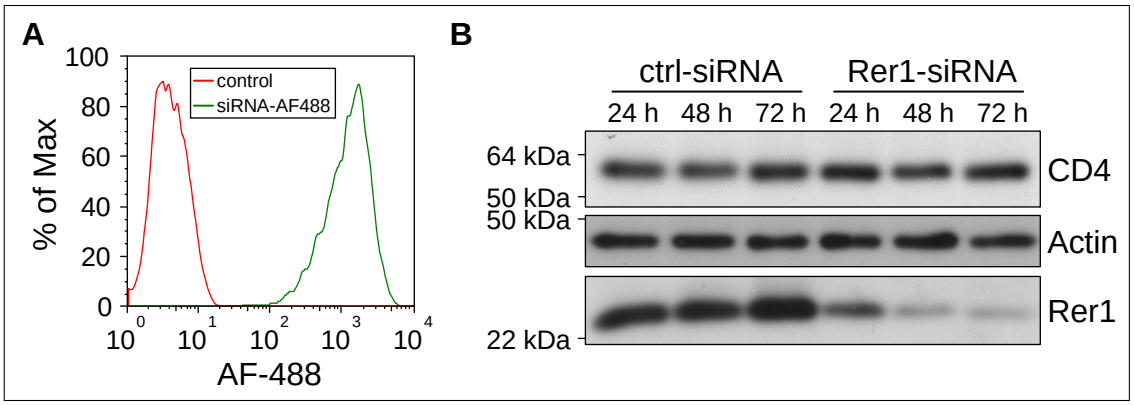

Figure 3.16: *siRNA was efficiently transfected into Swe cells and caused robust Rer1 knock down. A) Swe cells stably expressing CD4 were either transfected with Alexa Fluor® 488-labelled siRNA or left untreated. Transfection efficiency was measured after 6 hours by FACS analysis. The percentage of all measured cells that display a distinct fluorescence intensity (% of Max) is plotted against the fluorescence intensity. B) Swe cells stably expressing CD4 were transfected either with Rer1- or control-siRNA. STEN lysates of transfected cells were prepared after 24 h, 48 h and 72 h and analysed by Western blot for protein levels of CD4 and Rer1. Actin was used as an internal loading control.*

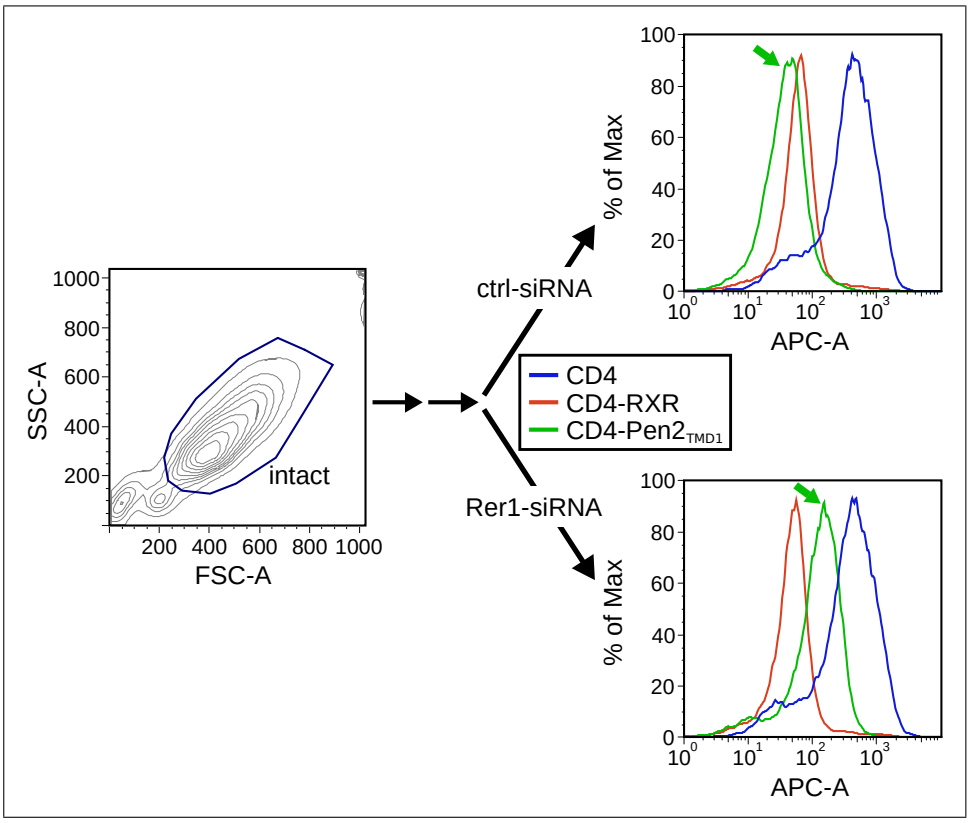

Figure 3.17: *Scheme for the combination of the FACS-based quantification assay with Rer1 knock down. Swe cells stably expressing different CD4 variants were transfected with Rer1-siRNA, control-siRNA or left untransfected (not shown here). After 72 hours cells were prepared and measured as described in chapter 3.1.2 and figure 3.4. Shown here are histograms of only surface stained samples. The percentage of all measured cells that display a distinct fluorescence intensity (% of Max) is plotted against the fluorescence intensity. APC-A reflects the amount of surface CD4. Note the increasing amount of surface CD4 for the Swe CD4-Pen2$_{TMD1}$ in the Rer1-siRNA transfected sample (green arrow).*

pended on other proteins but Rer1 (Yuan *et al.*, 2003; Nufer and Hauri, 2003). Swe CD4-RXR, CD4-Pen2$_{TMD1}$ and CD4-PS1$_{TMD4}$ were either left untransfected, transfected with control-siRNA or transfected with Rer1-siRNA. After 72 hours cells were harvested, counted and each sample was split into two subsamples of defined cell number. The subsamples were either stained for total CD4 antigen or for surface CD4 antigen as has been described earlier (chapter 3.1.2). All stained samples were measured by FACS analysis and the fraction of surface CD4 was calculated from the fluorescence. Figure 3.17 schematises the experiment. The histograms show the surface CD4 immunoreactivity in cells treated with control- or Rer1-siRNA. It is clearly visible that after Rer1 knock down the amount of surface CD4 increased in Swe CD4-Pen2$_{TMD1}$ cells (green arrow).

Swe CD4-RXR, CD4-Pen2$_{TMD1}$ and CD4-PS1$_{TMD4}$ cells displayed strong ER retention of the respective CD4 variant under non-treated or control-siRNA condi-

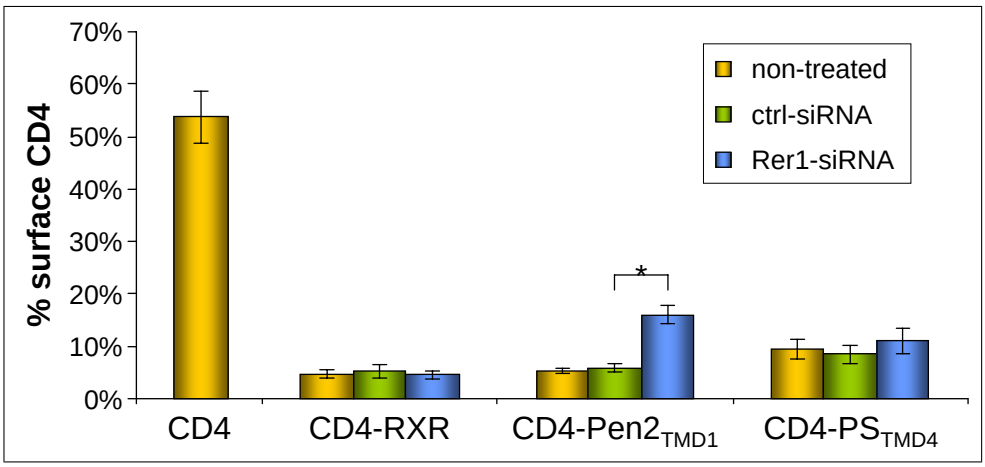

Figure 3.18: *Rer1 knock down caused the release of CD4-Pen2$_{TMD1}$ but not CD4-PS1$_{TMD4}$ towards the cell surface. Swe cell lines stably expressing the respective CD4 species were either left untreated, transfected with control-siRNA or with Rer1-siRNA. After 72 hours cells were either stained for surface CD4 or for total CD4 after permeabilisation. Cells were measured by FACS and the geometric mean of the fluorescence intensities was determined. The ratios of surface CD4 to total CD4 were calculated for the respective conditions and CD4 variants. The data for the Swe CD4 cells are identical to the data shown in figure 3.5. The error bars depict the standard error of n=3-4 experiments.*

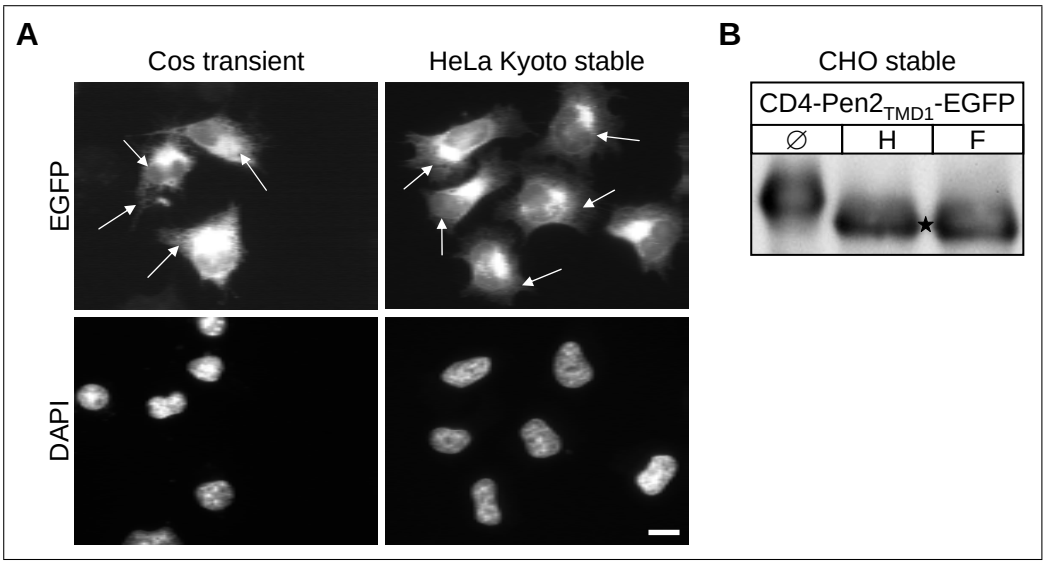

Figure 3.19: *C-terminally EGFP-tagged CD4-Pen2$_{TMD1}$ (CD4-Pen2$_{TMD1}$-EGFP) was retained in the ER. A) Cos-7 cells transiently expressing CD4-Pen2$_{TMD1}$-EGFP and HeLa Kyoto cells stably expressing CD4-Pen2$_{TMD1}$-EGFP were fixed and nuclei were stained with DAPI. Subsequently, cells were analysed by fluorescence microscopy. Scalebar 10 µm. Arrows, ER localisation (nuclear envelope and reticular ER). B) Lysates of CHO cells stably expressing CD4-Pen2$_{TMD1}$-EGFP were used for a deglycosylation assay. Star indicates endoH sensitive species.*

tions. After Rer1 knock down only CD4-Pen2$_{TMD1}$ showed a significant increase of surface CD4 levels. The percentage of surface CD4 immunoreactivity increased by a factor of 2.7 from 5.9 % to 16.1 % (figure 3.18). This result demonstrated the functional relevance of Rer1 for the ER retention signal in the Pen2-TMD1, whereas the ER localisation of the PS1-TMD4 was Rer1-independent.

The Rer1-dependence of CD4-Pen2$_{TMD1}$ retention was confirmed using fluorescence microscopy. To this end, CD4-Pen2$_{TMD1}$ with a C-terminally fused EGFP moiety was constructed. CD4-Pen2$_{TMD1}$-EGFP localised to the ER in transiently transfected Cos-7 cells and stably expressing HeLa Kyoto cells as demonstrated by the strong staining of the nuclear envelope (figure 3.19A). In the stable HeLa Kyoto cells some additional plasma membrane staining is visible due to the high expression level in this cell line. Moreover, CD4-Pen2$_{TMD1}$-EGFP stably expressed in CHO cells showed endoH sensitivity in a deglycosylation assay, confirming the ER retention observed by fluorescence microscopy (figure 3.19B).

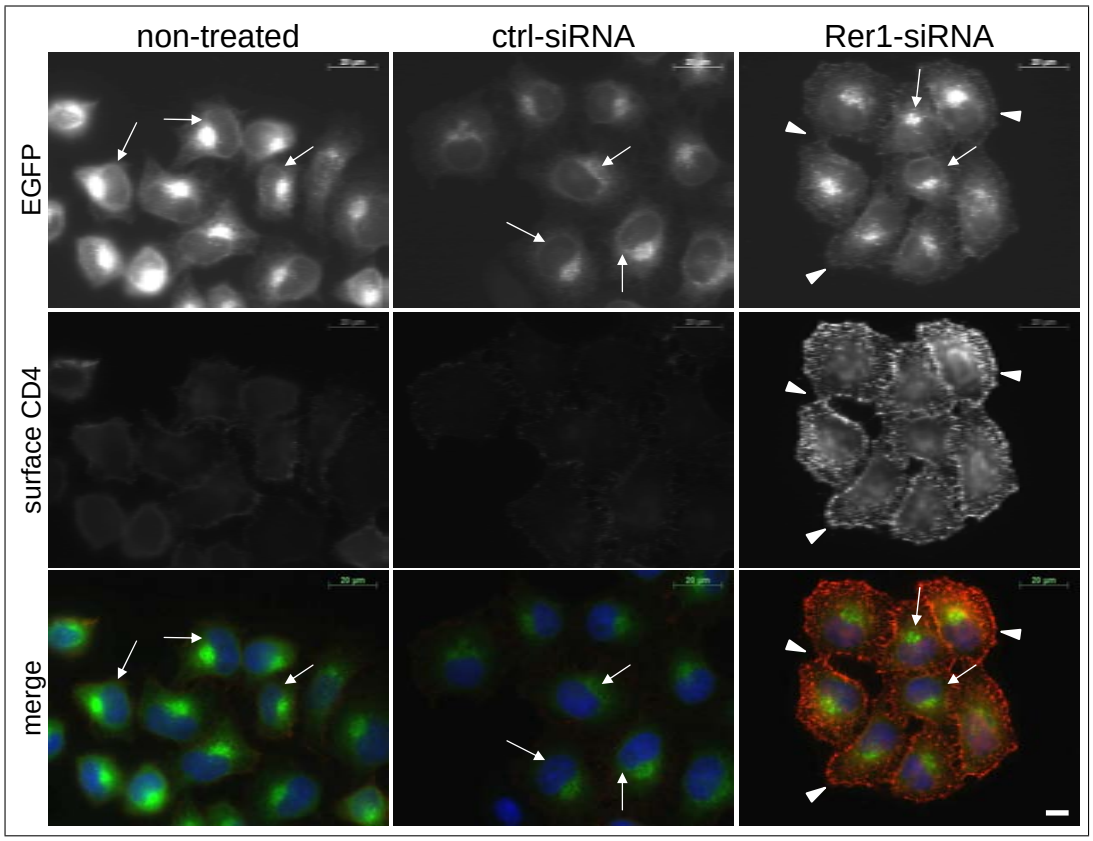

Figure 3.20: *CD4-Pen2$_{TMD1}$-EGFP was released to the cell surface after Rer1 knock down. HeLa Kyoto CD4-Pen2$_{TMD1}$-EGFP cells were seeded onto cover slips and transfected with siRNA or left untreated as indicated. 72 hours later cells were stained for surface CD4, fixed and the nuclei were stained with DAPI. All pictures were taken with identical exposure times and equally processed with Photoshop software. In the merge picture surface CD4 was coloured red, EGFP green and DAPI blue. Arrowheads, PM localisation; Arrows, ER localisation (nuclear envelope and reticular ER); Scalebar 10 μm.*

Similar to the FACS-based assay, the HeLa Kyoto cells stably expressing CD4-Pen2$_{TMD1}$-EGFP were either left untreated or transfected with control- and Rer1-siRNA, respectively. After 72 hours cells were processed for immunofluorescence staining of surface CD4 using an anti-CD4 antibody prior to fixation and permeabilisation. Thus, it is possible to compare surface CD4 levels with total CD4-Pen2$_{TMD1}$-EGFP expression, which is reflected by the EGFP signal. In figure 3.20 both siRNA-transfected samples displayed equal EGFP signals, whereas the surface CD4 signal was much stronger in the Rer1 knock down cells (second and third column, respectively). On the other hand, untreated cells showed some surface CD4 (though not as much as Rer1 knock down cells), but they also displayed an increased EGFP signal.

The effect of Rer1 knock down on the localisation of CD4-Pen2$_{TMD1}$-EGFP was quantified using automated microscopy and image analysis in a 96-well plate scale (see 2.4.1 for details). Briefly, pictures of the Alexa Fluor®555, EGFP and DAPI channels were automatically taken with equal exposure times. The software subsequently identified cells via the DAPI staining and expanded the nucleus by 7 pixels, thus creating a region of interest for the quantification. Within this region of interest the intensities of the Alexa Fluor®555 signal (reflecting surface CD4-Pen2$_{TMD1}$-EGFP) and the EGFP signal (reflecting total CD4-Pen2$_{TMD1}$-EGFP) were measured and the ratio was calculated (figure 3.21, left part). This ratio increased highly significantly from 0.76 for cells transfected with control-siRNA to 1.74 in Rer1 knock down cells (figure 3.21, right part). The obtained results perfectly matched the data obtained in the FACS assay (figure 3.18).

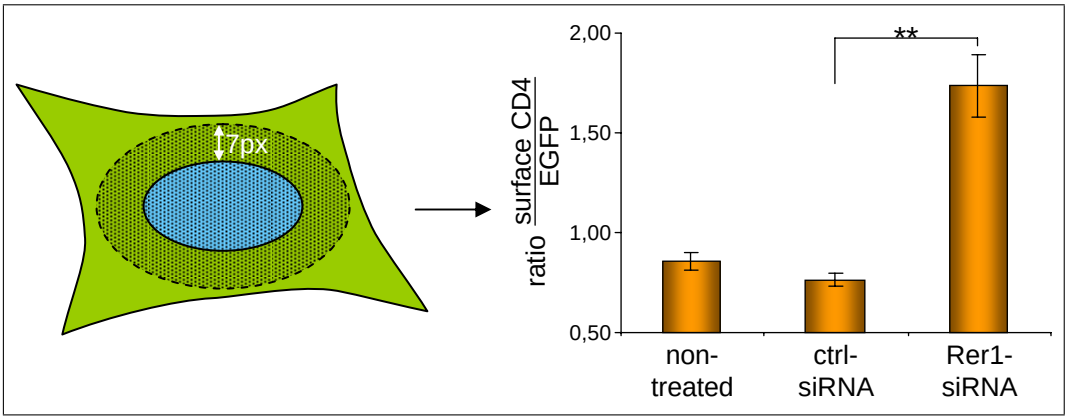

Figure 3.21: *Rer1 knock down triggered the release of CD4-Pen2$_{TMD1}$-EGFP towards the cell surface as revealed by quantitative immunofluorescence. HeLa Kyoto CD4-Pen2$_{TMD1}$-EGFP cells were seeded into 96-well plates and transfected with siRNA or left untreated as indicated. 72 hours later cells were stained for surface CD4, fixed and the nuclei were stained with DAPI. Using Cellomics ArrayScan HCS reader and Cellomics One software cellular structures were identified automatically and a region of interest was generated by expansion of the nucleus (dotted ellipse). The average intensities of EGFP- and surface CD4-derived fluorescence were quantified within these regions of interest and ratios were calculated.*

To sum up, it became evident that the ER-retention signal in the Pen2-TMD1 depended on Rer1. Rer1 bound exclusively unassembled Pen2 and this binding was mediated by the Pen2-TMD1 that contained a critical asparagine residue. Although PS1-TMD4 also contained an ER retention signal with a critical asparagine, the ER retention of the PS1-TMD4 was independent of Rer1.

3.4 Masking of ER retention signals in Pen2 and PS1

In the first two chapters evidence was presented that the Pen2-TMD1 and the PS1-TMD4 contained ER retention signals. Additionally, it was shown in 2005 by two research groups, that the PS1-TMD4 comprised the binding site for the Pen2 subunit. The binding site was narrowed down to a ″WNF″(Watanabe *et al.*, 2005) or ″NF″motif (Kim and Sisodia, 2005a). Hence, within in the PS1-TMD4 the binding site to Pen2 and an ER retention signal overlapped. On the other hand Kim and Sisodia, 2005b gave evidence, that the Pen2-TMD1 is indispensable for the binding of Pen2 to PS1, a finding that was supported by data from our lab (Christoph Kaether, unpublished data). Thus, Pen2-TMD1 likewise contained an interaction site and an ER retention signal. This led to the hypothesis that the Pen2-TMD1 and the PS1-TMD4 could exert a dual function during γ-secretase assembly. On the one hand, they could accomplish ER retention of the unassembled subunits or complex intermediates. On the other hand they could serve as interaction sites between the two subunits, thus promoting the last step in the assembly of the γ-secretase, namely the binding of Pen2 to the trimer of Nct, PS1 and Aph-1. In the course of this last step, the protein-protein interaction between the Pen2-TMD1 and the PS1-TMD4 could lead to the masking of the two ER-retention signals and thereby allow ER export of fully assembled complex.

3.4.1 Co-expression of Pen2-TMD1 and PS1-TMD4 causes mutual masking of ER retention signals

To test this hypothesis, the interaction of the Pen2-TMD1 and the PS1-TMD4 was examined in an isolated manner, since the analysis in the context of the entire complex was confined by the presence of other ER retention signals elsewhere in the γ-secretase complex. Hence, in a first approach C-terminally myc-tagged versions of CD4-PS1$_{TMD4}$ and CD4-RXR were generated by Michael Zocher from our lab. The addition of a myc tag allowed the distinction of CD4-PS1$_{TMD4}$-myc and CD4-RXR-myc from CD4-Pen2$_{TMD1}$-EGFP by fluorescence microscopy. The constructs are depicted in figure 3.22A.

HeLa Kyoto cells stably expressing CD4-Pen2$_{TMD1}$-EGFP were seeded onto cover slips and transiently transfected with either CD4-RXR-myc or CD4-PS1$_{TMD4}$-myc. After fixation cells were stained with mouse anti-myc antibodies to visualise transfected cells. The untransfected (myc negative) cells showed ER localisation of CD4-Pen2$_{TMD1}$-EGFP as was shown before (figure 3.19A). As a negative control CD4-RXR-myc was used that contained the CD4-TMD, which was not supposed

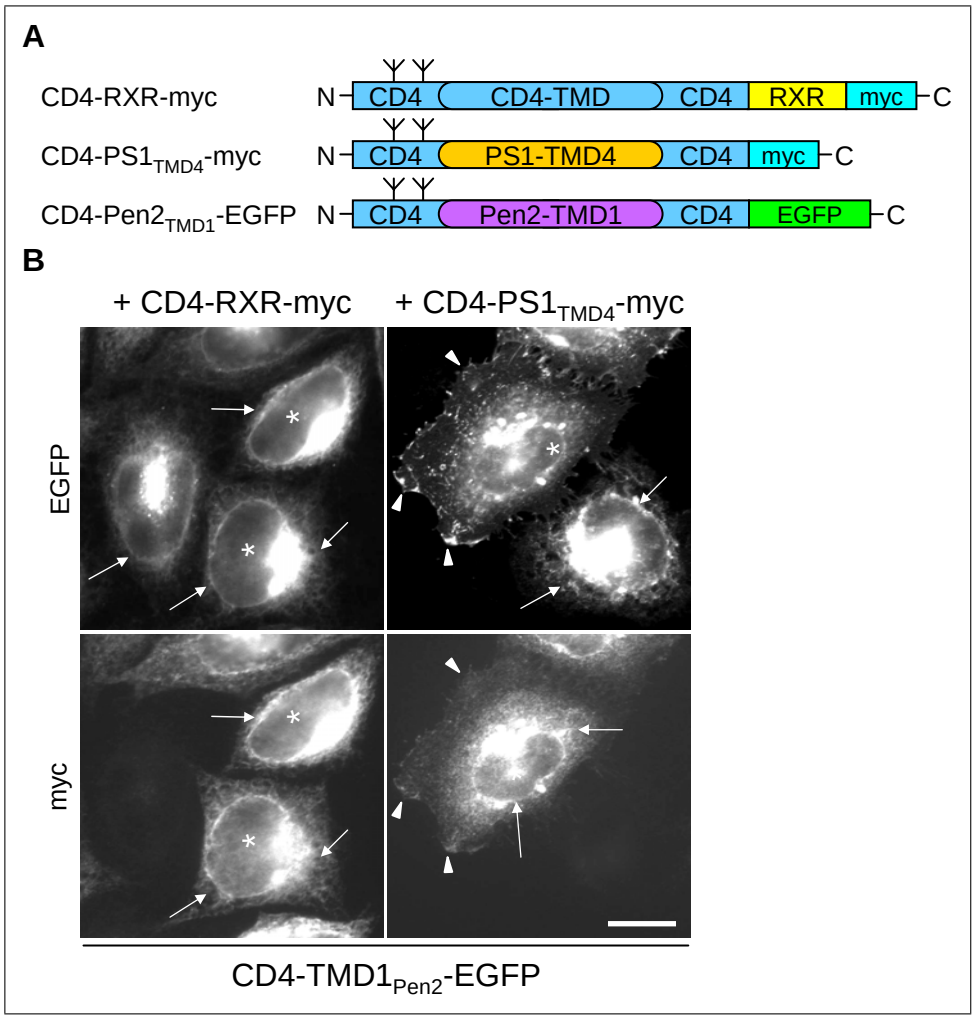

Figure 3.22: *CD4-Pen2$_{TMD1}$-EGFP was released to the cell surface after co-expression with CD4-PS1$_{TMD4}$-myc. HeLa Kyoto cells stably expressing CD4-Pen2$_{TMD1}$-EGFP were seeded onto cover slips and transfected with CD4-PS1$_{TMD4}$-myc or CD4-RXR-myc as a negative control. Cells were processed for immunofluorescence with an anti-myc antibody and nuclei were stained with DAPI. Subsequently, cells were analysed by fluorescence microscopy. Transfected (myc positive) cells were marked with an asterisk. Arrowheads, PM localisation; Arrows, ER localisation (nuclear envelope and reticular ER); Scalebar 10 µm.*

to interact with the Pen2-TMD1. As expected, cells co-expressing CD4-Pen2$_{TMD1}$-EGFP and CD4-RXR-myc did not show any plasma membrane localisation of neither construct (figure 3.22B, left column, asterisk-marked cells). In contrast, cells co-expressing CD4-Pen2$_{TMD1}$-EGFP and CD4-PS1$_{TMD4}$-myc displayed a strong PM staining (figure 3.22B, right column, asterisk-marked cell). Notably, both constructs CD4-PS1$_{TMD4}$-myc and CD4-Pen2$_{TMD1}$-EGFP were partially localised to the PM when they were co-expressed, demonstrating that both had overcome ER retention.

To confirm these results, the introduced Tac reporter proteins Tac-RXR and Tac-PS1$_{TMD4}$ were used. The use of Tac reporters rendered the myc-tagging of the tran-

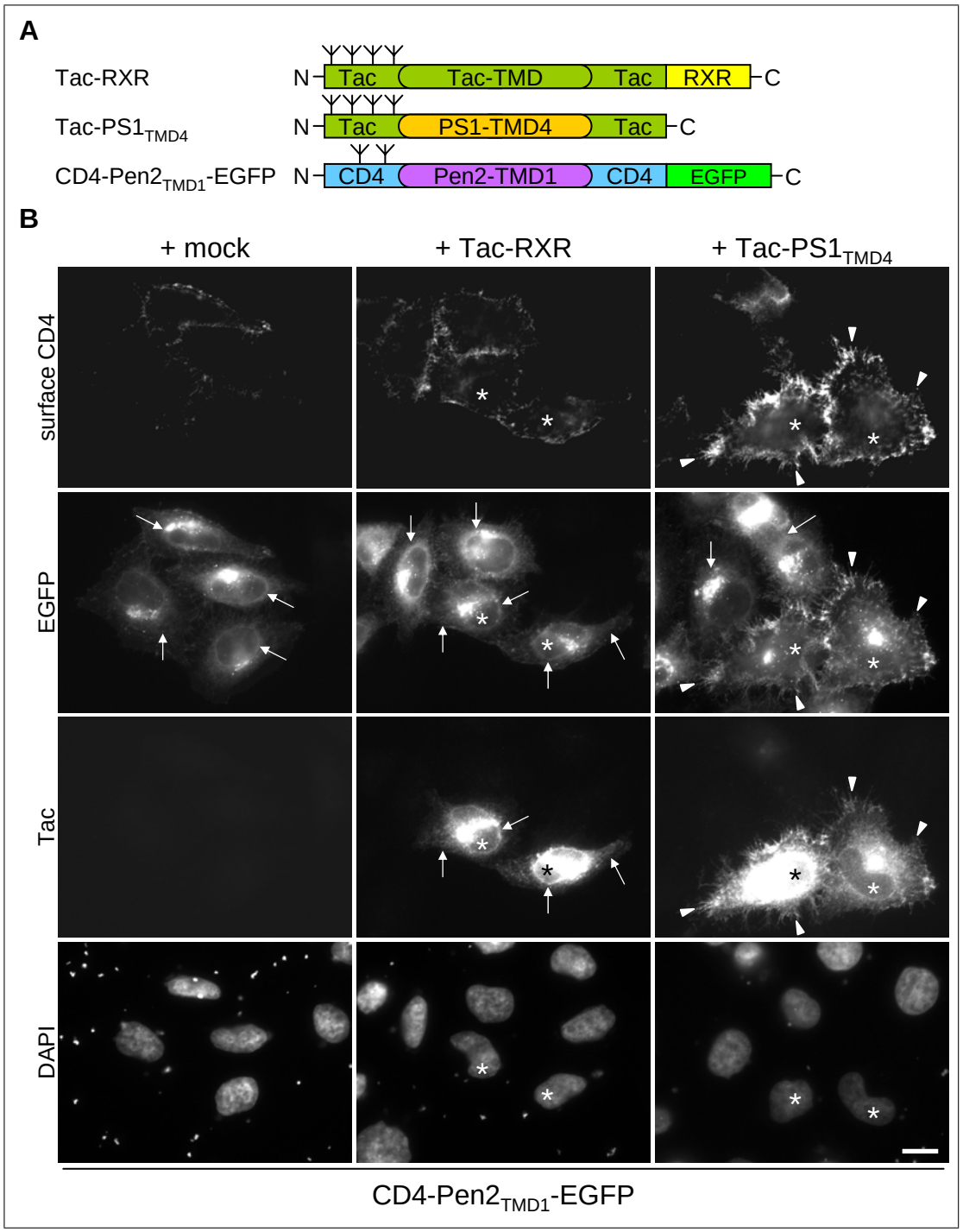

Figure 3.23: *The amount of surface CD4 antigen increased in HeLa Kyoto CD4-Pen2$_{TMD1}$-EGFP cells after co-expression of Tac-PS1$_{TMD4}$. HeLa Kyoto cells stably expressing CD4-Pen2$_{TMD1}$-EGFP were seeded onto cover slips and transfected with Tac-PS1$_{TMD4}$ or with Tac-RXR and mock vector as negative controls. Surface CD4 antigen was stained prior to fixation using an Alexa Fluore® 660-conjugated secondary antibody. Subsequently, Tac was stained with an Alexa Fluore® 555-conjugated secondary antibody and the nuclei were stained with DAPI. Transfected (Tac positive) cells were marked with an asterisk. Arrowheads, PM localisation; Arrows, ER localisation (nuclear envelope and reticular ER); Scalebar 10 µm.*

siently transfected reporters unnecessary, since the Tac antigen was used as a transfection marker. The used constructs are depicted in figure 3.23A. Additionally, the use of Tac reporters permitted the staining of surface CD4 by immunocytochemistry. This allowed a more sensitive view on the release of CD4-Pen2$_{TMD1}$-EGFP towards the cell surface, since the fluorescence of the surface localised CD4 was not biased by the total CD4-Pen2$_{TMD1}$-EGFP. HeLa Kyoto CD4-Pen2$_{TMD1}$-EGFP cells were seeded onto cover slips and transfected with mock vector, Tac-RXR or Tac-PS1$_{TMD4}$, respectively. Subsequently, cells were stained for surface CD4 prior to fixation using an Alexa Fluor®660-conjugated secondary antibody. Additionally, Tac antigen was stained after permeabilisation with an Alexa Fluor®555-conjugated secondary antibody. The EGFP signal served as an expression control, ruling out possible changes in localisation due to altered expression of the stable CD4-Pen2$_{TMD1}$-EGFP. Transfection with a mock vector or Tac-RXR did not result in an increase of surface CD4 levels and Tac-RXR was retained in the ER as expected (figure 3.23B, upper and middle row). In contrast, transfection of Tac-PS1$_{TMD4}$ caused an increase of surface CD4 antigen in the cells co-expressing the CD4 and the Tac reporter protein. Moreover, Tac-PS1$_{TMD4}$ likewise localised partially to the plasma membrane (figure 3.23B, lower row) in these cells, although it was nicely retained in the ER in Cos-7 cells when expressed alone (figure 3.11C).

3.4.2 Quantitative analysis of ER retention signal masking

To assess the effect of masking on the localisation of the reporter proteins in a more quantitative way, a FACS-based assay was performed. To this end, Cos-7 cells were transfected with CD4-Pen2$_{TMD1}$-EGFP, CD4-PS1$_{TMD4}$-myc or both constructs together. After 16 hours of expression cells were counted and split into two subsamples, which were stained for surface and total CD4 antigen, respectively. Additionally, the intracellular myc epitope of CD4-PS1$_{TMD4}$-myc was stained with a polyclonal anti-myc antibody and a PE-conjugated secondary antibody. This staining allowed gating on cells that expressed either CD4-PS1$_{TMD4}$-myc (PE$^+$) or CD4-Pen2$_{TMD1}$-EGFP (GFP$^+$) or both reporter proteins together (PE$^+$GFP$^+$) (see figure 3.24). This work was performed in collaboration with Michael Zocher from our lab.

For all three populations (PE$^+$, GFP$^+$, PE$^+$GFP$^+$) the fraction of surface CD4 antigen was calculated from the fluorescence intensities of the total and surface CD4 stained subsamples. In CD4-PS1$_{TMD4}$-myc or CD4-Pen2$_{TMD1}$-EGFP expressing cells only 6.9 % and 8.6 % of the CD4 reporter protein was at the cell surface, respectively. This indicates strong ER retention as was shown before by immunocytochemistry. In contrast, co-expression of both constructs caused the release of 14.0 % of total CD4 antigen to the cell surface. This constituted a significant 2-fold increase of surface CD4 antigen levels (figure 3.25B). This increase was not resulting from an overall increase of total CD4 reporter proteins in the double transfected cells as was shown by Western blot analysis (figure 3.25A).

Taken together the data provided evidence that the TMD-associated ER retention signals in the PS1-TMD4 and the Pen2-TMD1 overcame ER retention, when they were co-expressed in the same cell. This effect was not due to an overloading

of the ER retention machinery due to overexpression as was shown by figure 3.25A.

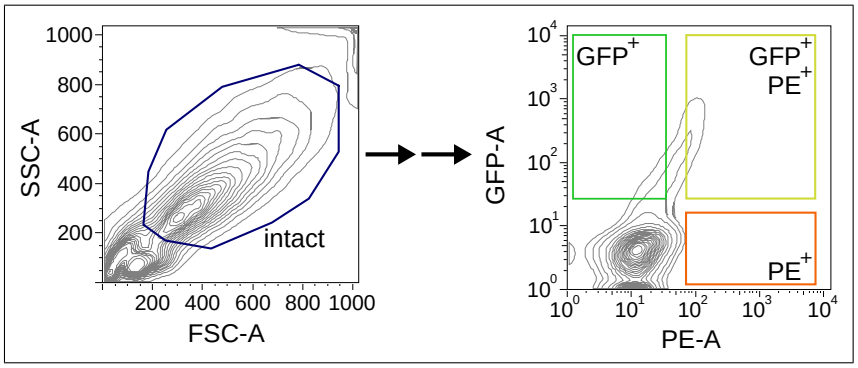

Figure 3.24: *Gating strategy for the FACS-based masking assay. Intact cells were gated using several steps of FSC and SSC gating. The gates used to isolate single positive or double positive cells are shown to the right. In this example co-transfected cells are shown. The intensities of CD4 signals of the gated cells were used to calculate the fraction of surface CD4 for the respective subpopulation.*

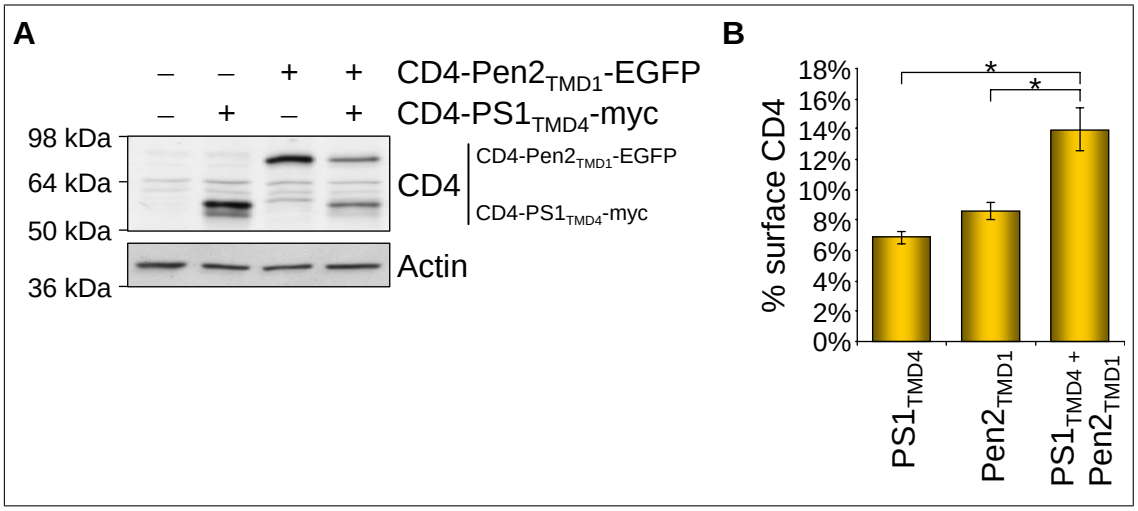

Figure 3.25: *Quantification confirmed increased surface CD4 levels after co-expression of CD4-Pen2$_{TMD1}$-EGFP with CD4-PS1$_{TMD4}$-myc. CD4-Pen2$_{TMD1}$-EGFP (Pen2$_{TMD1}$) and CD4-PS1$_{TMD4}$-myc (PS1$_{TMD4}$) were expressed separately or together in Cos-7 cells. A) Transfected Cos-7 cells were lysed using STEN lysis buffer and Western blot analysis was performed with anti-CD4 and anti-βActin antibodies. B) Transfected cells were stained for intracellular myc epitope and either for surface CD4 or for total CD4. Cells were measured by FACS using appropriate gates for the respective subpopulation (PE$^+$, GFP$^+$ or PE$^+$GFP$^+$) as described in figure 3.24. The geometric mean of the fluorescence intensities was determined and the ratios of surface CD4 to total CD4 were calculated for the respective subpopulations. The error bars depict of n=4 experiments.*

3.4.3 Overexpression of PS1-TMD4 interferes with γ-secretase assembly

As described before, it was initially speculated whether the overexpression of the Pen2-TMD1 could interfere with the γ-secretase assembly. In work from our lab and in the course of this work an interference of CD4-Pen2$_{TMD1}$ expression and γ-secretase maturation and activity was disproved (data not shown).

In a similar approach it was tested if the isolated overexpression of PS1-TMD4 interfered with γ-secretase assembly. To this end, CD4-PS1$_{TMD4}$ was stably expressed in HEK-293 cells. The processing of transiently transfected NotchΔE-EGFP (provided by Kerstin Hünniger) to Notch intracellular domain (NICD)-EGFP was used to assess γ-secretase activity. It was shown before that NotchΔE was an immediate substrate for γ-secretase (Schroeter *et al.*, 1998). The cleavage product NICD-EGFP was nicely detectable with a neoepitopic antibody against the NICD N-terminus. As an additional control HEK-293 cells stably expressing an shRNA against Pen2 were used.

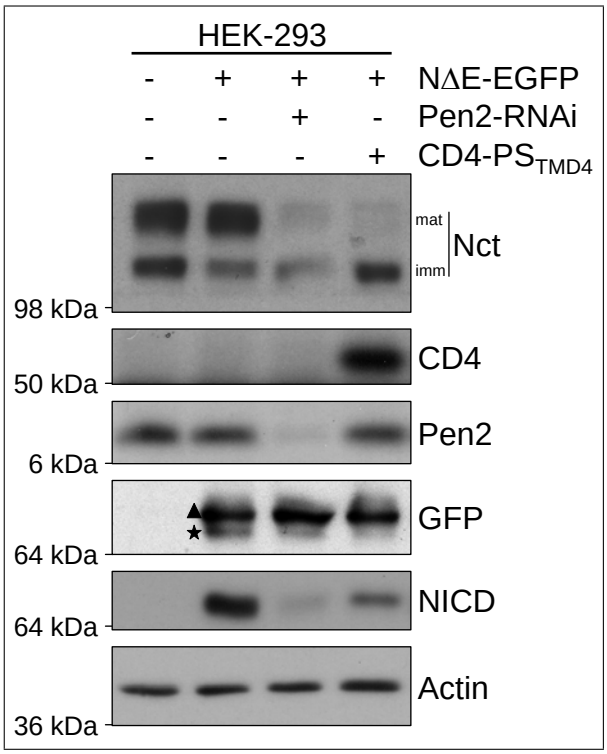

Figure 3.26: *Stable overexpression of PS1-TMD4 interfered with γ-secretase assembly. HEK-293 wt cells or HEK-293 stably expressing an shRNA against Pen2 or HEK-293 cells stably expressing CD4-PS1$_{TMD4}$ were transiently transfected with NotchΔE-EGFP (NΔE-EGFP). Cells were lysed 24 h later, subjected to Western blotting and probed with antibodies against the indicated proteins. The triangle marks the γ-secretase substrate NotchΔE-EGFP and the star the cleavage product Notch intracellular domain (NICD)-EGFP. Note that the anti-NICD antibody is neoepitopic, thus only cleaved NotchΔE-EGFP is detected.*

As expected, HEK-293 cells with a stable knock down of Pen2 lacked mature Nct, since the assembly and trafficking of γ-secretase was impaired by the lack of the rate-limiting subunit Pen2 (Steiner *et al.*, 2002; Prokop *et al.*, 2004). The reduced amount of mature γ-secretase resulted in a strong decrease in NotchΔE-EGFP cleavage as demonstrated by the reduced NICD-EGFP levels (figure 3.26B, lane 3). HEK-293 cells stably expressing CD4-PS1$_{TMD4}$ displayed a comparable reduction of mature Nct, although Pen2 levels remained unchanged. Likewise, the reduced levels of mature γ-secretase resulted in a decreased processing of NotchΔE-EGFP to NICD-EGFP (figure 3.26B, lane 4).

To confirm these results, we analysed the localisation of NotchΔE and its cleavage product via the fused EGFP moiety. To this end, HEK-293 cells, HEK-293 cells stably expressing a Pen2-shRNA and HEK-293 cells stably expressing CD4-PS1$_{TMD4}$ were transiently transfected with NotchΔE-EGFP. Subsequently, cells were fixed, stained with an anti-CD4 antibody and DAPI and subjected to immunofluorescence microscopy. Confocal-like optical sections through the nuclei were taken using an apotome slider module. As described by Schroeter *et al.*, 1998, NICD contained

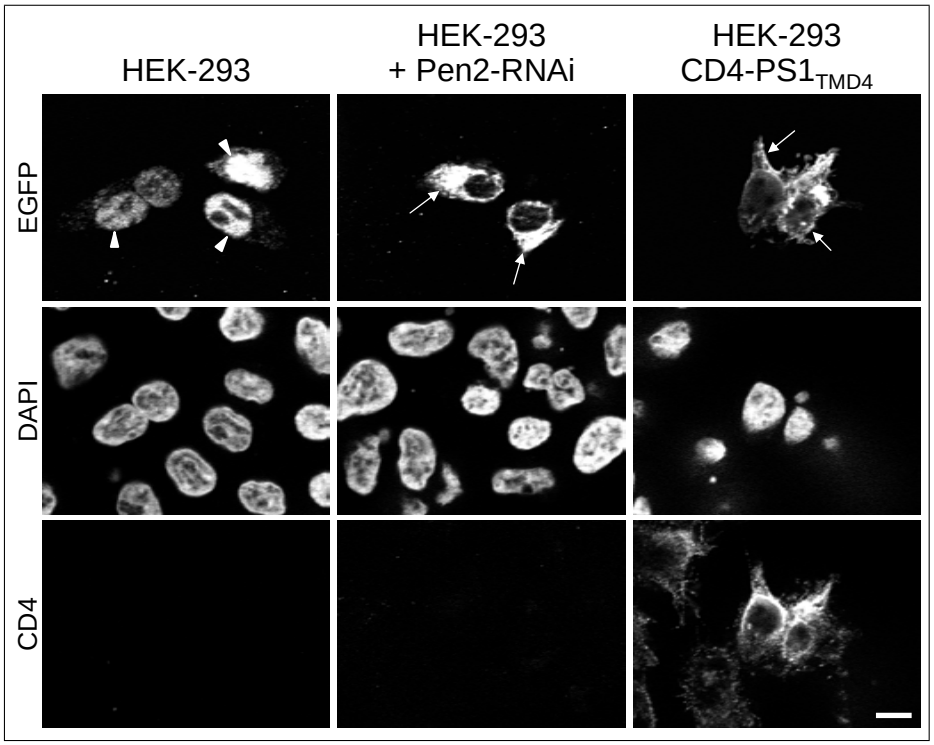

Figure 3.27: *Stable overexpression of PS1-TMD4 inhibited the cleavage of the γ-secretase substrate NotchΔE. HEK-293 wt cells or HEK-293 stably expressing an shRNA against Pen2 or HEK-293 cells stably expressing CD4-PS1$_{TMD4}$ were grown on cover slips and transiently transfected with NotchΔE-EGFP. Subsequently, cells were fixed, stained with an anti-CD4 antibody and DAPI and subjected to immunofluorescence microscopy. Confocal-like optical sections were taken using an apotome slider module. Scalebar 10 μm. Arrowheads, nuclear localisation; Arrows, extra-nuclear localisation (PM and secretory pathway).*

several nuclear localisation signals. Thus, NICD-EGFP accumulated in the nucleus of HEK-293 cells after the cleavage of NotchΔE-EGFP by γ-secretase (figure 3.27, left column). In HEK-293 cells stably expressing a Pen2-shRNA and HEK-293 cells stably expressing CD4-PS1$_{TMD4}$ NICD-EGFP was localised to the extra-nuclear space. Since these cells lacked γ-secretase activity, NICD-EGFP stayed attached to the membrane in its precursor form NotchΔE-EGFP. The lack of plasma membrane staining and the strong perinuclear staining resulted from the accumulation of the transiently overexpressed NotchΔE-EGFP in the ER and Golgi apparatus.

In summary, these results confirmed and extended the findings by Watanabe *et al.*, 2005, who demonstrated that the binding to CD4-PS1$_{TMD4}$ stabilised free Pen2. Moreover, overexpressed CD4-PS1$_{TMD4}$ acted dominant-negative on γ-secretase assembly, most probably by sequestering unassembled Pen2.

4 Discussion

It was the aim of this work to provide evidence for the quality control hypothesis for γ-secretase assembly proposed by Kaether *et al.*, 2004. This hypothesis suggests that all unassembled γ-secretase subunits and assembly intermediates are retained in the ER by specific ER retention signals. If the complex is properly assembled these signals are inactivated and thus complex export from the ER to the sites of γ-secretase activity is permitted. By employing such a quality control system the cell can assure that nonfunctional or even dysfunctional complexes do not interfere with normal cellular processes.

4.1 TMD-based ER retention signals are found in different γ-secretase subunits

It has been shown that γ-secretase assembles in the early compartments of the secretory pathway (Kim *et al.*, 2004; Capell *et al.*, 2005). Although, it was proposed that ER retention signals on unassembled subunits must exist (Kaether *et al.*, 2004), at the beginning of this work only one ER retention signal had been identified on all subunits. This signal is located in the C-terminus of PS1, consists of a stretch of 22 amino acids (ALPALPISITFGLVFYFATDYL)(Kaether *et al.*, 2004) and does not resemble other known ER retention signals. It is highly conserved between species (Tomita *et al.*, 2001) and at least partially contributes to the ninth TMD of PS1 (Kaether *et al.*, 2004; Spasic *et al.*, 2006).

The hypothesis by Kaether *et al.*, 2004 already implies the presence of ER retention signals on every single γ-secretase subunit. Otherwise, only some subunits would be retained in the ER while others proceed to later compartments of the secretory pathway. The resulting spatial separation would obviate a proper complex assembly. Thus, the first step in this work was the identification of further ER retention signals in γ-secretase subunits.

4.1.1 The Pen2-TMD1 contains an ER retention signal

Data from others (Bergman *et al.*, 2004a) and from our lab already suggested the presence of an ER retention signal in Pen2. The application of CD4 as a reporter for ER retention signals had been well established and a broad spectrum of methods is at hand to analyse the subcellular localisation of CD4 (Nilsson *et al.*, 1989;

Zerangue *et al.*, 1999; Kaether *et al.*, 2004). By applying this reporter protein the ER retention signal in Pen2 was narrowed down to the TMD1 while the presence of further retention signals in other parts of the protein was disproved (Kaether *et al.*, 2007).

To obtain ER retention of CD4-Pen2$_{TMD1}$ the Pen2-TMD1 and the three adjacent cytoplasmic residues (REA) had to be present (figure 3.1A). Individually, neither the Pen2-TMD1 nor the REA sequence were sufficient to confer ER retention to CD4. At present, no explanation for the necessity of the three residues exists. Eventually, they are needed to delimit the TMD and thereby facilitate the correct insertion of the TMD into the membrane. The relevance of the flanking amino acids for TMD-based ER retention signals was also described by others. Spasic *et al.*, 2007 described an ER retention signal in the Nct-TMD. To confer ER retention to their reporter protein telencephalin, 10 adjacent lumenal amino acids from Nct have to be exchanged together with the Nct-TMD.

In contrast to cytoplasmic ER retention signals no consensus sequence exists for TMD-based signals. In literature polar or even charged residues in the context of a hydrophobic TMD can act as an ER retention signal (Bonifacino *et al.*, 1990a; Letourneur and Cosson, 1998; Sato *et al.*, 2003). In the Pen2-TMD1 mutagenesis of a single asparagine at position 16 of the TMD to leucine results in the partial surface transport of CD4-Pen2$_{TMD1}$ (Johanna Scheuermann, published in Kaether *et al.*, 2007). This demonstrates that the retention signal in Pen2 follows the described pattern for other TMD-based retention signals. The signals described by Bonifacino *et al.*, 1990a and Letourneur *et al.*, 1995 not only target the bearing proteins to the ER but also for ERAD and unassembled Pen2 is targeted for ERAD as well (Bergman *et al.*, 2004a). Thus, it was tested if the retention signal in the Pen2-TMD1 is simultaneously responsible for the ERAD targeting and degradation of Pen2. Our results suggest the opposite. In case of Pen2 the presence of the polar asparagine stabilises the protein, clearly indicating that other mechanisms are involved. The observed destabilisation of Pen2 after mutagenesis of the asparagine was even more pronounced when the adjacent residues or the entire half of the TMD were mutated. These findings can be easily explained by the altered trafficking of the Pen2 mutants. In work from our lab is was shown that the trafficking of Pen2$_{N/L}$ to the cell surface is increased (Christoph Kaether, published in Kaether *et al.*, 2007, figure S2), most likely due to the reduced binding to the retention factor Rer1 (see section 4.2 and figure 3.14). The altered trafficking might result in lysosomal degradation of the Pen2 mutants. Similarly, lysosomal degradation was observed for the α-subunit of the nicotinic acetylcholine receptor (nAChR) which is released from the ER after Rer1 knockdown (Christina Valkova, unpublished data). Furthermore, Δ*rer1* yeast strains show vacuolar degradation of Rer1 substrates that are retained in the ER of wildtype strains (Sato *et al.*, 2003). However, to really prove this hypothesis, the experiment has to be repeated either in the presence of inhibitors of lysosomal protein degradation (e.g. NH_4Cl) or after Rer1 knockdown. The latter should result in a decreased stability of wildtype Pen2 (due to a lack of retention) whereas treatment with NH_4Cl should stabilise the Pen2 mutants. As an alternative explanation for the observed instability of the Pen2 mutants, it could be

speculated that the asparagine is needed for the stabilisation of other polar residues in the Pen2-TMD2. The Pen2-TMD2 contains a serine and a glutamine which might destabilise Pen2 in the absence of the opposing asparagine in the Pen2-TMD1. As a result the destabilised Pen2 mutants are degraded by ERAD. This hypothesis could be examined by the use of Brefeldin A (BFA) or inhibitors of the proteasome (e.g. MG-132) in the same experimental setup. BFA blocks the transport from the ER to the Golgi and thus would allow ER-associated degradation for all GFP-Pen2 variants without an overlaying trafficking effect. On the other hand, MG-132 blocks proteasomal degradation which is utilised by ERAD.

Similar experiments on the Pen2 stability were performed by Bergman *et al.*, 2004a. In comparison with their results it can be noticed that the observed halflife of Pen2 is much lower in their study. This discrepancy is most likely due to the fused EGFP moiety used here, which forms a very stable structure and attenuates protein ubiquitinylation and thus increases the halflife of Pen2 (Baens *et al.*, 2006).

4.1.2 A WNF motif is part of an ER retention signal in the PS1-TMD4

As aforementioned, the presence of polar amino acids is the only loose consensus for TMD-based ER retention signals found so far. Interestingly, an asparagine in the PS1-TMD4 was shown to be important in a totally different context. This asparagine is part of the binding site for Pen2 in the PS1-TMD4 (Kim and Sisodia, 2005a; Watanabe *et al.*, 2005). It was tested in the present work whether this asparagine is also part of an ER retention signal or not. By applying the same approaches as for the signal in the Pen2-TMD1 it was shown that the PS1-TMD4 indeed contains an ER retention signal. Moreover, the PS1-TMD4 not only confers ER retention to a CD4 reporter protein but also to Tac. Tac (IL-2 receptor α subunit) has been extensively used to study ER retention signals in the past (Bonifacino *et al.*, 1990b; Letourneur *et al.*, 1995; Wang *et al.*, 2002).

By mutating the polar asparagine and the two flanking residues to alanine (WNF→AAA mutation, CD4-PS1$_{TMD4mut}$) surface transport of the CD4 reporter is partially restored. For CD4-PS1$_{TMD4mut}$ twofold more CD4 reporter protein is transported to the plasma membrane in comparison to CD4-PS1$_{TMD4}$. Although this increase is statistically significant, it does not represent a complete loss of retention as can be seen in comparison to wildtype CD4. For wildtype CD4, which represents the upper limit of the assay scale and the complete absence of ER retention, 53.8 % of the reporter protein is at the cell surface. This finding can be explained by the rapid turnover of the protein. In contrast, inferring from the deglycosylation assay and the FACS analysis more than 50 % of the retention capacity is still intact in the mutated PS1-TMD4. Thus other residues in the PS1-TMD4 contribute to the ER retention signal.

To get an idea about the other involved residues, the PS1-TMD4 is compared with the TMD of the yeast protein Sec71p. The ER retention signal in the TMD of Sec71p was intensively studied and two critical polar residues (Tyr, Ser) were identified by mutagenesis (Sato *et al.*, 2003). Individual mutation of either residue

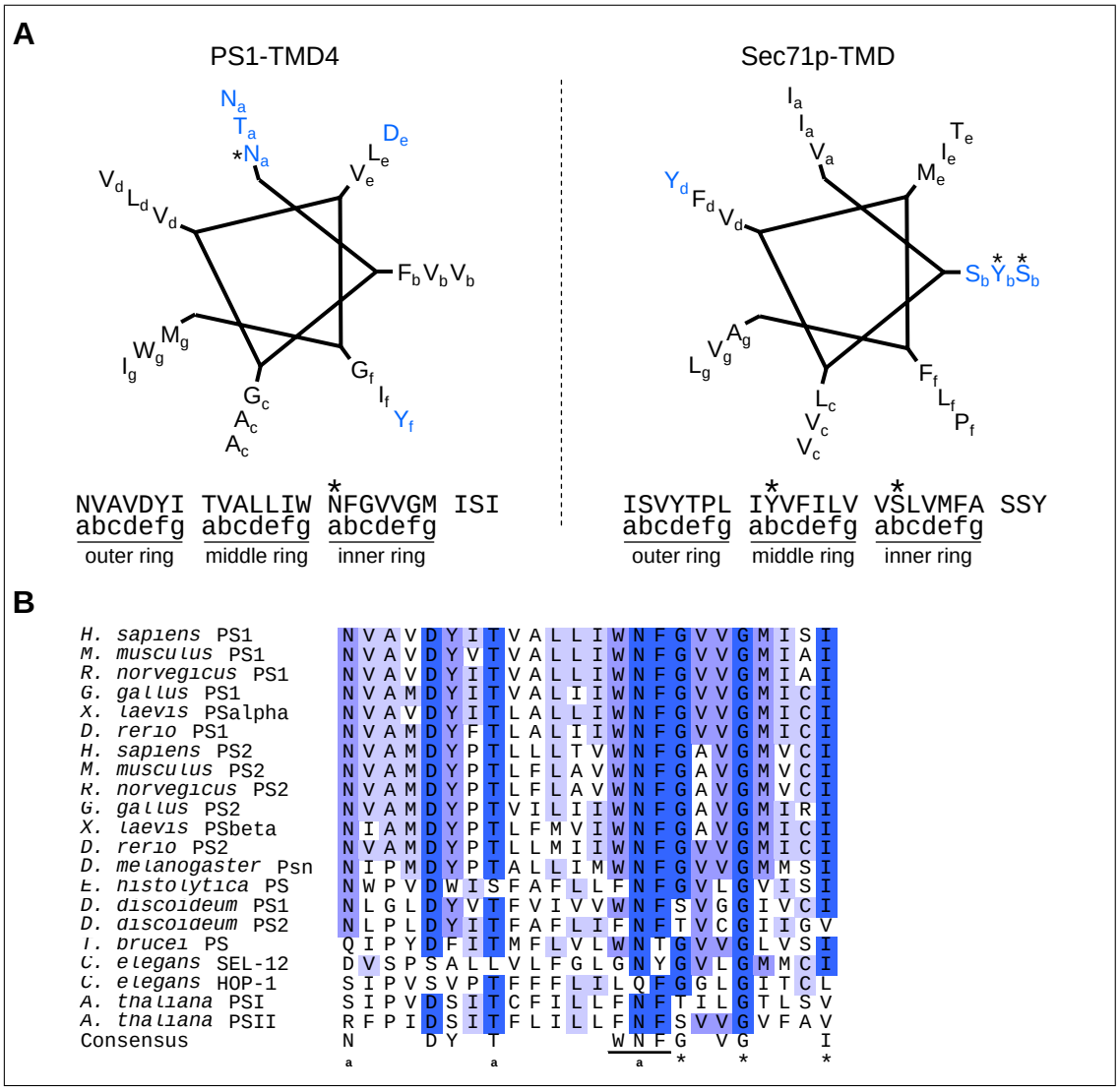

Figure 4.1: *TMD-based ER retention signals can be based on several polar residues with a defined interspace. A) Comparison between the PS1-TMD4 and the Sec71p-TMD in a simplified helical wheel projection. The projection assumes 3.5 amino acids per turn and the amino acids are labelled from a to g, which corresponds to two turns of the helix. Accordingly, for every seventh amino acid the same relative position is reached again. The last three (most C-terminal) amino acids of the helices are not shown to simplify the picture. The projection covers 3×7 amino acids resulting in three rings in the projection. Polar or charged residues are coloured in blue and residues that have been mutated in this study (PS1-TMD4) or in Sato* et al., *2003 (Sec71p-TMD) are marked with an asterisk. B) Alignment of PS-TMD4. Darker blue depicts a higher degree of conservation. The small a indicates residues that are located to the a-position in the helical wheel projection of PS1-TMD4. The WNF motif that has been mutated in this study is underlined. The small asterisks indicate residues that were found mutated in cases of FAD.*

to leucine in the context of a reporter protein led only to partial release of the reporter from the ER. In a helical wheel projection of Sec71p both residues are found at the same side of the α-helix of the TMD. Together with another serine at the same side a polar interface is formed rendering the α-helix of the Sec71p-TMD amphipathic (figure 4.1A, right helix, 3 o'clock). To permit ER exit, the polar interface has to be mutated completely . Similarly, the asparagine in the WNF motif of the PS1-TMD4 is part of a polar interface comprised of two asparagines, a threonine and an aspartate (figure 4.1A, left helix, 11 o'clock; figure 4.3). This polar interface of the helix is highly conserved over all species and even in cases where a residue is not conserved another polar residue is present instead (figure 4.1B). Thus, it is likely that these other polar residues of the PS1-TMD4 contribute to ER retention and that mutation of these residues to non-polar amino acids allows ER export of the CD4 reporter. A very similar polar interface comprising an ER retention signal was described for the Nct-TMD (Spasic *et al.*, 2007). The polar interface of the TMD4 is conserved between PS1 and PS2 (figure 4.1B). Hence, it is likely that the PS2-TMD4 also contains an ER retention signal, although this has not yet been tested explicitly.

The presence of two ER retention signals in the PS1-TMD4 (WNF) and the PS1-TMD9 (PALP) raises the question of the relevance of the individual signals. To address this question both signals were mutated individually or together in PS1-EGFP (PE). In contrast to the findings by Kaether *et al.*, 2004 no ER-located PE was visible in HeLa Kyoto cells (figure 3.12). This discrepancy can be explained by the different cell line used here (HeLa Kyoto instead of HEK-293) and/or the lower expression level of PE in the HeLa Kyoto cells. The low expression prevents accumulation of unassembled PE in the ER, since all newly synthesised PE is immediately bound by Nct/Aph-1 heterodimers and after the binding of Pen2 a complete γ-secretase complex is formed. Subsequently this complex is transported to the plasma membrane, resulting in the absence of ER staining in the steady-state. Although the absence of unassembled PE was not formally demonstrated here, other observations support this interpretation. It was shown by several groups, that exogenous expression of functional PS1 variants results in a reduced expression of endogenous PS1 and PS2 (reviewed in De Strooper, 2003). This phenomenon prevents the competition of the exogenously expressed PE species with endogenous PS1/PS2 for the binding to the Nct/Aph-1 heterodimer and allows the rapid incorporation of the exogenously expressed PE variants. Hence, the described reduction of ER staining for PE$_{-PALP}$ (Kaether *et al.*, 2004) could not be observed, because already for the stably expressed PE no ER staining was visible.

Interestingly, mutation of the second ER retention motif in the PS1-TMD4 (PE$_{-WNF}$) resulted in the ER localisation, a finding which was surprising at first glance. This observation can be explained by the altered assembly status of PE$_{-WNF}$, because the WNF motif also serves as a binding site for Pen2. In contrast to PE or PE$_{-PALP}$, PE$_{-WNF}$ does not assemble into complete γ-secretase complexes and accumulates in trimeric assembly intermediates with Nct and Aph-1. In these assembly intermediates additional ER retention signals are not inactivated and the heterotrimer of Aph-1, Nct and PE$_{-WNF}$ stays in the ER. In contrast, PE and

PE_{-PALP} are incorporated into a complete γ-secretase complex and ER retention signals are inactivated, resulting in the observed plasma membrane localisation of PE and PE_{-PALP} complexes. In summary, it becomes apparent that the comparison of PE_{-PALP} and PE_{-WNF} is impossible due to their different assembly status. Nevertheless, it is interesting that the double mutant $PE_{-PALP-WNF}$ was located to the ER. This implies that further ER retention signals contribute to the localisation of the trimeric assembly intermediate.

These signals are not necessarily limited to PE but could also be located in the other subunits Aph-1 and Nct. For instance, the folding status of the highly glycosylated Nct ectodomain could serve as an additional assembly sensor and ER retention signal. The folding of the Nct ectodomain into a trypsin-resistant conformation probably occurs in the ER, because it does not require the extensive glycosylation obtained in the later Golgi. This is demonstrated by an artificially ER-localised Nct that becomes trypsin-resistent after the complete assembly of an ER-localised γ-secretase complex (Capell *et al.*, 2005). The unfolded Nct ectodomain could be bound by chaperones like calnexin and calreticulin in the ER until it undergoes a conformational switch after the correct γ-secretase assembly. In this way, the Nct ectodomain could also serve as an assembly sensor, explaining why the Nct/Aph-1/$PE_{-PALP-WNF}$ heterotrimer was located in the ER. However, additional signals could be located in any of the three subunits.

To explicitly test if there are other ER retention signals in PS1 but the described ones in the TMD4 and the TMD9, the last seven amino acids were deleted in all PE variants. The resulting $PE_{\Delta 7}$ variants are not bound to assembly intermediates since the binding to Nct is obviated (Kaether *et al.*, 2004). All $PE_{\Delta 7}$ variants were located in the ER in stably expressing HeLa Kyoto cells, which indicates that additional ER retention signals have to exist within PS1. However, none of the classical RXR-type or KKXX-type ER retention signals can be found in the cytoplasmic domains of PS1. TMD-based or atypical cytoplasmic retention signals could exist that are responsible for the ER localisation of the $PE_{\Delta 7}$ variants. On the other hand, it is possible that the ER export of PS1 depends on the presence of ER export signals which might be provided by other subunits or which become exposed after the proper complex assembly. The presence of more than two ER retention signals in PS1 does not necessarily render the described signals insignificant. Rather, it is likely that each and every signal is involved in probing a particular aspect of the assembly of γ-secretase. Following the hypothesis proposed by Kaether *et al.*, 2004, every signal could for instance sense one subunit-subunit interaction (see section 4.3).

The observation that all $PE_{\Delta 7}$ variants were located in the ER is in contrast to the findings by Kaether *et al.*, 2004, who described that unassembled PE_{-PALP} was released from the ER in HEK-293 cells. Their results imply that the signal in the PS1-TMD9 (PALP) is the most important and dominating signal in PS1. This is disproven by the ER localisation of the $PE_{\Delta 7-PALP}$ observed in the present study.

Just like for Pen2, the question raises if the polar residues in the ER retention signal of the PS1-TMD4 are also a degradation signal. Additionally, the PS1-TMD9 also contains polar residues that contribute to ER retention (Kaether *et al.*, 2004). Both signals described for PS1 could provide an easy explanation for the observed

instability of non complex-associated presenilin (Edbauer *et al.*, 2002; Takasugi *et al.*, 2003), but this has to be tested experimentally.

4.2 Similar TMD-based ER retention signals are recognised by different mechanisms

Little knowledge exists on how TMD-based ER retention is accomplished. The only described protein that recognises TMD-based signals is the yeast protein Rer1p which is highly conserved from yeast to human (Sato *et al.*, 1995; Boehm *et al.*, 1997; Massaad *et al.*, 1999). It was tested if mammalian Rer1 accomplishes the ER localisation of PS1 and Pen2, because both contain potential Rer1-dependent signals. By applying CD4 reporter proteins it was shown that only the signal in the Pen2-TMD1 depends on Rer1 and thus Pen2 is the first identified substrate of mammalian Rer1. Knockdown of Rer1 using siRNA caused an increased surface localisation of CD4-Pen2$_{TMD1}$, although a complete release (meaning similar localisation like wildtype CD4) was not observed. The observed knockdown of Rer1 on the protein level was not complete and the residual Rer1 could be enough to ensure a partial ER retention of CD4-Pen2$_{TMD1}$. Moreover, it was observed in yeast that reporter proteins used to study Rer1p-dependent ER localisation, are partially ER retained even in a Δ*rer1* yeast strain (Sato *et al.*, 1996). It is possible that substrates of Rer1 are retained in the ER also by other mechanisms besides Rer1-dependent ER localisation, for instance by exclusion from ER exit sites (Barlowe, 2000).

In yeast it was shown that the Rer1p-dependent ER retention of reporter proteins is saturable. High overexpression of the reporter causes ER release which can be rescued by additional overexpression of Rer1p (Sato *et al.*, 1997). Similar effects have been observed in this study and the ER retention capacity seems to be cell type specific. Transient overexpression of CD4-Pen2$_{TMD1}$ in HEK-293 cells resulted in a prominent surface staining (data not shown), whereas the stable, more modest expression resulted in ER retention. On the other hand, transiently overexpressed CD4-Pen2$_{TMD1}$ was well retained in the ER in Cos-7 cells and to a lesser extent in HeLa Kyoto cells (data not shown). In summary, the mammalian Rer1-dependent ER retention of Pen2 follows the mechanisms described for yeast.

The interaction between Rer1 and unassembled Pen2 was demonstrated by co-immunoprecipitation with stably overexpressed proteins. The absence of other γ-secretase subunits but Pen2 in the co-immunoprecipitation under conditions that leave the γ-secretase intact pinpoint the specific binding of Rer1 to the unassembled Pen2. The amount of co-immunoprecipitating Pen2 was very low, most likely due to low levels of unassembled Pen2. These low levels result from the high instability of the unassembled protein (Bergman *et al.*, 2004a) and from the rate limiting character of the Pen2 incorporation into the γ-secretase (Takasugi *et al.*, 2003; Prokop *et al.*, 2004). Hence, unassembled Pen2 is either rapidly degraded or incorporated. Additionally, the amount of co-immunoprecipitating Pen2 is reduced by the transient character of the interaction with Rer1. Rer1 is a retrieval factor for Pen2 and only a minor amount of the unassembled Pen2 is in the process of retrieval from the ERGIC

or cis-Golgi. For this reasons, the co-immunoprecipitation of endogenous Pen2 is impeded since the levels of endogenous, unassembled Pen2 are even lower. Further evidence for the relevance of the Rer1-dependent ER retention of Pen2 results from HEK-293 cell stably overexpressing Rer1-V5. In these cells slightly elevated levels of Pen2 were observed (Christoph Kaether, published in Kaether *et al.*, 2007, figure 4). The increased binding of Rer1 to Pen2 in these cells might result in the protection of Pen2 against degradation in lysosomes and/or by ERAD.

In parallel to the present study, a report by Spasic *et al.*, 2007 failed to show the binding of Pen2 to Rer1. However, this contradictory finding might emerge from experimental differences. The use of chemical cross-linking by Spasic *et al.*, 2007 might be a bad choice since domains that could be cross-linked between Rer1 and Pen2 are very small. Rer1 has cytoplasmic domains but virtually no lumenal domains. In contrast, the cytoplasmic domain of Pen2 is relatively small and poor of lysines.

Interestingly, the signal in the PS1-TMD4 does not depend on Rer1, although it contains an asparagine in a similar position. The question raises what makes the difference between the PS1-TMD4 and the Pen2-TMD1. Both TMDs contain an ER retention signal based on polar residues and both TMDs are composed of amphipathic α-helices, because polar residues form a non-hydrophobic interface at one side of the helix (figure 4.3). From work in our lab and by others two other proteins are known that carry TMD-based ER retention signals but do not depend on Rer1. The TCRα chain contains an ER retention/degradation signal based on charged residues (Bonifacino *et al.*, 1990a) which does not depend on Rer1 (Slavomir Kacmar, unpublished data). On the other hand, the yeast protein Ufe1p possesses a TMD-based ER retention signal composed of a non-hydrophobic interface in the α-helix. Although this signal matches the signals in typical Rer1 substrates it does not depend on Rer1p (Rayner and Pelham, 1997). To allow a clearer view on differences that could determine the Rer1-dependency, the known substrate TMDs of Rer1 were compared with the TMDs of Ufe1p, TCRα and the PS1-TMD4 (table 4.1). Despite the heterogeneity of the amino acids that are important for the Rer1-mediated ER localisation it is remarkable that none of the TMDs interacting with Rer1 contains charged amino acids. In contrast, the TMDs of Ufe1p, TCRα and the PS1-TMD4 contain one or more charged residues. Eventually, the presence of charges within the hydrophobic context of a TMD interferes with the binding to Rer1 and instead other mechanisms are used for such signals.

To further substantiate this hypothesis the TMDs of Rer1 were examined, because they have to accomplish the interaction with substrate proteins that carry TMD-based retention signals. Especially the TMD4 of Rer1 exhibits a high degree of conservation from yeast to human (figure 4.2). This indicates that the Rer1-TMD4 could be of special importance for the interaction with Rer1 substrates. Furthermore, mutation of the tyrosine in the TMD4 to leucine resulted in a loss of interaction with Sec12p and the ER retention of Sec12p was abrogated, although the same mutation did not affect the interaction with Sec71p (Sato *et al.*, 2003)(figure 4.2, asterisk). It is known from the TCRα subunit that an interaction with amino acids of oppositional charge lead to stabilisation and ER release of TCRα (Bonifa-

Table 4.1: *TMDs that are recognised by Rer1 do not contain charged amino acids. The upper part of the table shows all TMDs that have been described to be substrates of Rer1. TMDs in the lower part are localised to the ER in a Rer1-independent manner. Residues that have been described to be critical for ER retention are underlined and charged amino acids have a yellow background.*

protein	TMD sequence	reference
Sec12p	LSFQLIYSLLVILIFNTFF	Sato *et al.*, 1995 Sato *et al.*, 1996
Sec71p	ISVYTPLIYVFILVVSLVMFASSY	Sato *et al.*, 1997 Sato *et al.*, 2003
Fet3p	IIAMTFSCFAGILGIITIAIYGMM	Sato *et al.*, 2004
Mns1p	WPVYYIAAIIAVITAISIGV	Massaad *et al.*, 1999 Massaad and Herscovics, 2001
Sed4p	YGLQIAGALVVLLLLVFNLFF	Sato *et al.*, 1996
Gas1p	VVFTSIISLSIAAGVGFA	Letourneur and Cosson, 1998
Nct	LITLTVGFGILIFSLIVTYCI	Spasic *et al.*, 2007
Pen2-TMD1	YYLGGFAFLPFLWLVNIFWFF	this study
Ufe1p	KLTTYGAIIMGVFILFLD	Rayner and Pelham, 1997
PS1-TMD4	NVAVDYITVALLIWNFGVVGMISI	this study
TCRα	NLSVMGLRILLLKVAGFNLLMTL	Bonifacino *et al.*, 1990a

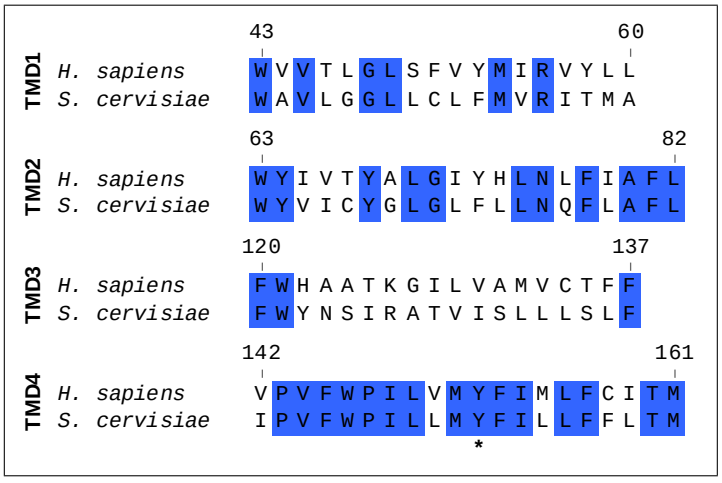

Figure 4.2: *The TMD4 of Rer1 is highly conserved from yeast to human. Alignment of the four TMDs of yeast and human Rer1. The TMD regions are in accordance with Boehm* et al.*, 1994. The asterisk depicts a tyrosine that is critical for the retention of Sec12p but not for the retention of Sec71p (Sato* et al.*, 2003).*

cino *et al.*, 1990a). It is likely that charged residues would be needed in the TMDs of Rer1 to stabilise an interaction with charged, TMD-based ER retention signals. However, the only conserved charged residue is an arginine in the less conserved TMD1.

Taken together, the retention signals in the Pen2-TMD1 and the PS1-TMD4 belong to two different classes of signals. On the one hand, retention signals in TMDs that contain charged residues like the ones in the PS1-TMD4 or the TCRα-TMD. These signals might also be involved in targeting the protein to ERAD, depending on the relative position of the charged residue within the TMD (Bonifacino *et al.*, 1991). These signals cannot be bound by Rer1 since Rer1 cannot stabilise the energetically unfavourable charge in the hydrophobic membrane. On the other hand, there are signals composed of polar residues like the one in the Pen2-TMD1. Those signals can be bound by Rer1 via interactions with polar residues in the TMDs of Rer1. However, this hypothesis is of course speculative at present and needs to be substantiated by experimental results.

4.3 Interaction of TMDs causes masking of ER retention signals

A quality control machinery that probes the assembly status of protein complexes via ER retention signals has to include mechanisms which finally permit the ER export of a correctly assembled complex. Accordingly, these retention signals have to be inactivated after the complex is properly assembled for instance by phosphorylation (Scott *et al.*, 2001), sterical masking (Margeta-Mitrovic *et al.*, 2000; Horak *et al.*, 2008), charge neutralisation (Bonifacino *et al.*, 1990a; Letourneur *et al.*, 1995) or binding of masking proteins (Standley *et al.*, 2000; Yuan *et al.*, 2003)(see also section 1.3.3). Both the PS1-TMD4 and the Pen2-TMD1 were implicated in the interaction between PS1 and Pen2 (Kim and Sisodia, 2005a,b; Watanabe *et al.*, 2005). Thus, it is an intriguing possibility that the protein-protein interaction between the two TMDs results in a masking of the respective ER retention signals.

This hypothesis was tested by co-expression of the isolated TMDs in the context of different reporter proteins. Indeed, a partial ER export was observed in cells co-expressing both reporter proteins. Since the Pen2-TMD1 and the PS1-TMD4 are retained in the ER by different mechanisms the observed effect is not due to a competition for limiting retention factors (see section 4.2). However, the proportion of released reporter proteins was rather small as can be judged from immunofluorescence and as was measured by FACS analysis. The reason for this could be the weakness of the interaction between the TMDs in the reporter proteins. In the full-length proteins the binding of Pen2 to PS1 is presumably stabilised by additional interactions between other parts of the subunits. A candidate region for such an interaction could be the C-terminus of Pen2, which is involved in the stabilisation of the PS1 NTF/CTF heterodimer (Prokop *et al.*, 2005; Kim and Sisodia, 2005b). The weak interaction between the isolated TMDs decreases the probability that the formed heterodimer of the reporter proteins stays tied together until it has passed

early Golgi compartments. Since later Golgi compartments do not contain further quality control checkpoints, both reporter proteins can proceed to the PM even if they fall apart again after having passed the cis-Golgi (Mezzacasa and Helenius, 2002).

For the PS1-TMD4 the interaction motif (WNF) is also part of the ER retention signal and thus the WNF sequence is bifunctional. However, for the Pen2-TMD1 the situation is less clear. Kim and Sisodia, 2005b provided evidence that the proximal two-thirds of the Pen2-TMD1 contain a binding site for PS1. In their work, transiently overexpressed Pen2 co-immunoprecipitated with PS1 even if the distal one-third of the TMD1 was replaced with a TMD from an unrelated protein. This construct lacks the asparagine which is important for the proper ER retention of Pen2. In contrast, work from our lab suggests that the distal part of the Pen2-TMD1 is of high relevance. Replacement of the nine most distal amino acids of the Pen2-TMD1 with the corresponding sequence from CD4 (GFP-Pen2$_{CD4}$) resulted in an increased instability of this GFP-Pen2 mutant (figure 3.6). Moreover, stably expressed GFP-Pen2$_{CD4}$ failed to rescue γ-secretase assembly and function in Pen2 knockdown cells (Johanna Scheuermann, published in Fassler *et al.*, 2009, figure 3). Both observations can be explained with an altered trafficking of GFP-Pen2$_{CD4}$ that leads to lysosomal degradation (see section 4.1). In the study of Kim and Sisodia, 2005b, the transient overexpression of the chimera that has one-third of the distal Pen2-TMD1 replaced might conceal this trafficking phenotype due to high expression levels. The overexpression of the Pen2 chimera results in an ER accumulation and thus allows binding to PS1, although both proteins would be spatially separated when expressed at lower levels. On the other hand, it is possible that the incapability of GFP-Pen2$_{CD4}$ to rescue the Pen2 knockdown is indeed due to an impaired binding to PS1. The proximal two-thirds of the Pen2-TMD1 could be needed for the correct spatial orientation of the distal one-third, which contains the asparagine. Additional experiments from our lab confirmed the binding of the Pen2-TMD1 as a whole to the PS1-TMD4, although this has not been dissected down to single amino acids or a motifs in the Pen2-TMD1 (Sebastian Klare, published in Fassler *et al.*, 2009, figure 3).

In summary, it was shown here for the first time how masking of TMD-based ER retention signals is achieved. Both, the PS1-TMD4 and the Pen2-TMD1 are bifunctional, since they contribute to the protein-protein interaction between PS1 and Pen2 and contain ER retention signals. This bifunctionality of TMDs in different complex subunits provides an effective way for the ER quality control to probe the assembly status of multimeric complexes. The binding of Pen2 to PS1 masks the ER retention signals in the PS1-TMD4 and the Pen2-TMD1 and thus marks this part of the complex as assembled. As assumed by Sato *et al.*, 2001, the higher affinity of the TMDs for the correct binding partner could ensure that components of the quality control mechanism do not interfere with complex assembly by competition. For the PS1-TMD4 the bifunctionality is provided by the WNF motif, which serves as a binding site for Pen2 and as an ER retention signal. The situation is less clear for the Pen2-TMD1. It was shown by our laboratory that the asparagine contributes to ER retention, whereas the localisation of the binding site for PS1 in the Pen2-TMD1

is still controversial.

The interaction between the PS1-TMD4 and the Pen2-TMD1 is schematised in figure 4.3. It is likely that the polar or charged residues in both TMDs face each other, because the exposure of hydrophilic amino acids to the hydrophobic environment of a membrane is energetically unfavourable. The interaction between non-hydrophobic amino acids in TMDs was shown before for several proteins (reviewed in Moore *et al.*, 2008). However, the detailed interactions between these amino acids and how they contribute to the specificity of the interaction between the Pen2-TMD1 and the PS1-TMD4 remains unclear. It could be tried to address this question with an *in silico* approach.

In the present study, the findings by Watanabe *et al.*, 2005 were confirmed and extended. The stable overexpression of the PS1-TMD4 via CD4-PS1$_{TMD4}$ resulted in an attenuation of γ-secretase assembly and thus in a decreased activity. The dominant-negative effect results most likely from a sequestration of Pen2 by the CD4 reporter protein. This would also explain the normal levels of Pen2 in these cells, since it was shown by Watanabe *et al.*, 2005 that CD4-PS1$_{TMD4}$ is sufficient to protect unassembled Pen2 from degradation. Taking into account our results on the masking, it could be argued that CD4-PS1$_{TMD4}$/Pen2 heterodimers should be transported to the plasma membrane. Indeed, cells stably expressing CD4-PS1$_{TMD4}$ showed significantly more CD4 at the plasma membrane than cells stably expressing CD4-Pen2$_{TMD1}$ or CD4-RXR. However, no elevated surface localisation could be observed by immunofluorescence. This might by due to the relatively high overexpression of CD4-PS1$_{TMD4}$ in comparison to the much lower levels of endogenous Pen2. The small fraction of released CD4-PS1$_{TMD4}$ is concealed by the much bigger fraction that does not bind to Pen2 and is accordingly retained in the ER. To ultimately test this hypothesis, CD4-PS1$_{TMD4}$ has to be expressed in stable Pen2 knockdown cells which should result in a stronger ER retention of the CD4 reporter protein.

Since stable overexpression of CD4-PS1$_{TMD4}$ interferes with γ-secretase assembly, it was analysed whether CD4-Pen2$_{TMD1}$ has the same effect. Stable overexpression of CD4-Pen2$_{TMD1}$ did not result in a reduction of γ-secretase assembly, although this finding is a little bit incomprehensible at first glance. In contrast to CD4-PS1$_{TMD4}$, CD4-Pen2$_{TMD1}$ could interfere with the assembly even in two ways. First and obviously, CD4-Pen2$_{TMD1}$ could compete with endogenous Pen2 for the binding to PS1. However, the big ectodomain of CD4 might constrain the binding to PS1 for sterical reasons, especially under consideration of the almost 20-fold smaller lumenal domains of Pen2. To address this issue, a CD4-Pen2$_{TMD1}$ stub construct was generated, lacking almost the entire ectodomain of CD4. Although this stub is localised to the ER as expected, no interference with the γ-secretase assembly was observed in preliminary experiments (data not shown). Secondly, stable, high level overexpression of CD4-Pen2$_{TMD1}$ should result in a saturation of the Rer1-dependent ER retention machinery as it was described in yeast (Sato *et al.*, 1997). As a consequence, the much lower expressed endogenous Pen2 should be transported to later Golgi compartments and eventually be degraded in the lysosomes (see section 4.1). The resulting spatial separation would then lead to an attenuation of

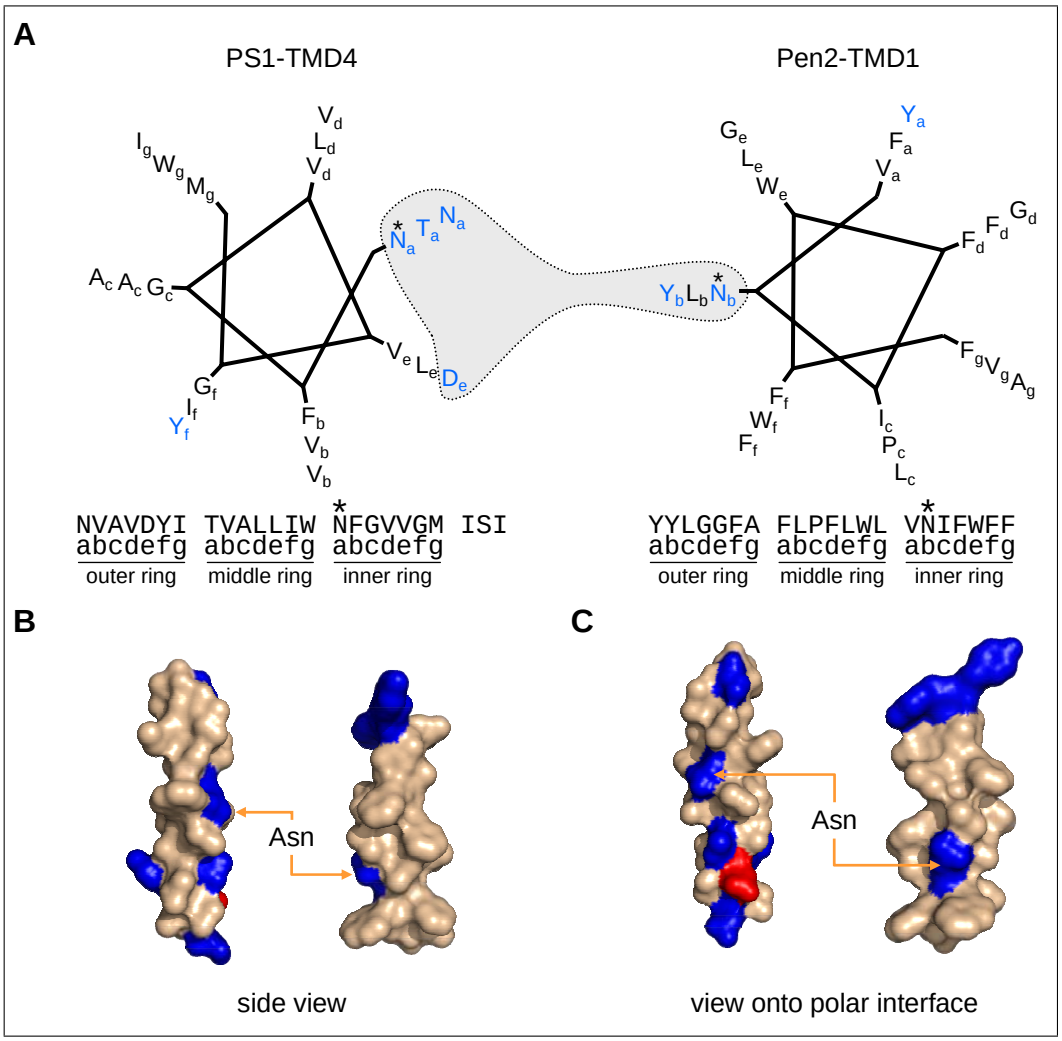

Figure 4.3: *The amphipathic helices of the PS1-TMD4 and the Pen2-TMD1 could interact via polar residues. A) Simplified helical wheel projection of the Pen2-TMD1 and the PS1-TMD4. The projection assumes 3.5 amino acids per turn and the amino acids are labelled from a to g, which corresponds to two turns of the helix. Accordingly, for every seventh amino acid the same relative position is reached again. The last three (most C-terminal) amino acids of PS1 are not shown to simplify the picture. The projection covers 3×7 amino acids resulting in three rings in the projection. Polar or charged residues are coloured in blue and residues that have been mutated in this study are marked with an asterisk. The polar interfaces of the helices could contribute to the protein-protein interaction between PS1 and Pen2 via their polar residues (highlighted in grey). B,C) Three-dimensional structures of the PS1-TMD4 and Pen2-TMD1 assuming an ideal α-helical structure for the TMDs. B) provides a side view with the polar interfaces facing each other. In C) a view onto the polar surfaces of the TMDs is shown. Pictures in B) and C) were generated with PyMOL (DeLano, 2008)*

the γ-secretase assembly. Although this experiment has not yet been performed, it mimics the situation of a long-time Rer1 knockdown. However, knockdown of Rer1 by siRNA over nine days did not lead to decreased levels of mature Nct, which would

be indicative of an impaired γ-secretase assembly (Christina Valkova, unpublished data). In contrast, Spasic *et al.*, 2007 observed a slightly decreased fraction of fully glycosylated Nct after 72 h of Rer1 knockdown. Although, their results match the predictions that were made here, their explanation is completely different. In summary, no convincing explanation can be given why the isolated overexpression of the Pen2-TMD1 does not interfere with the γ-secretase assembly. Sterical problems might be the reason for CD4-Pen2$_{TMD1}$, whereas this should not be the case for the stub construct. Further experiments with the stub and/or Pen2-TMD1 peptides might resolve this issue. Concerning the effect of an Rer1 knockdown or an overloading of the Rer1 machinery it is not clear to what extent the localisation of Pen2 to the ER depends on this mechanism. Experiments with Δ*rer1* yeast strains demonstrated that substrates of Rer1 are localised to the ER by additional mechanisms besides the Rer1 machinery (Sato *et al.*, 1996). Accordingly, it has to be analysed to what extent loss of Rer1 affects the ER localisation of Pen2. This question could be addressed with Rer1$^{-/-}$ MEF cells.

4.4 Conclusions and perspectives

In the present study, evidence was provided that supports the quality control hypothesis for the γ-secretase assembly which was initially proposed by Kaether *et al.*, 2004. New ER retention signals were identified in the PS1-TMD4 and the Pen2-TMD1. Both signals are based on polar residues that are part of a hydrophilic interface in the hydrophobic environment of a TMD. For the signal in the Pen2-TMD1 it was shown that it also affects the stability of Pen2, although it is not clear whether this happens via an interaction with a degradation machinery or via altered trafficking of Pen2. Furthermore, Pen2 was identified as the first substrate of Rer1-mediated ER retention in mammalian cells, whereas the signal in the PS1-TMD4 is Rer1-independent. In this context, first evidence suggests that there could be at least two different kinds of TMD-based ER retention signals, which are based on different machineries: TMD-based retention signals that are based on polar residues but lack charged amino acids are based on Rer1. On the other hand, signal-carrying TMDs that contain charged residues are Rer1-independent. The mechanism accomplishing the retention of such signals remains completely unknown.

As the major finding, it was shown that both the Pen2-TMD1 and the PS1-TMD4 are bifunctional. They confer ER localisation to their carrying proteins and constitute sites of protein-protein interaction. The bifunctionality of the TMDs provides a mechanism by which the ER retention signals can be masked in the properly assembled γ-secretase. Thus, they serve as a sensor for the ER quality control. The findings of the present work are summarised in the figure 4.4 which illustrates a model for the quality control of γ-secretase assembly.

For the first time detailed insight was provided into the mechanism that leads to the masking of TMD-based ER retention signals. Under consideration of the obtained results one can speculate that the masking of the retention signals in the Nct-TMD and the PS1-TMD9 results from similar a mechanism. Both domains are bifunctional as well, since they contain ER retention signals and are involved

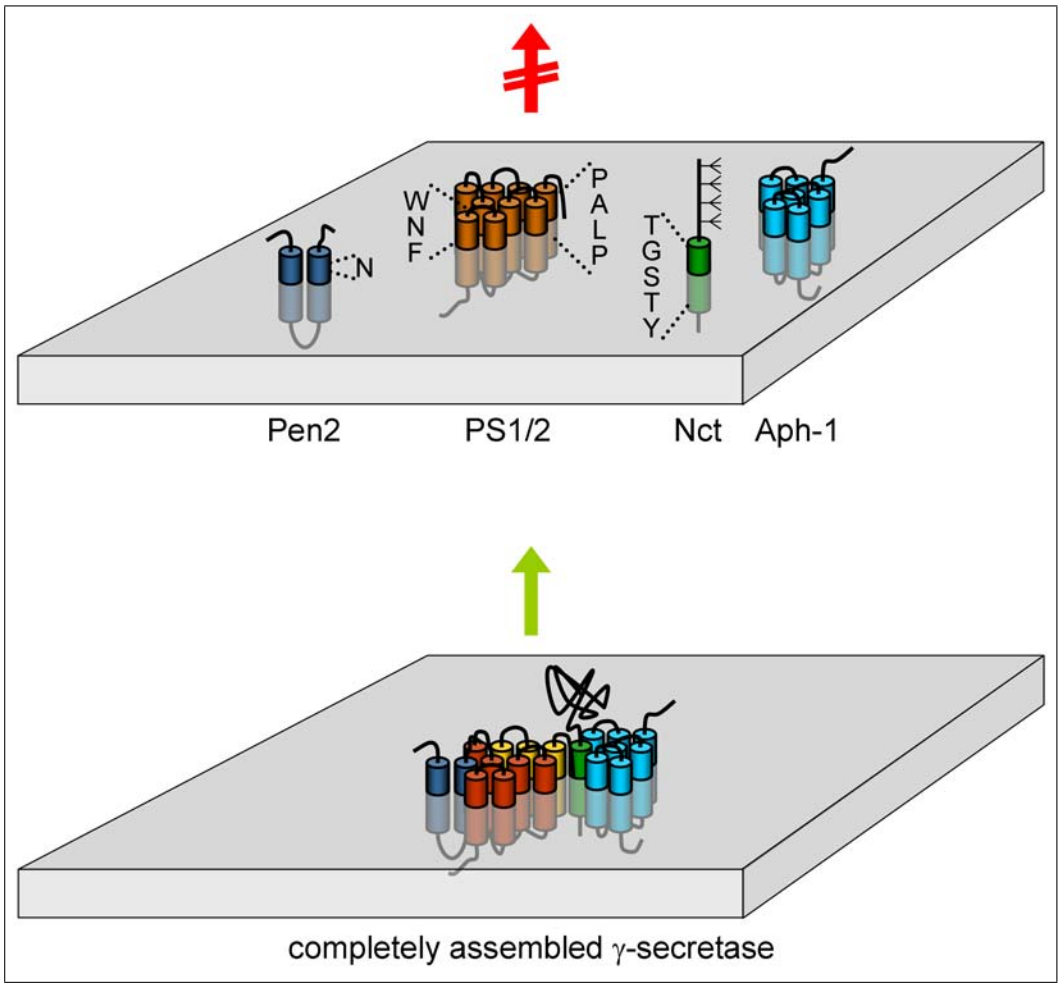

Figure 4.4: *Correct assembly of γ-secretase results in the inactivation of ER retention signals. ER retention signals have been identified in Pen2 (dark blue), PS1 (orange) and Nct (green). The signals in Pen2 and Nct depend on Rer1, whereas the machinery recognising the signals in PS1 is unknown. The binding of the Pen2-TMD1 to the PS1-TMD4 masks the signals in the two TMDs. The binding of the PS1 C-terminus to the Nct-TMD could cause the masking of the signals in the Nct-TMD and the spatially close PS1-TMD9, although this is speculative at present. Correct assembly of the γ-secretase results in the folding of the Nct ectodomain and in the endoproteolytic cleavage of PS1 holoprotein to PS1-NTF (red) and PS1-CTF (yellow). The completely assembled complex lacks open ER retention signals and is transported to the plasma membrane and/or endosomes.*

in protein-protein interaction either directly (Nct-TMD) or via adjacent regions (PS1-TMD9)(Kaether *et al.*, 2004; Spasic *et al.*, 2007). The binding of the last amino acids of the PS1 C-terminus to the Nct-TMD could mask the signals in the Nct-TMD. In parallel, this binding could result in a sterical masking of the closely neighbouring PS1-TMD9. Moreover, the findings of the present study could be generalised for the quality control of other multimeric membrane proteins, like cell surface receptors or ion channels. For instance, a TMD-based ER retention signal

has been described for the nAChR (Wang *et al.*, 2002) and data from out lab suggest that this signal depends on Rer1 (Christina Valkova, unpublished data). This signal could be masked by interactions between the multiplicity of TMDs found in the α-, β-, δ- and ϵ-subunit which finally form the functional nAChR with an $\alpha_2\beta\delta\epsilon$ stoichiometry.

The present study points to the relevance of the TMDs of γ-secretase for the proper assembly of the enzyme. Others showed that the TMDs are also of importance for the activity of γ-secretase. Besides the fact that the catalytically active residues are located in the TMDs 6 and 7 of presenilin, evidence emerges that the targeting of TMDs might be a promising approach for pharmacological intervention. It was demonstrated that isolated TMD peptides derived from the γ-secretase modulator TMP21 can reduce γ-secretase activity (Pardossi-Piquard *et al.*, 2009). Furthermore, recent findings suggest that some of the known γ-secretase modulators (GSMs, e.g. fenofibrate and flurbiprofen) target a region of the Aβ domain that is located in the TMD of APP (Kukar *et al.*, 2008). Another option described in the literature is the usage of computed helical anti-membrane proteins (CHAMPs). Experimental evidence demonstrated that CHAMPs can be used to disrupt TMD-based interactions between α- and β-integrins (Yin *et al.*, 2007). Similarly, it is possible that PS1-TMD4 derived peptides can be used to disrupt the γ-secretase complex and thereby inhibit γ-secretase activity in pathological situations.

Bibliography

Allinson, T. M. J., Parkin, E. T., Turner, A. J., and Hooper, N. M. ADAMs family members as amyloid precursor protein alpha-secretases. *J Neurosci Res* **74**(3), 342–352 (2003).

Alzheimer Disease & Frontotemporal Dementia Mutation Database. `http://www.molgen.ua.ac.be/ADMutations` (as of November 2009).

Aoe, T., Lee, A. J., van Donselaar, E., Peters, P. J., and Hsu, V. W. Modulation of intracellular transport by transported proteins: insight from regulation of COPI-mediated transport. *Proc Natl Acad Sci U S A* **95**(4), 1624–1629 (1998).

Baens, M., Noels, H., Broeckx, V., Hagens, S., Fevery, S., Billiau, A. D., Vankelecom, H., and Marynen, P. The dark side of EGFP: defective polyubiquitination. *PLoS One* **1**, e54 (2006).

Barlowe, C. Traffic COPs of the early secretory pathway. *Traffic* **1**(5), 371–377 (2000).

Bergman, A., Hansson, E. M., Pursglove, S. E., Farmery, M. R., Lannfelt, L., Lendahl, U., Lundkvist, J., and Näslund, J. Pen-2 is sequestered in the endoplasmic reticulum and subjected to ubiquitylation and proteasome-mediated degradation in the absence of presenilin. *J Biol Chem* **279**(16), 16744–16753 (2004a).

Bergman, A., Laudon, H., Winblad, B., Lundkvist, J., and Näslund, J. The extreme C terminus of presenilin 1 is essential for gamma-secretase complex assembly and activity. *J Biol Chem* **279**(44), 45564–45572 (2004b).

Bertram, L., McQueen, M. B., Mullin, K., Blacker, D., and Tanzi, R. E. Systematic meta-analyses of Alzheimer disease genetic association studies: the AlzGene database. *Nat Genet* **39**(1), 17–23 (2007).

Bertram, L. and Tanzi, R. E. The genetic epidemiology of neurodegenerative disease. *J Clin Invest* **115**(6), 1449–1457 (2005).

Bertram, L. and Tanzi, R. E. Thirty years of Alzheimer's disease genetics: the implications of systematic meta-analyses. *Nat Rev Neurosci* **9**(10), 768–778 (2008).

Bickel, H. Demenzsyndrom und Alzheimer Krankheit: Eine Schätzung des Krankenbestandes und der jährlichen Neuerkrankungen in Deutschland. *Gesundheitswesen* **62**(04), 211–218 (2000).

Boehm, J., Letourneur, F., Ballensiefen, W., Ossipov, D., Demolliere, C., and Schmitt, H. D. Sec12p requires Rer1p for sorting to coatomer (COPI)-coated vesicles and retrieval to the ER. *J Cell Sci* **110 (Pt 8)**, 991–1003 (1997).

Boehm, J., Ulrich, H. D., Ossig, R., and Schmitt, H. D. Kex2-dependent invertase secretion as a tool to study the targeting of transmembrane proteins which are involved in ER→Golgi transport in yeast. *EMBO J* **13**(16), 3696–3710 (1994).

Bonifacino, J. S., Cosson, P., and Klausner, R. D. Colocalized transmembrane determinants for ER degradation and subunit assembly explain the intracellular fate of TCR chains. *Cell* **63**(3), 503–513 (1990a).

Bonifacino, J. S., Cosson, P., Shah, N., and Klausner, R. D. Role of potentially charged transmembrane residues in targeting proteins for retention and degradation within the endoplasmic reticulum. *EMBO J* **10**(10), 2783–2793 (1991).

Bonifacino, J. S., Suzuki, C. K., and Klausner, R. D. A peptide sequence confers retention and rapid degradation in the endoplasmic reticulum. *Science* **247**(4938), 79–82 (1990b).

Capell, A., Beher, D., Prokop, S., Steiner, H., Kaether, C., Shearman, M. S., and Haass, C. Gamma-secretase complex assembly within the early secretory pathway. *J Biol Chem* **280**(8), 6471–8 (2005).

Capell, A., Kaether, C., Edbauer, D., Shirotani, K., Merkl, S., Steiner, H., and Haass, C. Nicastrin interacts with gamma-secretase complex components via the N-terminal part of its transmembrane domain. *J Biol Chem* **278**(52), 52519–52523 (2003).

Chen, F., Hasegawa, H., Schmitt-Ulms, G., Kawarai, T., Bohm, C., Katayama, T., Gu, Y., Sanjo, N., Glista, M., Rogaeva, E., Wakutani, Y., Pardossi-Piquard, R., Ruan, X., Tandon, A., Checler, F., Marambaud, P., Hansen, K., Westaway, D., George-Hyslop, P. S., and Fraser, P. TMP21 is a presenilin complex component that modulates gamma-secretase but not epsilon-secretase activity. *Nature* **440**(7088), 1208–1212 (2006).

Citron, M., Oltersdorf, T., Haass, C., McConlogue, L., Hung, A. Y., Seubert, P., Vigo-Pelfrey, C., Lieberburg, I., and Selkoe, D. J. Mutation of the beta-amyloid precursor protein in familial Alzheimer's disease increases beta-protein production. *Nature* **360**(6405), 672–674 (1992).

Cole, S. L. and Vassar, R. The role of amyloid precursor protein processing by BACE1, the beta-secretase, in Alzheimer disease pathophysiology. *J Biol Chem* **283**(44), 29621–29625 (2008).

Corder, E. H., Saunders, A. M., Strittmatter, W. J., Schmechel, D. E., Gaskell, P. C., Small, G. W., Roses, A. D., Haines, J. L., and Pericak-Vance, M. A. Gene dose of apolipoprotein E type 4 allele and the risk of Alzheimer's disease in late onset families. *Science* **261**(5123), 921–923 (1993).

Cosson, P. and Letourneur, F. Coatomer (COPI)-coated vesicles: role in intracellular transport and protein sorting. *Curr Opin Cell Biol* **9**(4), 484–487 (1997).

Dalbey, R. E. and Heijne, G. v. *Protein targeting, transport & translocation.* Academic Press, Amsterdam; San Diego, CA (2002).

De Strooper, B. Aph-1, Pen-2, and Nicastrin with Presenilin generate an active gamma-Secretase complex. *Neuron* **38**(1), 9–12 (2003).

DeLano, W. The PyMOL Molecular Graphics System. DeLano Scientific LLC, Palo Alto, CA, USA. `http://www.pymol.org` (2008).

Dries, D. R. and Yu, G. Assembly, maturation, and trafficking of the gamma-secretase complex in Alzheimer's disease. *Curr Alzheimer Res* **5**(2), 132–146 (2008).

Edbauer, D., Winkler, E., Haass, C., and Steiner, H. Presenilin and nicastrin regulate each other and determine amyloid beta-peptide production via complex formation. *Proc Natl Acad Sci U S A* **99**(13), 8666–8671 (2002).

Edbauer, D., Winkler, E., Regula, J. T., Pesold, B., Steiner, H., and Haass, C. Reconstitution of gamma-secretase activity. *Nat Cell Biol* **5**(5), 486–488 (2003).

Ellgaard, L. and Helenius, A. Quality control in the endoplasmic reticulum. *Nat Rev Mol Cell Biol* **4**(3), 181–191 (2003).

Fassler, M., Zocher, M., Klare, S., Guzman de la Fuente, A., Scheuermann, J., Capell, A., Haass, C., Valkova, C., Veerappan, A., Schneider, D., and Kaether, C. Masking of transmembrane-based retention signals controls ER-export of gamma-secretase. *Traffic* (*in press*) (2009).

Francis, R., McGrath, G., Zhang, J., Ruddy, D. A., Sym, M., Apfeld, J., Nicoll, M., Maxwell, M., Hai, B., Ellis, M. C., Parks, A. L., Xu, W., Li, J., Gurney, M., Myers, R. L., Himes, C. S., Hiebsch, R., Ruble, C., Nye, J. S., and Curtis, D. aph-1 and pen-2 are required for Notch pathway signaling, gamma-secretase cleavage of betaAPP, and presenilin protein accumulation. *Dev Cell* **3**(1), 85–97 (2002).

Frigerio, C. S., Piscopo, P., Calabrese, E., Crestini, A., Campeggi, L. M., di Fava, R. C., Fogliarino, S., Albani, D., Marcon, G., Cherchi, R., Piras, R., Forloni, G., and Confaloni, A. PEN-2 gene mutation in a familial Alzheimer's disease case. *J Neurol* **252**(9), 1033–1036 (2005).

Fullekrug, J., Boehm, J., Rottger, S., Nilsson, T., Mieskes, G., and Schmitt, H. D. Human Rer1 is localized to the Golgi apparatus and complements the deletion of the homologous Rer1 protein of Saccharomyces cerevisiae. *Eur J Cell Biol* **74**(1), 31–40 (1997).

Glenner, G. G. and Wong, C. W. Alzheimer's disease: initial report of the purification and characterization of a novel cerebrovascular amyloid protein. *Biochem Biophys Res Commun* **120**(3), 885–890 (1984).

Goldgaber, D., Lerman, M. I., McBride, O. W., Saffiotti, U., and Gajdusek, D. C. Characterization and chromosomal localization of a cDNA encoding brain amyloid of Alzheimer's disease. *Science* **235**(4791), 877–880 (1987).

Gu, Y., Chen, F., Sanjo, N., Kawarai, T., Hasegawa, H., Duthie, M., Li, W., Ruan, X., Luthra, A., Mount, H. T. J., Tandon, A., Fraser, P. E., and George-Hyslop,

P. S. APH-1 interacts with mature and immature forms of presenilins and nicastrin and may play a role in maturation of presenilin.nicastrin complexes. *J Biol Chem* **278**(9), 7374–7380 (2003).

Haass, C., Schlossmacher, M. G., Hung, A. Y., Vigo-Pelfrey, C., Mellon, A., Ostaszewski, B. L., Lieberburg, I., Koo, E. H., Schenk, D., and Teplow, D. B. Amyloid beta-peptide is produced by cultured cells during normal metabolism. *Nature* **359**(6393), 322–325 (1992).

Haass, C. and Selkoe, D. J. Soluble protein oligomers in neurodegeneration: lessons from the Alzheimer's amyloid beta-peptide. *Nat Rev Mol Cell Biol* **8**(2), 101–112 (2007).

Harter, C. and Wieland, F. The secretory pathway: mechanisms of protein sorting and transport. *Biochim Biophys Acta* **1286**(2), 75–93 (1996).

Hasegawa, H., Sanjo, N., Chen, F., Gu, Y.-J., Shier, C., Petit, A., Kawarai, T., Katayama, T., Schmidt, S. D., Mathews, P. M., Schmitt-Ulms, G., Fraser, P. E., and George-Hyslop, P. S. Both the sequence and length of the C terminus of PEN-2 are critical for intermolecular interactions and function of presenilin complexes. *J Biol Chem* **279**(45), 46455–46463 (2004).

Helenius, A. and Aebi, M. Intracellular functions of N-linked glycans. *Science* **291**(5512), 2364–2369 (2001).

Helenius, A. and Aebi, M. Roles of N-linked glycans in the endoplasmic reticulum. *Annu Rev Biochem* **73**, 1019–1049 (2004).

Horak, M., Chang, K., and Wenthold, R. J. Masking of the endoplasmic reticulum retention signals during assembly of the NMDA receptor. *J Neurosci* **28**(13), 3500–3509 (2008).

Ikonen, E. and Simons, K. Protein and lipid sorting from the trans-Golgi network to the plasma membrane in polarized cells. *Semin Cell Dev Biol* **9**(5), 503–509 (1998).

Jamieson, J. D. and Palade, G. E. Intracellular transport of secretory proteins in the pancreatic exocrine cell. I. Role of the peripheral elements of the Golgi complex. *J Cell Biol* **34**(2), 577–596 (1967a).

Jamieson, J. D. and Palade, G. E. Intracellular transport of secretory proteins in the pancreatic exocrine cell. II. Transport to condensing vacuoles and zymogen granules. *J Cell Biol* **34**(2), 597–615 (1967b).

Jamieson, J. D. and Palade, G. E. Intracellular transport of secretory proteins in the pancreatic exocrine cell. 3. Dissociation of intracellular transport from protein synthesis. *J Cell Biol* **39**(3), 580–588 (1968a).

Jamieson, J. D. and Palade, G. E. Intracellular transport of secretory proteins in the pancreatic exocrine cell. IV. Metabolic requirements. *J Cell Biol* **39**(3), 589–603 (1968b).

Kaether, C., Capell, A., Edbauer, D., Winkler, E., Novak, B., Steiner, H., and Haass, C. The presenilin C-terminus is required for ER-retention, nicastrin-binding and gamma-secretase activity. *Embo J* **23**(24), 4738–48 (2004).

Kaether, C., Haass, C., and Steiner, H. Assembly, trafficking and function of gamma-secretase. *Neurodegener Dis* **3**(4-5), 275–83 (2006).

Kaether, C., Lammich, S., Edbauer, D., Ertl, M., Rietdorf, J., Capell, A., Steiner, H., and Haass, C. Presenilin-1 affects trafficking and processing of betaAPP and is targeted in a complex with nicastrin to the plasma membrane. *J Cell Biol* **158**(3), 551–561 (2002).

Kaether, C., Scheuermann, J., Fassler, M., Zilow, S., Shirotani, K., Valkova, C., Novak, B., Kacmar, S., Steiner, H., and Haass, C. Endoplasmic reticulum retention of the gamma-secretase complex component Pen2 by Rer1. *EMBO Rep* **8**(8), 743–748 (2007).

Kang, J., Lemaire, H. G., Unterbeck, A., Salbaum, J. M., Masters, C. L., Grzeschik, K. H., Multhaup, G., Beyreuther, K., and Müller-Hill, B. The precursor of Alzheimer's disease amyloid A4 protein resembles a cell-surface receptor. *Nature* **325**(6106), 733–736 (1987).

Kang, J. and Müller-Hill, B. Differential splicing of Alzheimer's disease amyloid A4 precursor RNA in rat tissues: PreA4(695) mRNA is predominantly produced in rat and human brain. *Biochem Biophys Res Commun* **166**(3), 1192–1200 (1990).

Khalil, H., Brunet, A., Saba, I., Terra, R., Sékaly, R. P., and Thibodeau, J. The MHC class II beta chain cytoplasmic tail overcomes the invariant chain p35-encoded endoplasmic reticulum retention signal. *Int Immunol* **15**(10), 1249–1263 (2003).

Khalil, H., Brunet, A., and Thibodeau, J. A three-amino-acid-long HLA-DRbeta cytoplasmic tail is sufficient to overcome ER retention of invariant-chain p35. *J Cell Sci* **118**(Pt 20), 4679–87 (2005).

Kim, S.-H. and Sisodia, S. S. Evidence that the NFmotif in transmembrane domain 4 of presenilin 1 is critical for binding with PEN-2. *J Biol Chem* **280**(51), 41953–41966 (2005a).

Kim, S. H. and Sisodia, S. S. A sequence within the first transmembrane domain of PEN-2 is critical for PEN-2-mediated endoproteolysis of presenilin 1. *J Biol Chem* **280**(3), 1992–2001 (2005b).

Kim, S. H., Yin, Y. I., Li, Y. M., and Sisodia, S. S. Evidence that assembly of an active gamma-secretase complex occurs in the early compartments of the secretory pathway. *J Biol Chem* **279**(47), 48615–9 (2004).

Kimberly, W. T., LaVoie, M. J., Ostaszewski, B. L., Ye, W., Wolfe, M. S., and Selkoe, D. J. Gamma-secretase is a membrane protein complex comprised of presenilin, nicastrin, Aph-1, and Pen-2. *Proc Natl Acad Sci U S A* **100**(11), 6382–7 (2003).

Klumperman, J. The growing Golgi: in search of its independence. *Nat Cell Biol* **2**(12), E217–E219 (2000).

Kukar, T. L., Ladd, T. B., Bann, M. A., Fraering, P. C., Narlawar, R., Maharvi, G. M., Healy, B., Chapman, R., Welzel, A. T., Price, R. W., Moore, B., Rangachari, V., Cusack, B., Eriksen, J., Jansen-West, K., Verbeeck, C., Yager, D., Eckman, C., Ye, W., Sagi, S., Cottrell, B. A., Torpey, J., Rosenberry, T. L., Fauq, A., Wolfe, M. S., Schmidt, B., Walsh, D. M., Koo, E. H., and Golde, T. E. Substrate-targeting gamma-secretase modulators. *Nature* **453**(7197), 925–929 (2008).

Kuwana, T., Peterson, P. A., and Karlsson, L. Exit of major histocompatibility complex class II-invariant chain p35 complexes from the endoplasmic reticulum is modulated by phosphorylation. *Proc Natl Acad Sci U S A* **95**(3), 1056–1061 (1998).

Lai, M.-T., Chen, E., Crouthamel, M.-C., DiMuzio-Mower, J., Xu, M., Huang, Q., Price, E., Register, R. B., Shi, X.-P., Donoviel, D. B., Bernstein, A., Hazuda, D., Gardell, S. J., and Li, Y.-M. Presenilin-1 and presenilin-2 exhibit distinct yet overlapping gamma-secretase activities. *J Biol Chem* **278**(25), 22475–22481 (2003).

Lee, S.-F., Shah, S., Li, H., Yu, C., Han, W., and Yu, G. Mammalian APH-1 interacts with presenilin and nicastrin and is required for intramembrane proteolysis of amyloid-beta precursor protein and Notch. *J Biol Chem* **277**(47), 45013–45019 (2002).

Letourneur, F. and Cosson, P. Targeting to the endoplasmic reticulum in yeast cells by determinants present in transmembrane domains. *J Biol Chem* **273**(50), 33273–33278 (1998).

Letourneur, F., Hennecke, S., Démollière, C., and Cosson, P. Steric masking of a dilysine endoplasmic reticulum retention motif during assembly of the human high affinity receptor for immunoglobulin E. *J Cell Biol* **129**(4), 971–978 (1995).

Li, Y. M., Lai, M. T., Xu, M., Huang, Q., DiMuzio-Mower, J., Sardana, M. K., Shi, X. P., Yin, K. C., Shafer, J. A., and Gardell, S. J. Presenilin 1 is linked with gamma-secretase activity in the detergent solubilized state. *Proc Natl Acad Sci U S A* **97**(11), 6138–6143 (2000).

Lodish, H. F. *Molecular cell biology.* W.H. Freeman, New York, 6th edition (2007). Harvey Lodish ... [et al.]. col. ill. ; 29 cm.

Margeta-Mitrovic, M., Jan, Y. N., and Jan, L. Y. A trafficking checkpoint controls GABA(B) receptor heterodimerization. *Neuron* **27**(1), 97–106 (2000).

Massaad, M. J., Franzusoff, A., and Herscovics, A. The processing alpha1,2-mannosidase of Saccharomyces cerevisiae depends on Rer1p for its localization in the endoplasmic reticulum. *Eur J Cell Biol* **78**(7), 435–40 (1999).

Massaad, M. J. and Herscovics, A. Interaction of the endoplasmic reticulum alpha 1,2-mannosidase Mns1p with Rer1p using the split-ubiquitin system. *J Cell Sci* **114**(Pt 24), 4629–35 (2001).

Masters, C. L., Simms, G., Weinman, N. A., Multhaup, G., McDonald, B. L., and Beyreuther, K. Amyloid plaque core protein in Alzheimer disease and Down syndrome. *Proc Natl Acad Sci U S A* **82**(12), 4245–4249 (1985).

Mastrangelo, P., Mathews, P. M., Chishti, M. A., Schmidt, S. D., Gu, Y., Yang, J., Mazzella, M. J., Coomaraswamy, J., Horne, P., Strome, B., Pelly, H., Levesque, G., Ebeling, C., Jiang, Y., Nixon, R. A., Rozmahel, R., Fraser, P. E., George-Hyslop, P. S., Carlson, G. A., and Westaway, D. Dissociated phenotypes in presenilin transgenic mice define functionally distinct gamma-secretases. *Proc Natl Acad Sci U S A* **102**(25), 8972–8977 (2005).

McCarthy, J. V., Twomey, C., and Wujek, P. Presenilin-dependent regulated intramembrane proteolysis and gamma-secretase activity. *Cell Mol Life Sci* **66**(9), 1534–1555 (2009).

McGowan, E., Pickford, F., Kim, J., Onstead, L., Eriksen, J., Yu, C., Skipper, L., Murphy, M. P., Beard, J., Das, P., Jansen, K., Delucia, M., Lin, W.-L., Dolios, G., Wang, R., Eckman, C. B., Dickson, D. W., Hutton, M., Hardy, J., and Golde, T. Abeta42 is essential for parenchymal and vascular amyloid deposition in mice. *Neuron* **47**(2), 191–199 (2005).

Mezzacasa, A. and Helenius, A. The transitional ER defines a boundary for quality control in the secretion of tsO45 VSV glycoprotein. *Traffic* **3**(11), 833–849 (2002).

Michelsen, K., Schmid, V., Metz, J., Heusser, K., Liebel, U., Schwede, T., Spang, A., and Schwappach, B. Novel cargo-binding site in the beta and delta subunits of coatomer. *J Cell Biol* **179**(2), 209–17 (2007).

Michelsen, K., Yuan, H., and Schwappach, B. Hide and run. Arginine-based endoplasmic-reticulum-sorting motifs in the assembly of heteromultimeric membrane proteins. *EMBO Rep* **6**(8), 717–722 (2005).

Moore, D. T., Berger, B. W., and DeGrado, W. F. Protein-protein interactions in the membrane: sequence, structural, and biological motifs. *Structure* **16**(7), 991–1001 (2008).

Nikolaev, A., McLaughlin, T., O'Leary, D. D. M., and Tessier-Lavigne, M. APP binds DR6 to trigger axon pruning and neuron death via distinct caspases. *Nature* **457**(7232), 981–989 (2009).

Nilsson, T., Jackson, M., and Peterson, P. A. Short cytoplasmic sequences serve as retention signals for transmembrane proteins in the endoplasmic reticulum. *Cell* **58**(4), 707–718 (1989).

Nishikawa, S. and Nakano, A. Identification of a gene required for membrane protein retention in the early secretory pathway. *Proc Natl Acad Sci U S A* **90**(17), 8179–8183 (1993).

Nufer, O. and Hauri, H.-P. ER export: call 14-3-3. *Curr Biol* **13**(10), R391–R393 (2003).

O'Kelly, I., Butler, M. H., Zilberberg, N., and Goldstein, S. A. N. Forward transport. 14-3-3 binding overcomes retention in endoplasmic reticulum by dibasic signals. *Cell* **111**(4), 577–588 (2002).

Ott, A., Breteler, M. M., van Harskamp, F., Claus, J. J., van der Cammen, T. J., Grobbee, D. E., and Hofman, A. Prevalence of Alzheimer's disease and vascular dementia: association with education. The Rotterdam study. *BMJ* **310**(6985), 970–973 (1995).

Pardossi-Piquard, R., Böhm, C., Chen, F., Kanemoto, S., Checler, F., Schmitt-Ulms, G., George-Hyslop, P. S., and Fraser, P. E. TMP21 transmembrane domain regulates gamma-secretase cleavage. *J Biol Chem* **284**(42), 28634–28641 (2009).

Pelham, H. R. Sorting and retrieval between the endoplasmic reticulum and Golgi apparatus. *Curr Opin Cell Biol* **7**(4), 530–535 (1995).

Pelham, H. R. The dynamic organisation of the secretory pathway. *Cell Struct Funct* **21**(5), 413–419 (1996).

Pelham, H. R. Traffic through the Golgi apparatus. *J Cell Biol* **155**(7), 1099–1101 (2001).

Prokop, S., Haass, C., and Steiner, H. Length and overall sequence of the PEN-2 C-terminal domain determines its function in the stabilization of presenilin fragments. *J Neurochem* **94**(1), 57–62 (2005).

Prokop, S., Shirotani, K., Edbauer, D., Haass, C., and Steiner, H. Requirement of PEN-2 for stabilization of the presenilin N-/C-terminal fragment heterodimer within the gamma-secretase complex. *J Biol Chem* **279**(22), 23255–61 (2004).

Qi-Takahara, Y., Morishima-Kawashima, M., Tanimura, Y., Dolios, G., Hirotani, N., Horikoshi, Y., Kametani, F., Maeda, M., Saido, T. C., Wang, R., and Ihara, Y. Longer forms of amyloid beta protein: implications for the mechanism of intramembrane cleavage by gamma-secretase. *J Neurosci* **25**(2), 436–445 (2005).

R Development Core Team. *R: A Language and Environment for Statistical Computing*. R Foundation for Statistical Computing, Vienna, Austria (2009). ISBN 3-900051-07-0 `http://www.R-project.org`.

Radde, R., Bolmont, T., Kaeser, S. A., Coomaraswamy, J., Lindau, D., Stoltze, L., Calhoun, M. E., Jäggi, F., Wolburg, H., Gengler, S., Haass, C., Ghetti, B., Czech, C., Hölscher, C., Mathews, P. M., and Jucker, M. Abeta42-driven cerebral amyloidosis in transgenic mice reveals early and robust pathology. *EMBO Rep* **7**(9), 940–946 (2006).

Rayner, J. C. and Pelham, H. R. Transmembrane domain-dependent sorting of proteins to the ER and plasma membrane in yeast. *Embo J* **16**(8), 1832–41 (1997).

Robakis, N. K., Wisniewski, H. M., Jenkins, E. C., Devine-Gage, E. A., Houck, G. E., Yao, X. L., Ramakrishna, N., Wolfe, G., Silverman, W. P., and Brown, W. T. Chromosome 21q21 sublocalisation of gene encoding beta-amyloid peptide in cerebral vessels and neuritic (senile) plaques of people with Alzheimer disease and Down syndrome. *Lancet* **1**(8529), 384–385 (1987).

Rogaev, E. I., Sherrington, R., Rogaeva, E. A., Levesque, G., Ikeda, M., Liang, Y., Chi, H., Lin, C., Holman, K., and Tsuda, T. Familial Alzheimer's disease in kindreds with missense mutations in a gene on chromosome 1 related to the Alzheimer's disease type 3 gene. *Nature* **376**(6543), 775–778 (1995).

Sambrook, J. and Russell, D. W. *Molecular cloning : a laboratory manual*. 3. Cold Spring Harbor Laboratory Press, Cold Spring Harbor, N.Y., 3rd edition (2001). 00064380 Joseph Sambrook, David W. Russell. ill. ; 28 cm. Includes bibliographical references and index.

Sato, K., Nishikawa, S., and Nakano, A. Membrane protein retrieval from the Golgi apparatus to the endoplasmic reticulum (ER): characterization of the RER1 gene product as a component involved in ER localization of Sec12p. *Mol Biol Cell* **6**(11), 1459–77 (1995).

Sato, K., Sato, M., and Nakano, A. Rer1p as common machinery for the endoplasmic reticulum localization of membrane proteins. *Proc Natl Acad Sci U S A* **94**(18), 9693–8 (1997).

Sato, K., Sato, M., and Nakano, A. Rer1p, a retrieval receptor for endoplasmic reticulum membrane proteins, is dynamically localized to the Golgi apparatus by coatomer. *J Cell Biol* **152**(5), 935–44 (2001).

Sato, K., Sato, M., and Nakano, A. Rer1p, a retrieval receptor for ER membrane proteins, recognizes transmembrane domains in multiple modes. *Mol Biol Cell* **14**(9), 3605–16 (2003).

Sato, M., Sato, K., and Nakano, A. Endoplasmic reticulum localization of Sec12p is achieved by two mechanisms: Rer1p-dependent retrieval that requires the transmembrane domain and Rer1p-independent retention that involves the cytoplasmic domain. *J Cell Biol* **134**(2), 279–93 (1996).

Sato, M., Sato, K., and Nakano, A. Endoplasmic reticulum quality control of unassembled iron transporter depends on Rer1p-mediated retrieval from the golgi. *Mol Biol Cell* **15**(3), 1417–24 (2004).

Sato, T., Diehl, T. S., Narayanan, S., Funamoto, S., Ihara, Y., Strooper, B. D., Steiner, H., Haass, C., and Wolfe, M. S. Active gamma-secretase complexes contain only one of each component. *J Biol Chem* **282**(47), 33985–33993 (2007).

Schroeter, E. H., Ilagan, M. X. G., Brunkan, A. L., Hecimovic, S., ming Li, Y., Xu, M., Lewis, H. D., Saxena, M. T., Strooper, B. D., Coonrod, A., Tomita, T., Iwatsubo, T., Moore, C. L., Goate, A., Wolfe, M. S., Shearman, M., and Kopan, R. A presenilin dimer at the core of the gamma-secretase enzyme: insights from parallel analysis of Notch 1 and APP proteolysis. *Proc Natl Acad Sci U S A* **100**(22), 13075–13080 (2003).

Schroeter, E. H., Kisslinger, J. A., and Kopan, R. Notch-1 signalling requires ligand-induced proteolytic release of intracellular domain. *Nature* **393**(6683), 382–386 (1998).

Schutze, M. P., Peterson, P. A., and Jackson, M. R. An N-terminal double-arginine motif maintains type II membrane proteins in the endoplasmic reticulum. *EMBO J* **13**(7), 1696–1705 (1994).

Scott, D. B., Blanpied, T. A., Swanson, G. T., Zhang, C., and Ehlers, M. D. An NMDA receptor ER retention signal regulated by phosphorylation and alternative splicing. *J Neurosci* **21**(9), 3063–3072 (2001).

Selkoe, D. J. Alzheimer's disease: genes, proteins, and therapy. *Physiol Rev* **81**(2), 741–766 (2001).

Serneels, L., Dejaegere, T., Craessaerts, K., Horré, K., Jorissen, E., Tousseyn, T., Hébert, S., Coolen, M., Martens, G., Zwijsen, A., Annaert, W., Hartmann, D., and Strooper, B. D. Differential contribution of the three Aph1 genes to gamma-secretase activity in vivo. *Proc Natl Acad Sci U S A* **102**(5), 1719–1724 (2005).

Shah, S., Lee, S.-F., Tabuchi, K., Hao, Y.-H., Yu, C., LaPlant, Q., Ball, H., Dann, C. E., Südhof, T., and Yu, G. Nicastrin functions as a gamma-secretase-substrate receptor. *Cell* **122**(3), 435–447 (2005).

Sherrington, R., Rogaev, E. I., Liang, Y., Rogaeva, E. A., Levesque, G., Ikeda, M., Chi, H., Lin, C., Li, G., and Holman, K. Cloning of a gene bearing missense mutations in early-onset familial Alzheimer's disease. *Nature* **375**(6534), 754–760 (1995).

Shirotani, K., Edbauer, D., Capell, A., Schmitz, J., Steiner, H., and Haass, C. Gamma-secretase activity is associated with a conformational change of nicastrin. *J Biol Chem* **278**(19), 16474–16477 (2003).

Shirotani, K., Edbauer, D., Kostka, M., Steiner, H., and Haass, C. Immature nicastrin stabilizes APH-1 independent of PEN-2 and presenilin: identification of nicastrin mutants that selectively interact with APH-1. *J Neurochem* **89**(6), 1520–1527 (2004a).

Shirotani, K., Edbauer, D., Prokop, S., Haass, C., and Steiner, H. Identification of distinct gamma-secretase complexes with different APH-1 variants. *J Biol Chem* **279**(40), 41340–41345 (2004b).

Spasic, D., Raemaekers, T., Dillen, K., Declerck, I., Baert, V., Serneels, L., Füllekrug, J., and Annaert, W. Rer1p competes with APH-1 for binding to nicastrin and regulates gamma-secretase complex assembly in the early secretory pathway. *J Cell Biol* **176**(5), 629–40 (2007).

Spasic, D., Tolia, A., Dillen, K., Baert, V., Strooper, B. D., Vrijens, S., and Annaert, W. Presenilin-1 maintains a nine-transmembrane topology throughout the secretory pathway. *J Biol Chem* **281**(36), 26569–26577 (2006).

Standley, S., Roche, K. W., McCallum, J., Sans, N., and Wenthold, R. J. PDZ domain suppression of an ER retention signal in NMDA receptor NR1 splice variants. *Neuron* **28**(3), 887–898 (2000).

Steiner, H., Fluhrer, R., and Haass, C. Intramembrane proteolysis by gamma-secretase. *J Biol Chem* **283**(44), 29627–31 (2008a).

Steiner, H., Kostka, M., Romig, H., Basset, G., Pesold, B., Hardy, J., Capell, A., Meyn, L., Grim, M. L., Baumeister, R., Fechteler, K., and Haass, C. Glycine 384 is required for presenilin-1 function and is conserved in bacterial polytopic aspartyl proteases. *Nat Cell Biol* **2**(11), 848–851 (2000).

Steiner, H., Winkler, E., Edbauer, D., Prokop, S., Basset, G., Yamasaki, A., Kostka, M., and Haass, C. PEN-2 is an integral component of the gamma-secretase complex required for coordinated expression of presenilin and nicastrin. *J Biol Chem* **277**(42), 39062–39065 (2002).

Steiner, H., Winkler, E., and Haass, C. Chemical cross-linking provides a model of the gamma-secretase complex subunit architecture and evidence for close proximity of the C-terminal fragment of presenilin with APH-1. *J Biol Chem* **283**(50), 34677–34686 (2008b).

Strittmatter, W. J., Saunders, A. M., Schmechel, D., Pericak-Vance, M., Enghild, J., Salvesen, G. S., and Roses, A. D. Apolipoprotein E: high-avidity binding to beta-amyloid and increased frequency of type 4 allele in late-onset familial Alzheimer disease. *Proc Natl Acad Sci U S A* **90**(5), 1977–1981 (1993).

Takasugi, N., Tomita, T., Hayashi, I., Tsuruoka, M., Niimura, M., Takahashi, Y., Thinakaran, G., and Iwatsubo, T. The role of presenilin cofactors in the gamma-secretase complex. *Nature* **422**(6930), 438–41 (2003).

Tanzi, R. E., Gusella, J. F., Watkins, P. C., Bruns, G. A., George-Hyslop, P. S., Keuren, M. L. V., Patterson, D., Pagan, S., Kurnit, D. M., and Neve, R. L. Amyloid beta protein gene: cDNA, mRNA distribution, and genetic linkage near the Alzheimer locus. *Science* **235**(4791), 880–884 (1987).

Thathiah, A., Spittaels, K., Hoffmann, M., Staes, M., Cohen, A., Horré, K., Vanbrabant, M., Coun, F., Baekelandt, V., Delacourte, A., Fischer, D. F., Pollet, D., Strooper, B. D., and Merchiers, P. The orphan G protein-coupled receptor 3 modulates amyloid-beta peptide generation in neurons. *Science* **323**(5916), 946–951 (2009).

Thinakaran, G., Borchelt, D. R., Lee, M. K., Slunt, H. H., Spitzer, L., Kim, G., Ratovitsky, T., Davenport, F., Nordstedt, C., Seeger, M., Hardy, J., Levey, A. I., Gandy, S. E., Jenkins, N. A., Copeland, N. G., Price, D. L., and Sisodia, S. S. Endoproteolysis of presenilin 1 and accumulation of processed derivatives in vivo. *Neuron* **17**(1), 181–190 (1996).

Thinakaran, G. and Koo, E. H. Amyloid precursor protein trafficking, processing, and function. *J Biol Chem* **283**(44), 29615–29619 (2008).

Tomita, T., Watabiki, T., Takikawa, R., Morohashi, Y., Takasugi, N., Kopan, R., Strooper, B. D., and Iwatsubo, T. The first proline of PALP motif at the C terminus of presenilins is obligatory for stabilization, complex formation, and gamma-secretase activities of presenilins. *J Biol Chem* **276**(35), 33273–33281 (2001).

Walter, J., Grünberg, J., Capell, A., Pesold, B., Schindzielorz, A., Citron, M., Mendla, K., George-Hyslop, P. S., Multhaup, G., Selkoe, D. J., and Haass, C. Proteolytic processing of the Alzheimer disease-associated presenilin-1 generates an in vivo substrate for protein kinase C. *Proc Natl Acad Sci U S A* **94**(10), 5349–5354 (1997).

Wang, J.-M., Zhang, L., Yao, Y., Viroonchatapan, N., Rothe, E., and Wang, Z.-Z. A transmembrane motif governs the surface trafficking of nicotinic acetylcholine receptors. *Nat Neurosci* **5**(10), 963–970 (2002).

Wang, R., Sweeney, D., Gandy, S. E., and Sisodia, S. S. The profile of soluble amyloid beta protein in cultured cell media. Detection and quantification of amyloid beta protein and variants by immunoprecipitation-mass spectrometry. *J Biol Chem* **271**(50), 31894–31902 (1996).

Wang, X., Matteson, J., An, Y., Moyer, B., Yoo, J.-S., Bannykh, S., Wilson, I. A., Riordan, J. R., and Balch, W. E. COPII-dependent export of cystic fibrosis transmembrane conductance regulator from the ER uses a di-acidic exit code. *J Cell Biol* **167**(1), 65–74 (2004).

Watanabe, N., Tomita, T., Sato, C., Kitamura, T., Morohashi, Y., and Iwatsubo, T. Pen-2 is incorporated into the gamma-secretase complex through binding to transmembrane domain 4 of presenilin 1. *J Biol Chem* **280**(51), 41967–75 (2005).

WebPath: The Internet Pathology Laboratory. `http://library.med.utah.edu/WebPath/webpath.html` (as of November 2009).

Weiner, H. L. and Frenkel, D. Immunology and immunotherapy of Alzheimer's disease. *Nat Rev Immunol* **6**(5), 404–416 (2006).

Wolfe, M. S., Xia, W., Ostaszewski, B. L., Diehl, T. S., Kimberly, W. T., and Selkoe, D. J. Two transmembrane aspartates in presenilin-1 required for presenilin endoproteolysis and gamma-secretase activity. *Nature* **398**(6727), 513–517 (1999).

Yin, H., Slusky, J. S., Berger, B. W., Walters, R. S., Vilaire, G., Litvinov, R. I., Lear, J. D., Caputo, G. A., Bennett, J. S., and DeGrado, W. F. Computational design of peptides that target transmembrane helices. *Science* **315**(5820), 1817–1822 (2007).

Yoshida, Y., Chiba, T., Tokunaga, F., Kawasaki, H., Iwai, K., Suzuki, T., Ito, Y., Matsuoka, K., Yoshida, M., Tanaka, K., and Tai, T. E3 ubiquitin ligase that recognizes sugar chains. *Nature* **418**(6896), 438–442 (2002).

Yu, G., Nishimura, M., Arawaka, S., Levitan, D., Zhang, L., Tandon, A., Song, Y. Q., Rogaeva, E., Chen, F., Kawarai, T., Supala, A., Levesque, L., Yu, H., Yang, D. S., Holmes, E., Milman, P., Liang, Y., Zhang, D. M., Xu, D. H., Sato, C., Rogaev, E., Smith, M., Janus, C., Zhang, Y., Aebersold, R., Farrer, L. S., Sorbi, S., Bruni, A., Fraser, P., and George-Hyslop, P. S. Nicastrin modulates presenilin-mediated notch/glp-1 signal transduction and betaAPP processing. *Nature* **407**(6800), 48–54 (2000).

Yuan, H., Michelsen, K., and Schwappach, B. 14-3-3 dimers probe the assembly status of multimeric membrane proteins. *Curr Biol* **13**(8), 638–46 (2003).

Zerangue, N., Malan, M. J., Fried, S. R., Dazin, P. F., Jan, Y. N., Jan, L. Y., and Schwappach, B. Analysis of endoplasmic reticulum trafficking signals by combinatorial screening in mammalian cells. *Proc Natl Acad Sci U S A* **98**(5), 2431–6 (2001).

Zerangue, N., Schwappach, B., Jan, Y. N., and Jan, L. Y. A new ER trafficking signal regulates the subunit stoichiometry of plasma membrane K(ATP) channels. *Neuron* **22**(3WebPath: The Internet Pathology Laboratory), 537–48 (1999).

Zhou, S., Zhou, H., Walian, P. J., and Jap, B. K. CD147 is a regulatory subunit of the gamma-secretase complex in Alzheimer's disease amyloid beta-peptide production. *Proc Natl Acad Sci U S A* **102**(21), 7499–7504 (2005).

Publications

Publications in peer-reviewed journals:

Kaether, C., Scheuermann, J., Fassler, M., Zilow, S., Shirotani, K., Valkova, C., Novak, B., Kacmar, S., Steiner, H., and Haass, C. Endoplasmic reticulum retention of the gamma-secretase complex component Pen2 by Rer1. EMBO Rep 8(8), 743–748 (2007).

Fassler, M., Zocher, M., Klare, S., Guzman de la Fuente, A., Scheuermann, J., Capell, A., Haass, C., Valkova, C., Veerappan, A., Schneider, D., and Kaether, C. Masking of transmembrane-based retention signals controls ER-export of γ-secretase. Traffic, *in press.*

Poster presentations:

Fassler, M., Valkova, C., Reichenbach, D., Schwappach, B., and Kaether, C. Mammalian Rer1 - a novel protein involved in the assembly of multimeric complexes. 58. Mosbacher Kolloquium der GBM, Mosbach, March 2007.

Fassler, M., Valkova, C., Reichenbach, D., and Kaether, C. Rer1 interacts with an ER-retention/retrieval signal in the γ-secretase subunit Pen2. ELSO 2007, Dresden, September 2007.

Fassler, M., Zocher, M., Hänel, F., Pepperkok, R., and Kaether, C. The role of ER retention signals in γ-secretase assembly. Eighth Eibsee Meeting on Cellular Mechanisms of Alzheimer´s Disease, Garmisch-Partenkirchen, October 2008.

Fassler, M., Zocher, M., Klare, S., Guzman de la Fuente, A., Valkova, C., Veerappan, A., Schneider, D., and Kaether, C. Masking of ER retention signals during γ-secretase assembly. Ninth Eibsee Meeting on Cellular Mechanisms of Alzheimer´s Disease, Garmisch-Partenkirchen, November 2009

Selbstständigkeitserklärung

Hiermit erkläre ich, dass ich die eingereichte Dissertation selbständig und nur unter Verwendung der angegebenen Hilfsmittel und Literatur erstellt habe. Weiterhin erkläre ich, dass die in der Arbeit enthaltenen Abbildungen nur die originalen Daten enthalten und in keinem Fall inhaltsverändernder Bildbearbeitung unterzogen wurden.
Ich versichere, dass diese Dissertation nicht als Diplomarbeit oder ähnliches verwendet und abgesehen von den am Ende angegebenen Teilveröffentlichungen nicht publiziert wurde. Die Promotionsordnung der Biologisch-Pharmazeutischen Fakultät der FSU Jena ist mir bekannt.

Jena, den 15.12.2009

Lebenslauf

Persönliche Daten

Name:	Matthias Faßler
Geburtsdatum:	28. Oktober 1980
Geburtsort:	Jena
Staatsangehörigkeit:	deutsch
Familienstand:	verheiratet, 2 Kinder

Ausbildung

1993-1999:	**Carl Zeiss Gymnasium, Jena**
07/1999	Abitur (1.0)
10/2000-10/2005:	**Studium der Biochemie und Molekularbiologie Friedrich Schiller Universität, Jena** (Wahlfach: Molekulare Medizin)
01/2003:	Vordiplom (1.4)
11/2004-10/2005:	Diplomarbeit: ″Studien zur molekularen Interaktion von rekombinanten Skorpion α-Toxinen mit Spannungssensoren von Natriumkanälen″ Betreuer: Prof. Stefan H. Heinemann, FSU Jena
12/2005:	Diplom (1.3)

Promotion

seit 11/2005	**Doktorand am Leibniz Institut für Alters-forschung - Fritz Lipmann Institut (FLI), Jena** Arbeitsgruppe: ″Membrane Trafficking of Proteins involved in Alzheimer's Disease″ Betreuer: Dr. habil. Christoph Kaether

Stipendien

2008-2009	**Promotionsstipendium der Hans und Ilse Breuer Stiftung für Forschung über die Alzheimer-Krankheit**

Danksagungen

Zunächst möchte ich meinem Betreuer Dr. Christoph Kaether für die Bereitstellung des interessanten Themas für meine Dissertation danken. Er hat diese Arbeit mit wertvoller Kritik und Diskussion bereichert und mich während meiner Zeit am FLI immer verständnisvoll unterstützt. Er hat mir auch zur Bewerbung für das Stipendium der Hans und Ilse Breuer Stiftung geraten und diesen Prozess positiv begleitet. Letztendlich ist er dafür verantwortlich, dass ich mein Interesse an neurodegenerativen Erkrankungen wohl nicht wieder verlieren werde.

Auch danken möchte ich den Mitgliedern meines Thesis Committees Dr. Helen Morrison und Dr. Ignacio Rubio, welche mir gerade in der schwierigen Anfangszeit immer mit guten Ideen und praktischen Ratschlägen geholfen haben.

Ein besonderes Dankeschön gebührt auch Dr. Christina Valkova und Prof. Karl Bauer, welche diese Arbeit gelesen und durch ihre Vorschläge verbessert haben. Lesen mussten diese Arbeit natürlich auch alle Gutachter. Für diese sicher zeitaufwendige Arbeit möchte ich mich recht herzlich bedanken.

Der Hans und Ilse Breuer Stiftung danke ich für die Finanzierung meiner Arbeit über zwei Jahre.

Während des ganzen Zeitraums in dem diese Arbeit entstanden ist habe ich die positive Atmosphäre in unserem Labor sehr geschätzt. Von der Slavo-Krise bis zu akutem Kohlehydratmangel - für alles gab es immer eine Lösung. Für diese gute Zeit bedanke ich mich bei Kerstin, Christina, Dani, Sigrun und Sabine. Danke auch für gute Ideen, praktische Ratschläge und tröstende Worte wenn die Banden wiedermal nicht da waren wo sie sein sollten. Ein besonderer Dank geht dabei noch an Sigrun für das tolle Latex-Layout und ihre Geduld mit mir.

Ein Dankeschön für viele Seminare und Ausflüge geht auch an alle anderen (ehemaligen) Mitarbeiter der AGs Heuer und Kaether. Insbesondere auch an unsere beiden Diplomanden Micha und Sebastian, die durch ihre Ergebnisse auch zum Erfolg des Projektes beigetragen haben. Außerdem konnte ich so mal erleben, wie es ist, der Lehrer zu sein. Ich glaube ihr hattet es nicht immer leicht mit mir.

Bei Simone Tänzer möchte ich mich für das (die) viele(n) FACSen bedanken. So unterhaltsam habe ich noch nie etwas Neues gelernt.

Die wichtigste Unterstützung bei diesem Projekt kam aber von meiner Familie. Meine Frau Nicky hat mich immer aufgerichtet wenn es Probleme gab und mir immer den Rücken frei gehalten. Meinen wundervollen Kindern Emma und Anton danke ich dafür, dass sie einem keine Zeit lassen über die Arbeit nachzudenken solange sie noch wach sind. Das ist auch eine Möglichkeit den Kopf frei zu bekommen. Meinen Eltern danke ich für die Unterstützung während der gesamten Zeit meines Studiums und dieser Arbeit. Ohne euch wäre ich nicht hier. Zuletzt möchte ich noch meinem Paten Prof. Dieter Faßler danken, dem diese Arbeit gewidmet ist. Als ich hinschmeißen wollte hat er mich vom Gegenteil überzeugt. Er hätte das Ergebnis seiner Überzeugungskunst sicher gerne noch erlebt.

A
Appendix

A.1 Vector maps

Leibniz Institute for Age Research
Fritz Lipmann Institute (FLI)
Group: Membrane Trafficking of Proteins involved in Alzheimer´s Disease
Head: Dr. Christoph Kather
Tel +49 3641 656052 Email: mfassler@fli-leibniz.de

PLASMID DATA SHEET

Name:	CD4-TM1-EGFP / pcDNA3.1/Hygro(+)
Constructed by:	Matthias Faßler
Plasmid:	pcDNA3.1/Hygro(+)
Insert:	fusion protein hCD4-TM1 and EGFP
Cloning sites:	BamHI / ApaI
Resistance:	Amp , Hygro
Diagnostic REN:	NdeI (4135, 3516)
Reference:	

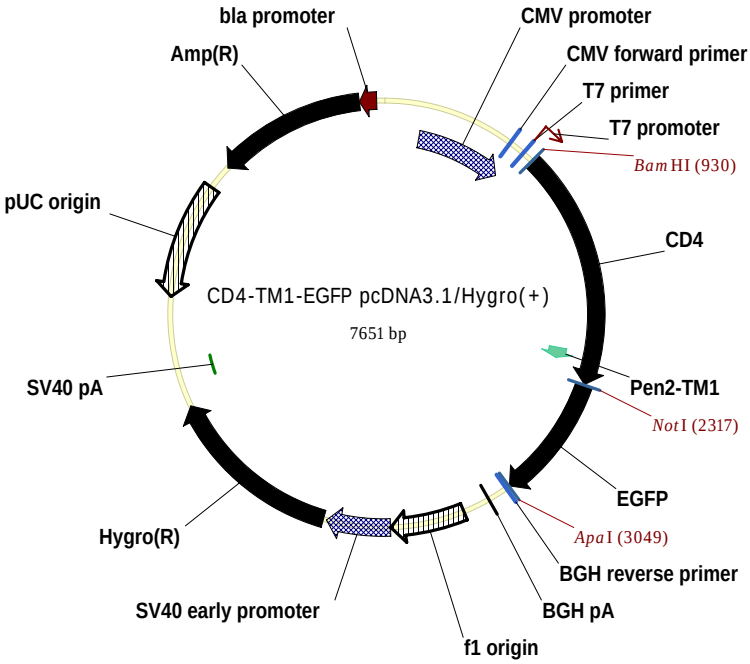

Construction: EGFP was amplified using primer EGFP-F NotI GCGGCCGCGATGGTGAGCAAGGGC (introducing NotI) and EGFP-R ApaI GGGCCCTTACTTGTACAGCTCGTC (introducing ApaI). CD4-TM1 was amplified using primer CD4-F BamHI *alt* GGATCCGCCACCATGAACCGGGGAGTCCC (introducing BamHI and Kozak sequence) and CD4-R NotI GCGGCCGCAATGGGGCTACATGT (introducing NotI). PCR products were TOPO TA cloned, cut with their respective RENs and then subsequently cloned into pcDNA3.1/Hygro(+) using BamHI, NotI and ApaI sites. Transition site: SPIaaaMVSK. The fusion leads to the insertion of 3 alanin (aaa).

Leibniz Institute for Age Research
Fritz Lipmann Institute (FLI)
Group: Membrane Trafficking of Proteins involved in Alzheimer´s Disease
Head: Dr. Christoph Kather
Tel +49 3641 656052 Email: mfassler@fli-leibniz.de

PLASMID DATA SHEET

Name:	CD4-TM4 / pcDNA3.1 Zeo(+)
Constructed by:	Matthias Faßler, Alerie Guzman
Plasmid:	pcDNA3.1 Zeo(+)
Insert:	hCD4 with PS1-TMD4
Cloning sites:	BamHI, XhoI
Resistance:	Amp , Zeo
Diagnostic REN:	PvuII (3451 bp, 1749 bp, 1151 bp)
Reference:	

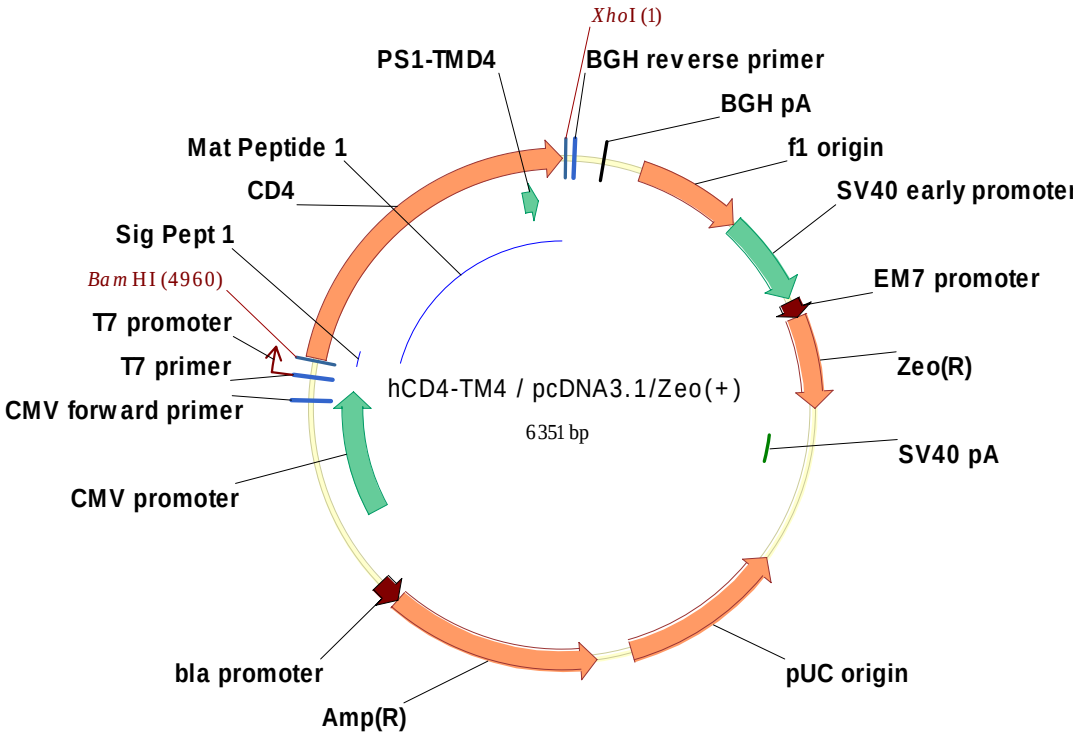

Construction: CD4-TM4 was generated by a standard deletion/insertion protocol for site directed mutagenesis from CD4/pcDNA3.1 Zeo(+). SP CD4-TM4PS 5'-GCACTCCTGATCTGGAATTTTGGTGTGGTGGGAATGATTT CCATTAGGTGCCGGCACCGAAGG-3'; ASP CD4-TM4PS 5'-ATTCCAGATCAGGAGTGCAACAGTAATGT AGTCCACAGCAACGTTCATTGGCTGCACCGGG-3'

Leibniz Institute for Age Research
Fritz Lipmann Institute (FLI)
Group: Membrane Trafficking of Proteins involved in Alzheimer´s Disease
Head: Dr. Christoph Kather
Tel +49 3641 656052 Email: mfassler@fli-leibniz.de

PLASMID DATA SHEET

Name:	CD4-TM4mut / pcDNA3.1 Zeo(+)
Constructed by:	Matthias Faßler, Alerie Guzman
Plasmid:	pcDNA3.1 Zeo(+)
Insert:	hCD4 with PS1-TMD4; introduced WNF->AAA mutation
Cloning sites:	BamHI, XhoI
Resistance:	Amp , Zeo
Diagnostic REN:	PvuII (3451 bp, 1749 bp, 1151 bp)
Reference:	

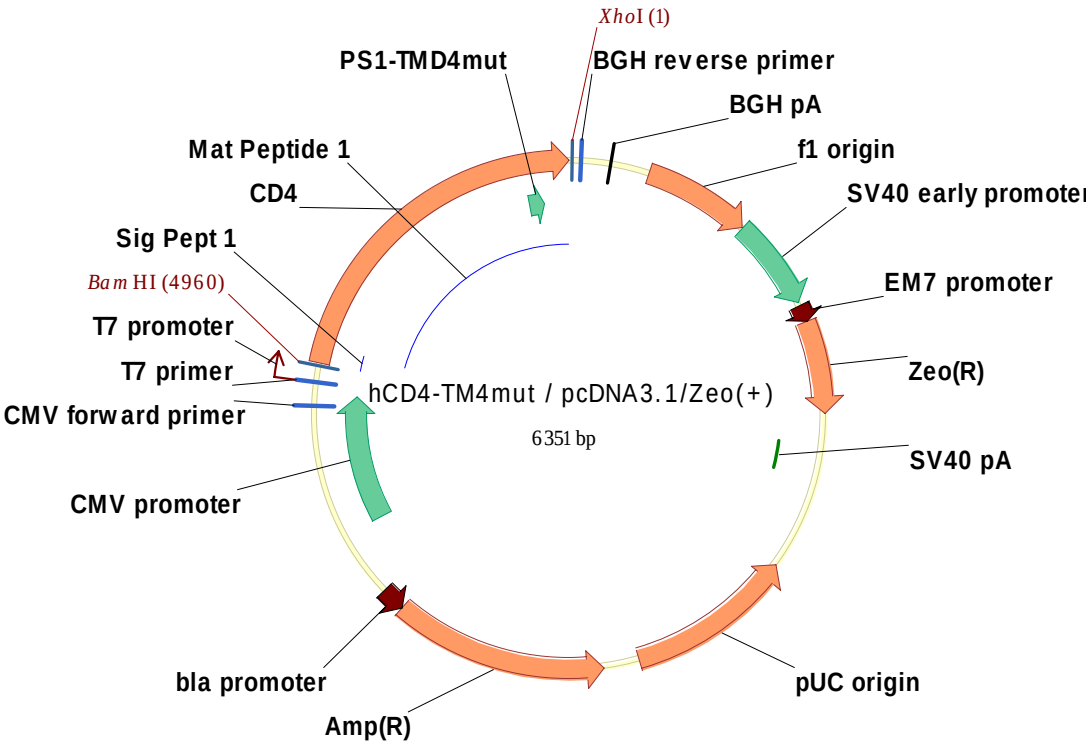

Construction: CD4-TM4mut was obtained using site directed mutagenesis on CD4-TM4 / pcDNA3.1 Zeo(+). SP TM4 WNF->AAA 5'-ATTACTGTTGCACTCCTGATCGCGGCTGCTGGTGTGGTGGGAATG-3'; ASP TM4 WNF->AAA 5'-CATTCCCACCACACCAGCAGCCGCGATCAGGAGTGCAACAGTAAT-3'.

Leibniz Institute for Age Research
Fritz Lipmann Institute (FLI)
Group: Membrane Trafficking of Proteins involved in Alzheimer´s Disease
Head: Dr. Christoph Kather
Tel +49 3641 656052 Email: mfassler@fli-leibniz.de

PLASMID DATA SHEET

Name:	PE Δ7 -PALP -WNF / pcDNA3.1 Zeo(+)
Constructed by:	Matthias Faßler
Plasmid:	pcDNA3.1 Zeo(+)
Insert:	PS1-EGFP Δ7 -PALP with a WNF->AAA mutation in the TMD4
Cloning sites:	EcoRI, XhoI
Resistance:	Amp , Zeo
Diagnostic REN:	PvuII + NotI (4011 bp, 1749 bp, 723 bp, 623 bp)
Reference:	Kaether *et al.*, 2004; Kaether *et al.*, 2002

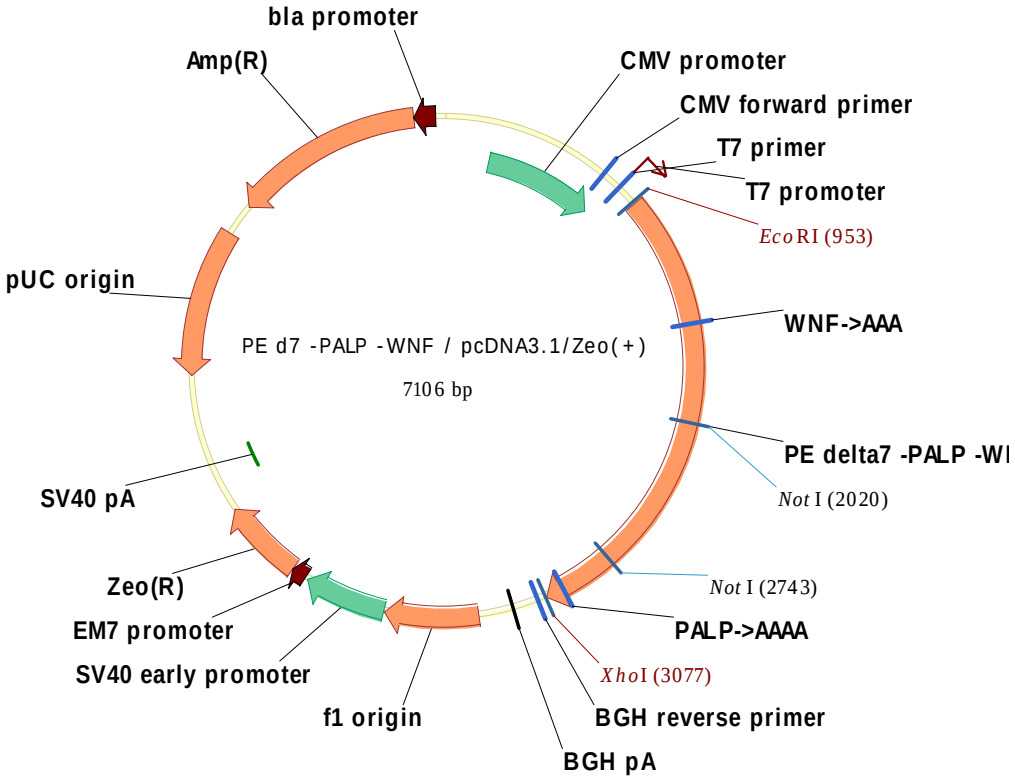

Construction: PE Δ7 -PALP -WNF was generated from PE Δ7 -PALP using site directed mutagenesis. SP TM4 WNF->AAA 5'-ATTACTGTTGCACTCCTGATCGCGGCTGCTGGTGTGGTGGGAATG-3'; ASP TM4 WNF->AAA 5'-CATTCCC ACCACACCAGCAGCCGCGATCAGGAGTGCAACAGTAAT-3'.

Leibniz Institute for Age Research
Fritz Lipmann Institute (FLI)
Group: Membrane Trafficking of Proteins involved in Alzheimer´s Disease
Head: Dr. Christoph Kather
Tel +49 3641 656052 Email: mfassler@fli-leibniz.de

PLASMID DATA SHEET

Name:	PE Δ7 -WNF / pcDNA3.1 Zeo(+)
Constructed by:	Matthias Faßler, Christoph Kaether
Plasmid:	pcDNA3.1 Zeo(+)
Insert:	PS1-EGFP Δ7 with a WNF->AAA mutation in the TMD4
Cloning sites:	EcoRI, XhoI
Resistance:	Amp , Zeo
Diagnostic REN:	PvuII + NotI (4011 bp, 1749 bp, 723 bp, 623 bp)
Reference:	Kaether *et al.*, 2004; Kaether *et al.*, 2002

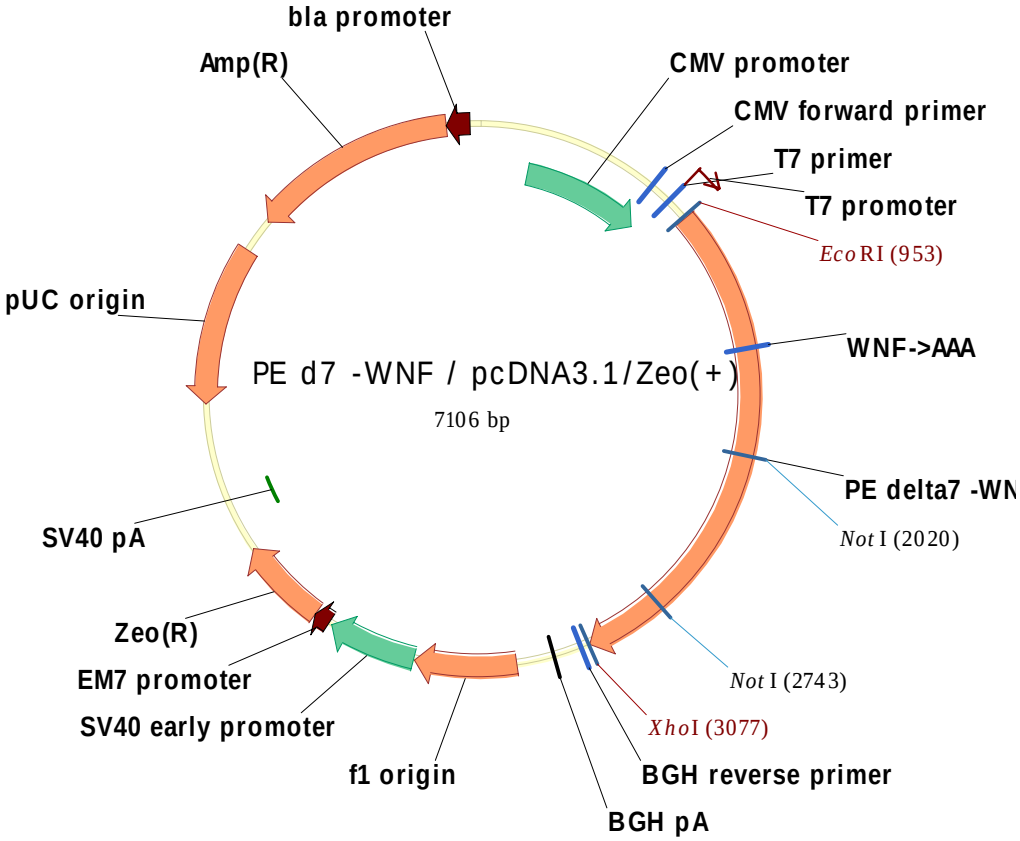

Construction: PE Δ7 -WNF was generated from PE Δ7 using site directed mutagenesis. SP TM4 WNF->AAA 5'-ATTACTGTTGCACTCCTGATCGCGGCTGCTGGTGTGGTGGGAATG-3'; ASP TM4 WNF->AAA 5'-CATTCCC ACCACACCAGCAGCCGCGATCAGGAGTGCAACAGTAAT-3'.

Leibniz Institute for Age Research
Fritz Lipmann Institute (FLI)
Group: Membrane Trafficking of Proteins involved in Alzheimer´s Disease
Head: Dr. Christoph Kather
Tel +49 3641 656052 Email: mfassler@fli-leibniz.de

PLASMID DATA SHEET

Name:	PE -PALP -WNF / pcDNA3.1 Zeo(+)
Constructed by:	Matthias Faßler, Christoph Kaether
Plasmid:	pcDNA3.1 Zeo(+)
Insert:	PS1-EGFP -PALP with a WNF->AAA mutation in the TMD4
Cloning sites:	EcoRI, EcoRI
Resistance:	Amp , Zeo
Diagnostic REN:	PvuII + NotI (4011 bp, 1749 bp, 838 bp, 723 bp, 295 bp)
Reference:	Kaether *et al.*, 2004; Kaether *et al.*, 2002

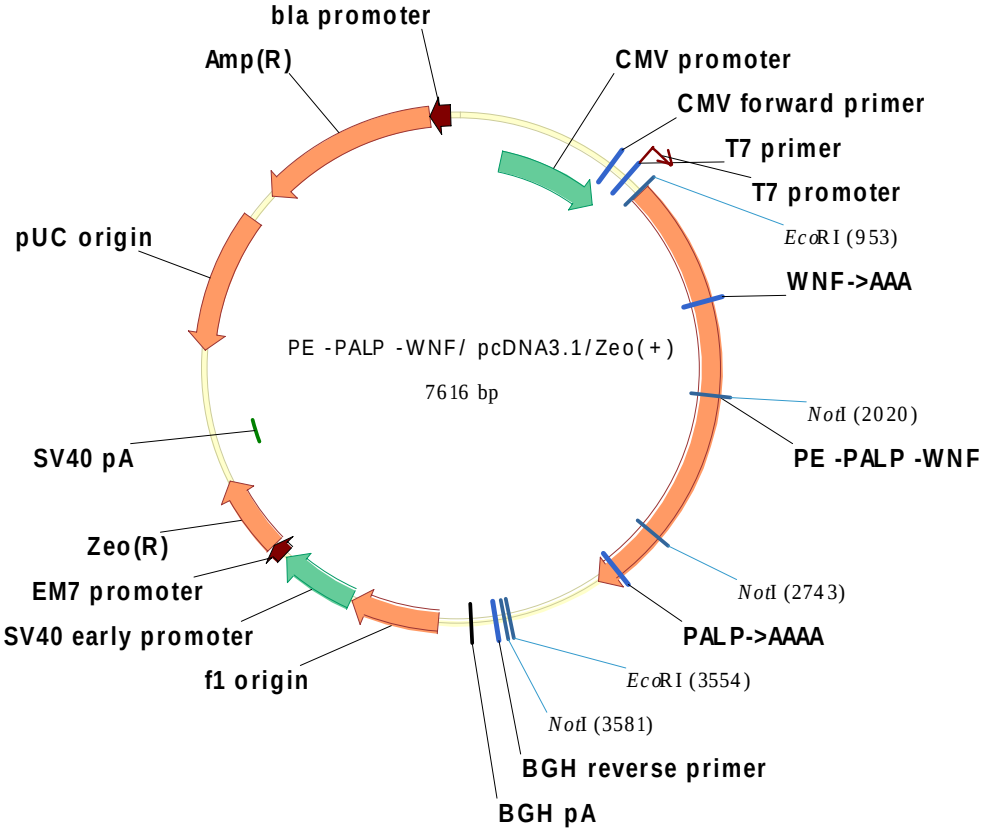

Construction: PE -PALP -WNF was generated from PE -PALP using site directed mutagenesis. SP TM4 WNF->AAA 5'-ATTACTGTTGCACTCCTGATCGCGGCTGCTGGTGTGGTGGGAATG-3'; ASP TM4 WNF->AAA 5'-CATTCCC ACCACACCAGCAGCCGCGATCAGGAGTGCAACAGTAAT-3'.

Leibniz Institute for Age Research
Fritz Lipmann Institute (FLI)
Group: Membrane Trafficking of Proteins involved in Alzheimer´s Disease
Head: Dr. Christoph Kather
Tel +49 3641 656052 Email: mfassler@fli-leibniz.de

PLASMID DATA SHEET

Name:	PE -WNF / pcDNA3.1 Zeo(+)
Constructed by:	Matthias Faßler, Christoph Kaether
Plasmid:	pcDNA3.1 Zeo(+)
Insert:	PS1-EGFP with a WNF->AAA mutation in the TMD4
Cloning sites:	EcoRI, EcoRI
Resistance:	Amp , Zeo
Diagnostic REN:	PvuII + NotI (4011 bp, 1749 bp, 838 bp, 723 bp, 295 bp)
Reference:	Kaether *et al.*, 2002

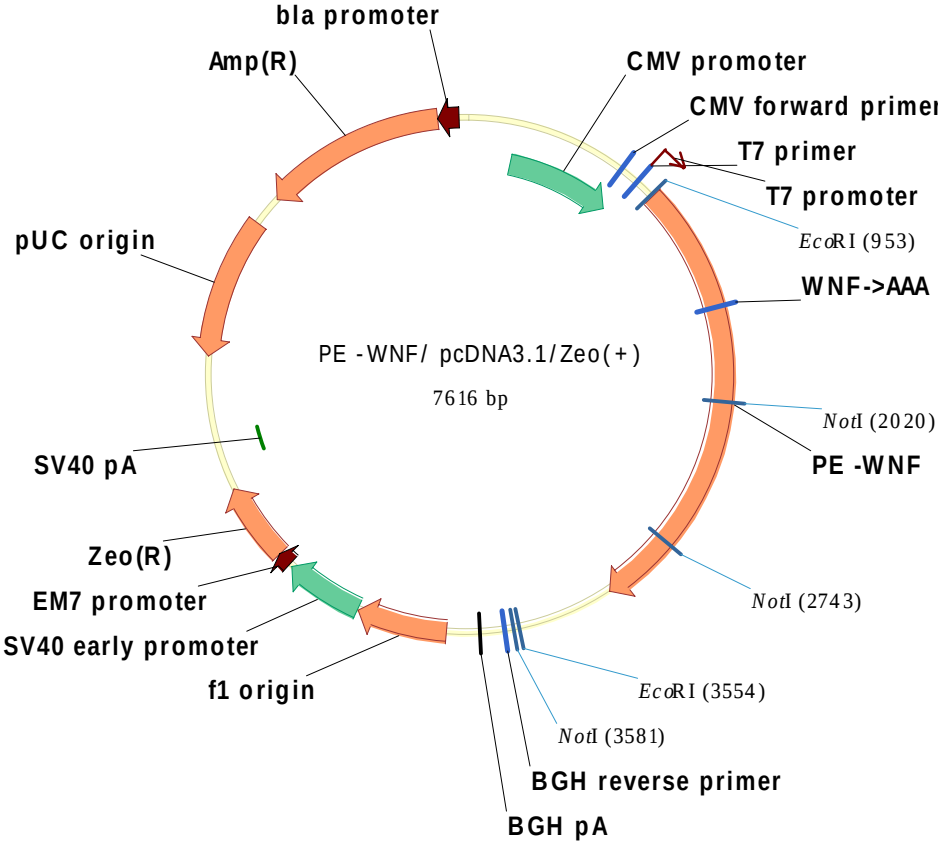

Construction: PE -WNF was generated from PE using site directed mutagenesis. SP TM4 WNF->AAA 5'-ATTACTGTTGCACTCCTGATCGCGGCTGCTGGTGTGGTGGGAATG-3'; ASP TM4 WNF->AAA 5'-CATTCCC ACCACACCAGCAGCCGCGATCAGGAGTGCAACAGTAAT-3'.

Leibniz Institute for Age Research
Fritz Lipmann Institute (FLI)
Group: Membrane Trafficking of Proteins involved in Alzheimer´s Disease
Head: Dr. Christoph Kather
Tel +49 3641 656052 Email: mfassler@fli-leibniz.de

PLASMID DATA SHEET

Name:	Tac-RXR / pcDNA3.1/Zeo(+)
Constructed by:	Matthias Faßler
Plasmid:	pcDNA3.1/Zeo(+)
Insert:	fusion protein mTac and 36 AA from Kir 6.2 containing an RXR motif
Cloning sites:	BamHI, NotI, XbaI
Resistance:	Amp , Zeo
Diagnostic REN:	PvuII (3654 bp, 1749 bp, 491 bp)
Reference:	Zerangue *et al.*, 1999

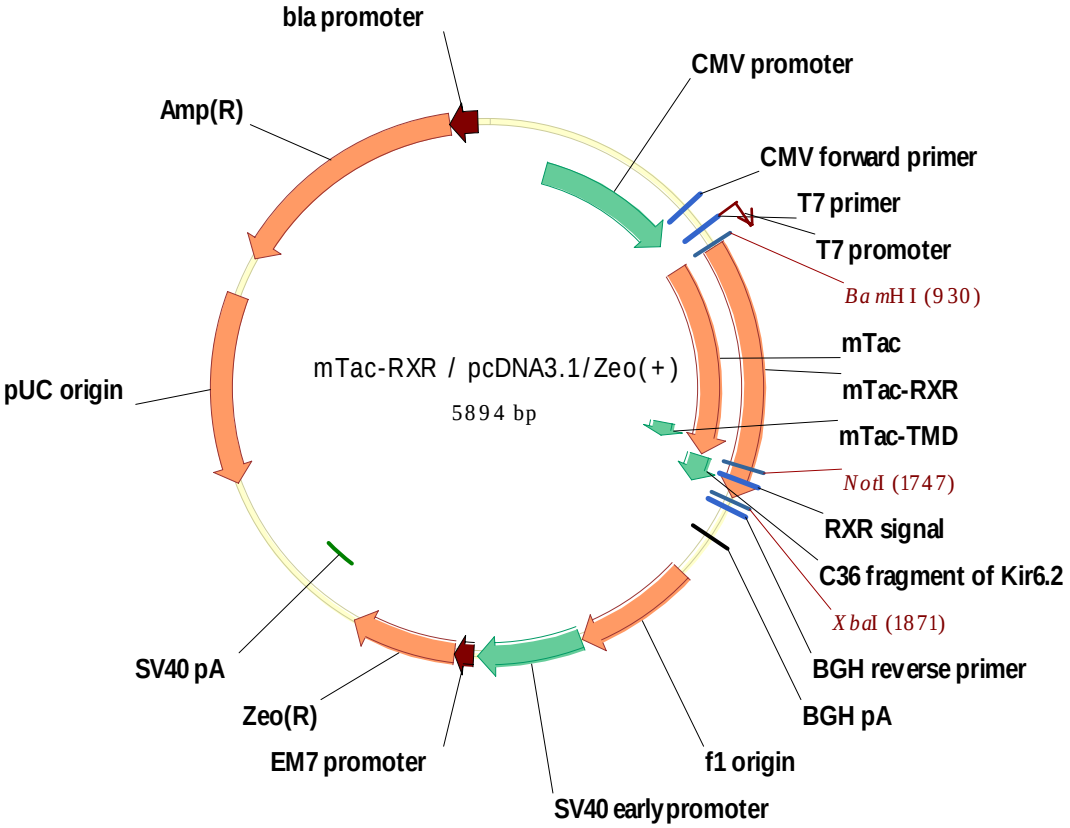

Construction: mTac was amplified from a mTac construct from Christina Valkova. Primers SP mTac BamHI Kozak 5'-GGATCCAGGACCATGGAGCCACGCTTGCTG-3' (introducing BamHI and Kozak sequence) and ASP mTac NotI 5'-TGCGGCCGCGATGGTTCTTCTGCT-3' (removing STOP and introducing NotI) were used. PCR product was TOPO-TA cloned and excised with BamHI and NotI. Excised fragment was ligated into BamHI-NotI-cut CD4-RXR / Zeo.

Leibniz Institute for Age Research
Fritz Lipmann Institute (FLI)
Group: Membrane Trafficking of Proteins involved in Alzheimer´s Disease
Head: Dr. Christoph Kather
Tel +49 3641 656052 Email: mfassler@fli-leibniz.de

PLASMID DATA SHEET

Name:	Tac-TM4 / pcDNA3.1 Zeo (+)
Constructed by:	Matthias Faßler
Plasmid:	pcDNA3.1 Zeo (+)
Insert:	mTac with PS1-TMD4
Cloning sites:	BamHI, XhoI
Resistance:	Amp , Zeo
Diagnostic REN:	PvuII (4032 bp, 1749 bp)
Reference:	

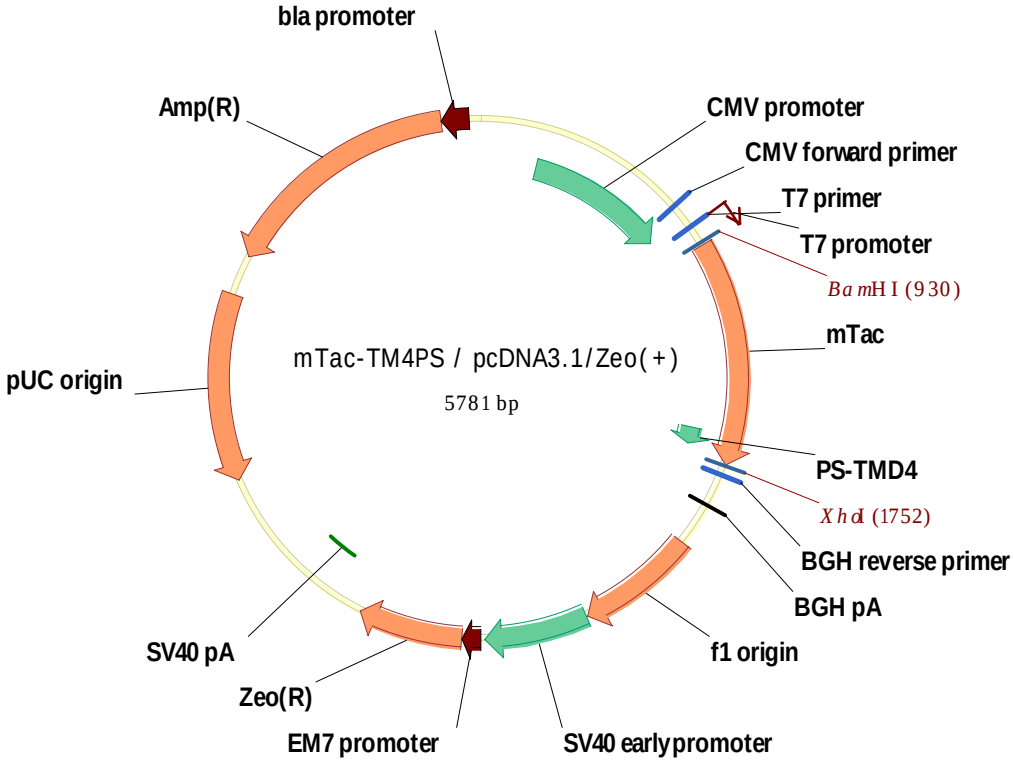

Construction: mTac was ampflified from a mouse cDNA library (C. Valkova): SP mTac BamHI Kozak 5'-GGATCCAGGACCATGGAGCCACGCTTGCTG-3' (introducing BamHI site and Kozak sequence), ASP mTac STOP XhoI 5'-CTCGAGCTAGATGGTTCTTCTGCTC-3' (introducing XhoI site). PCR product was TOPO-TA cloned and subsequently transferred to pcDNA3.1 Zeo (+). The Tac-TMD was swapped with the PS1-TMD4 using a standard protocol for PCR-based mutagenesis: SP mTac-TM4PS 5'-GCACTCCTGATCTGGAATTTTGGTGTGGTGGGAATGATTTCCATTCAACACAGATGGAGGAAG-3', ASP mTac-TM4PS 5'-ATTCCAGATCAGGAGTGCAACAGTAATGTAGTCCACAGCAACGTTCTCCATTGTGAGCACAAATG-3'.